UCLouvain

FACULTE DES SCIENCES

Faculté des sciences

Synthesis and characterisation of (4,4)-Connected Iron(II) Coordination Polymers

Research of Spin crossover Properties

Auteur·es : Constance Vandenbulcke

Encadrante : PhD. Student Li Sun

Promoteur·rices : Professeur Yann Garcia

Lecteur·rices : Dr.K. Robeyns, Prof. M. Singleton, Prof. O. Riant (remplace J. Wong)

Année académique 2021-2022

Master en chimie à finalité spécialisée

Table of Content

Acknowledgement

I would like to personally thank Professor Garcia for guiding me over the course of the process. Thanks to this I had the opportunity of realising the extent of research work in a lab. Previously, during an internship in a company I had learned to be independent and to manage practical aspects of experimentation (quantities, time,…). Whereas working on a research project allowed me to face the difficulties of scientific research, but also to experience the enthusiasm resulting from a conclusive result. I would also point out that Professor Garcia allowed practise specific technics, among which a training to the Mössbauer.

I would also like to thank all my post-doc, PhD and student colleagues that brightened up the atmosphere and always tried their best to help me when I encountered difficulties: Dr. Joanne Wong, PhD Afaf Oulmidi, PhD Yousra Bahjou, PhD Xiaochun Li, PhD Weiyang, Master student Arnaud Nizet, student Guerin Dewert.

I have a special thought for PhD Li Sun, who mentored and accompanied me over the whole course of this work. I thank her for taking the time to teach me the necessary basis. I also thank PhD Afaf Oulmidi for her involvement as supervisor of the original project.

I also want to give a special mention to Arnaud who helped me a lot on the design of the Sorai fit. He has taken a lot of his time to make the data fit and I wanted to underline it.

I would like to thank Jean-François Statsyns for his logistic help and his availability to answer technical questions.

Finally, I want to thank the jury members: Dr.K. Robeyns, Prof. M. Singleton, Prof. O. Riant for the time and energy they involve to grade this work.

Abbreviations

Acn : acetonitrile

Bpac : bis(4-pyridyl)acetylene

Bpe : 1,2-di(pyridin-4-yl)ethene

Bpeben : 1,4-bis(4-pyridylethynyl)-benzene

Bpp : 2,5-bis(pyrid-4-yl)pyridine

Btr : 4,4'-bis(1,2,4-triazol-4-yl)

Bz : benzene

HS : high spin

LS : low spin

MOF : metal organic framework

SCO : Spin crossover

Ph : phenyl

Phen : 1,10-phénanthroline

Phpy : 4-phenylpyridine

Py : pyridine

Pz: pyrazine

3-NH_2py : 3-aminopyridine

Foreword

I want to explain in a few words the reasons there was a subject in relation to the original theme. Indeed, the original subject was about the synthesis of transition spin Co(II) materials with the purpose of storage and display of digital information. Due to particular and extended difficulties in resupplying reagents, we decided to change the subject. Nonetheless, it is still in the same research domain, but the method and the foundations of the research are different.

Introduction

Objectives

When conducting a scientific research, defining clearly the objectives to achieve, as well as the course of action, is essential. This is why we will now elaborate on the stakes related to this project.

First of all, the core of this project is a research currently conducted by our colleague, PhD student Li Sun. Indeed, our research can be considered the extension of the work she had started. In fact, the organic ligands used right here are in the continuity of the ligands previously used and the Fe (II) is also at the core of this research. The objective is to synthesise and characterise coordination polymers of the Fe (II) (4, 4)-connected. The coordination polymers in question can show a solvent effect that is to say that the solvent enters the network and in this manner, it can influence the structure and the interactions happening in it. At the same time, this solvent can grant particular properties to this material that would not be possible without its presence. Consequently, researches are conducted on this subject. We will address this effect a bit farther into the thesis. The understanding of this phenomenon is also a route of study associated to this project. However, you will have the chance to note that this effect will only be partially studied here as it is only a secondary goal.

We have previously stated our desire to synthesise three-dimensional coordination polymers from organic ligands and Fe(II) compounds. Their shaping is a crucial issue. Thus, we wanted to define synthetic routes allowing the production of crystals. Indeed, it is vital to the characterisation of the compound, in particular in terms of magnetic properties. Moreover, another goal is to study these compounds in terms of spin transitions. The use of iron as a metal centre in these materials prompts us to study its magnetic characteristics. In fact, iron is a well-known transition metal in the field of spin transition compounds.

Over the course of this project, we wanted to establish synthetic routes based on liquid-liquid diffusion with buffer. This synthesis process is practically very simple and is here used to determine if the products can be easily formed. The core of this procedure is, at first, the characterisation of potential final compounds produced from an empirical point of view, and then the refining of the modus operandi is necessary. Finally, if the stability conditions allow it and if the collection is satisfactory and simple, a more in-depth analysis is done.

Spin crossover

Brief definition [1-6]

Some compounds based of centres from metals belonging to transition metals show a particular effect. This one is in fact the commutation between spin states, more precisely between low-spin and high-spin states. They correspond to electronic configurations well defined depending on the metal. We will detail later how we can define those metals. The nature of the phenomenon, that is to say the tendency to transit two states of different multiplicity, is generally considered to be a form of molecular bistability. The specificity is that those electronic states are interconvertible by external stimulation. Indeed, by changing the pressure, the temperature, the light irradiation, the magnetic or electronic field by example, it is possible to transform a low-spin system into a high-spin one and vice-versa. For this to happen, the free energies of the two spin states must be really close, so that their difference is approximatively equivalent to their nullification. That is to say that $\Delta G_{SCO} = \Delta H_{SCO} - T\Delta S_{SCO} \approx_0$ in the transition conditions [1-4]. The enthalpies and entropies attributed to the process do not encourage the same spin state. In fact, the contributions to each of those terms are different in nature. The enthalpy ΔH_{SCO} work in favour of the low-spin state since it comes in majority from electronic variations happening in the first sphere of coordination during the transition. In contrast, the entropy ΔH_{SCO} related to geometrical changes due to the spin transition and, more precisely, to the distance and force differences of the metal-ligand [3,5] bonds. We can try to summarise their influence to a tendency of the enthalpy favouring a low temperature ($\Delta G>0$) fundamental state low on energy, while the entropy tends to favour, in high temperature ($\Delta G<0$), the more disordered state. The vibrational and electronic aspects of the spin transition impact directly this thermodynamic data. Until then, the value of the variations of enthalpy and entropy observed most of the time are respectively in the range of 6-15 kJ/mol and 50-80 J/molK [137].

A spin crossover is a phenomenon attributed mainly to the d^4 to d^7 elements of the first period of the transition metals (3d) when to show a coordination in octahedron.

There are several ways to represent the spin crossover. Among those, the graphics representing the fractions in high-spin state in accordance to the temperature enable to visualise the spin transition. We can also call those graphics: SCO thermo-induced curves. With the observation of those, it appears obvious that several types of spin crossover can be identified (see figure 30) [6]. To do this, several characteristics are analysed, such as: the curve, the inflexion points, the reversibility or the final fraction obtained. In fact, on this basis, it is possible to establish a type for each profile of transition. First of all, a transition can be gradual or sharp if the gradient of the curve is respectively small or significant. The first type is characteristic of an almost absence of cooperative interactions. A transition can show an hysteresis loop if the curves related to the warming and freezing do not match, there are then two temperatures $T_{1/2}$ or T_c depending if the conversation is gradual or sharp. If the transition shows a threshold, it is defined as in two steps (possibly three steps if there is two thresholds). Finally, if the final fraction in high-spin state does not match with one, then transition is called incomplete.

Concept of spin [7-9]

During the twenties, the physicians Otto Stern and Walther Gerlach developed a quantum mechanics experience that was named after them. It allowed to reveal the spin. [7,8]

The idea was to apply a vertical non-uniform magnetic field to silver atoms. The magnetic moment attributed to the atoms was null because they were in the fundamental state, and thus at a null orbital angular moment. If it were true, whatever the magnetic field applied, the trajectory of the beam should not have been altered. But it did. In fact, the beam was divided into two beams. The phenomenon was explained by introducing the angular momentum of spin or, more generally, spin. There is an interpretation to this concept: the rotation of the electron around its axis. However, this interpretation is wrong and demonstrates the will to interpret the fact that the spin is considered as an intrinsic angular momentum. Indeed, the spin is the only observable quantum that does not have a classical physics counterpart. The partition of the atom beam means that the spin attributed to those atoms can be in two distinct states. Later, it was determined by mathematical means that the states could have two values: - ½ and + ½.

We know the spin more notably as a quantum number: the spin magnetic quantum number $m_s = \pm ½$. Indeed, it is one of the four quantum numbers defining the behaviour of the electrons of an atom based on the model created by Friedrich Hund and Robert Mulliken. [7-9]

If we add the exclusion principle of Pauli[1] to this, it appears that only two electrons can do an atomic orbital and that they can only be of opposed magnetic quantum spin numbers. This leads to a rule: only two electrons (a spin up and a spin down) can be contained in each atomic orbital.

Moreover, the spin is involved in other famous rules: Hund's rules. Indeed, thanks to those, it is possible to establish spectroscopic fundamental term of an atom. However, there have been some hypotheses to simplify the determination of this term. Among those, we can note that the coupling spin-orbit can be neglected regarding the electronic repulsion on the external layer. Furthermore, only the valence electrons are involved in the determination of the energy levels order. We can deduce this from the fact that empty and full orbitals do not impact the full spin and the full orbital angular momentum. The first rule of Hund claims that for all electronic configurations, the more energetically stable term maximizes the total spin S and its multiplicity 2S+1. Having states with high multiplicity being favoured can be surprising. However, it has been mathematically demonstrated that the electrons being alone in an orbit are less screened. Thus allowing to amplify the attraction energy between nucleus and electrons. The second rule is based on the « Orbital Angular Momentum Quantum Number » L and makes it possible to determine, between two states of maximised spin S total, which corresponds to the fundamental state. To do this, we just need to determine for which of those two the value L is greater. It highlights the fact that those rules apply consecutively. This rule allows to select the state in which the electronic repulsive energy is the weaker. Finally, the last rule takes into account the energy related to the coupling spin-orbit, in other words to the contribution of each electron in this value. Depending on the fullness of the layer, the fundamental state corresponds to the value that minimises or maximises, respectively, J = |L+S| [9].

[1] The exclusion principle of Pauli is based on the fact that an electron is a fermion, that is to say a particle with a spin of ½ (in opposition to the boson, the spin of which is complete). He describes the behaviour of fermions, and thus that of electrons. It results that two electrons from a system are not in the same quantum state at the same time.

Crystal field and ligand field theories

To establish the concept of low and high spin, it is necessary to understand their origins. To do this, we will elaborate on two essential theories of coordination chemistry: the theory of the crystal field and the theory of the ligand field. They both came from a different hypothesis, but lead to a similar conclusion.

Crystal field theory (CFT) [10-12]

It aims to explain the structures and properties of the complexes formed from transition metals. Even if the model [10] is quite simple and the base hypothesis is not applicable to most of the complexes, it gives an explanation on some characteristics of those compounds such as: the structure, the colouration, the spin, the stability, the reactivity and the magnetic type. This model refers to metal-ligand interactions by assuming they are only electrostatic, meaning that it is the electronic repulsions that are taken into account. Thus, it is not applicable in research about neutral complexes, by example: the CO. Since this theory applies to transition metals, they are studied, in particular, through their d-levels and the electrons that fill them. Meanwhile ligands are neglected here because assimilated to punctual negative charges. It is how this model determines the electronic configuration corresponding to a complex.

The metal centre of the compound is first considered as a metal cation M^{n+} without ligand or spherical symmetry. This free ion representation contrasts with the complexed state that can happen with all types of symmetry. Considering the ligands as such results in what we call the loss of degeneracy. In fact, it results from the fact that, initially, the five d-orbitals are considered as equivalent in energy since they have energy levels which can be more or less diverse depending on the type of geometry. In the case of an octahedral complex, the orbitals are always degenerated once the six negative charges have been assimilated evenly to the ligands spread on the surface of the sphere, but have a greater energy since there are repulsive electrostatic interactions. De facto, the d electrons and the negative charges interact and destabilise the d-orbitals. The next stage is to position the ligands at the top of an octahedral structure, that way the individual energies cannot be equivalent anymore. They are then divided into 2 orbital groups, with the d_{xy}, d_{xz} and d_{yz} being more stable than the $d_{x^2-y^2}$ et d_{z^2}. In the case of a tetrahedral complex, it is the opposite. The energy levels and the distribution of the orbitals fluctuate even more for a square plan, a square-base pyramid and a trigonal or pentagonal bipyramid. The geometry of a complex is determined by the coordination number, that is to say NC (or C) = m_L+n_X for a simple complex AX_nL_m in which

A represents the central atom for a studied molecule, n the number ligands involving two electrons in the bond with metal. Add to this effects that aims to divert expected geometries such the hindering or Jahn-Teller's distorsion.

The octahedral example being the simplest, we will elaborate on it a bit more. It will be interesting since the same methodology can be applied to the other arrangements, one only has to know the energies associated to each d-orbitals. In the case of an octahedral metal complex, the metal cation is surrounded by six negative charge ligands. According to Gillepsie's theory, more commonly called VSEPR[2] theory, the octahedron represents the more stable arrangement from an energetic point of view, for six identical negative charges via minimized repulsive interactions. As specified previously, the d_{xy}, d_{xz} and d_{yz} orbitals are more stable than the $d_{x^2-y^2}$ and d_{z^2} orbitals, it depends only of the orientation of those orbitals and thus of a diminution or augmentation of the electrostatic repulsions, respectively with the negative charges of the ligands. In addition, the first orbitals are regrouped under the name t_{2g} and the second ones e_g, in which t and e represent the number of degenerated orbitals (t for three/triple and e for deux/double) and g marks the fact to have the same symmetry in relation to an inversion center (g for the German word "gerade"). It is also to note that the t_{2g} are not only more stable in comparison with e_g, but also in comparison with the five degenerated d-orbitals and this by 0,4 Δ_o (or 4 Dq). On the contrary, the e_g are destabilised in relation to the degenerated d-orbitals of 0,6 Δ_o (or 6 Dq). In fact, Δ_o is the splitting of the octahedral crystal field, it represents the energetic difference between the t_{2g} and e_g levels. If we compare the total energy attributed to this system to the one of degenerated orbitals, we note that there is no variation since $3(-0{,}4\ \Delta_o) + 2(0{,}6\ \Delta_o)$ is null. However, it is important to highlight that, depending on the transition metal, the cation's charge and the nature of the ligands, the splitting of the crystal field fluctuates.

[2] Valence Shell Electron Pair Repulsion: method to define easily the geometry of low-complexity atoms or molecules in the form: AX_nE_m.

We will now turn to the highlighting of the low and high spin states thanks to the analysis of the electronic configurations of transition metals d^n for octahedral complexes:

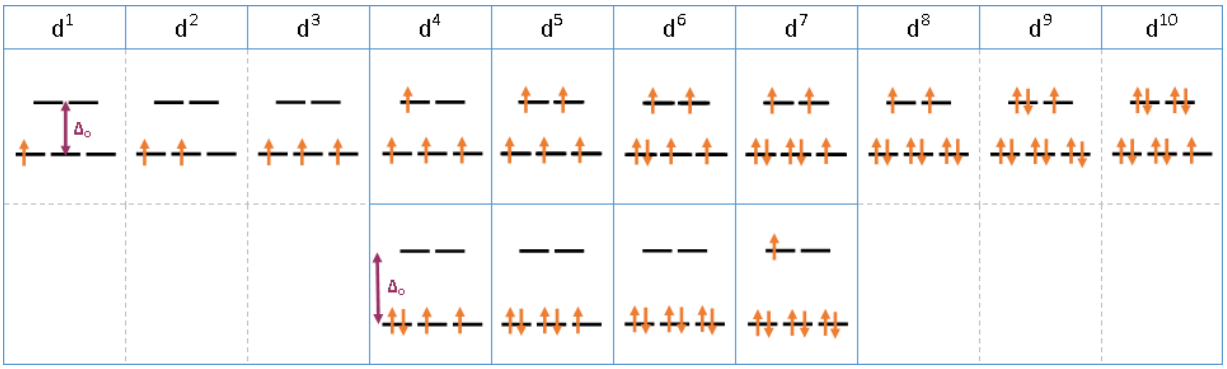

Representation of the different electronic configurations of the d^1 to d^{10} transition metals following an octahedral geometry. The first row represents the high spin state and the second row represents the low spin state when there is one.

These representations have been drawn following several principles. First, the electronic filling is done while following the exclusion principle of Pauli, separating the electrons and filling different orbitals in priority. However, it has its limits. Indeed, only one configuration is possible as long as we fill the stabilised orbitals. But, from d^4, a choice must be done: either we continue to follow this principle; or we abandon it and we fill an orbital of the level e_g. In the first case, we are in the low-spin state, while in the second case we are in the high-spin state. There are thus two different configurations possible for the transition metals corresponding. The more stable electronic arrangement is defined by two factors: the value of the splitting crystal field and the spin pairing energy. The latest represents the destabilisation, the energy gain caused by the pairing of two electrons in an orbital because of electrostatic repulsions. Therefore, if the splitting of the crystal field has lower value than the pairing energy it is preferable to fill an e_g orbital, this way the high-spin state is favoured. In the opposite case, the low-spin state is stabilizing since the energy gain related to the pairing of the electrons is lower than the stabilization induced by the filling of a t_{2g} orbital. From d^8, there is only one configuration possible. The existence of these two states is a source of

bistability and is at the foundation of the interest for these metals in research in field of the transitions of spin. [11,12]

Ligand field theory (LFT) [13-16]

This model is based on the theory of molecular orbitals and allows us to study the reactivity of transition metal-based compounds in coordination Chemistry. It is more complex, but also more exact than the crystal field theory, from which she comes from. It is bases on metal-ligand interactions and describes optical, chemical, and magnetic properties of the coordination compounds.

Thanks to this theory, Orgel and Griffith were able to comprehend colour variations between metal complexes. In fact, the colour of these complexes is easily linked to their absorption spectrum. The latter is impacted by the bonds, more precisely, by the occupation of the orbitals involved in interactions with the ligands. Thus, the colour of these complexes directly depends on the partial occupation of the orbitals from the d underlayer. Actually, the unoccupied orbitals are the ones being involved in the bonding to the ligands. [13,14]

It is based on the influence of the donor atoms on the energy related to the metal complex d-orbitals. The ones being mainly studied are the interactions between the metal d-orbitals and the ligands d-orbitals in a bond. Indeed, the interactions between these electrons lead to an increasing of the system's energy. As before, the geometrical arrangement of the ligands has an impact on their effects. Since we refer to a transition metal ion, we must consider the valence atomic orbitals: three (n+1)p orbitals, one (n+1)s orbital, and five nd orbitals, which are here enounced following the descending order of their energy. As there are nine of them and they can each be filled by coupled electrons, there are, in total, eighteen electrons available. The energy of those orbitals is influenced by the field of the involved ligands and by the force of the interaction.

Consider an octahedral complex in which six ligands are coordinated around a specific metal ion. The molecular orbitals can be represented, and each σ donor ligand gives two electrons to the d-orbitals for coordination. Some orbitals, such as the d_{xy}, d_{xz} and d_{yz}, are non-bonding, thus there is no energy variation because they hardly interact with the donor ligands. However, they do not exclude the π bonds. Others become antibonding, such as the $d_{x^2-y^2}$ or d_{z^2}, or bonding. Those interactions are regulated by the s and p orbitals. Therefore, there are six bonding orbitals and the same number of antibonding orbitals. The occupied d-orbitals are

stable or keep their energy while the unoccupied orbitals are unstable. From the t_{2g} et e_g , it is possible to determine the value of Δ_o.

The π bonds can also happen in these compounds based on LUMO[3] frontier orbitals of the ligands, that is to say π* antibonding orbitals. Their combination with the d_{xy}, d_{xz} and d_{yz} orbitals results in the creation of bonding orbitals. These antibonding orbitals are more destabilised than the antibonding orbitals from σ bonds. Consequently, the value of Δ_o is increasing and metal-ligand bond is stronger. It is the π metal-ligand backbonding, in which the ligand is π-acceptor [15,16].

There are other π interactions. This time, they involve a π-donor ligand. The p or π full orbitals interact with the d_{xy}, d_{xz} and d_{yz} to give electrons to the binding π orbitals formed with the metal. Unlike in the previous case, the energy of the antibinding molecular orbital is not superior to the σ antibinding orbital one. The d electrons of the metal will then occupy the π antibinding molecular orbital for it to become the HOMO. Just like the previous case, the Δ_o decreases.

From there, it appears obvious that the nature of the ligands influences the value of Δ_o and at the same time the way in which the electrons will spread in the binding and antibinding orbitals for the d^4 à d^7 transition metals. Some complexes will therefore be in the high-spin or low-spin state depending on the ligands associated with the metal ion. The first case represents the filling of the two types of orbitals, whole the second one favours the pairing and the filling of the antibinding orbitals. Indeed, the π interactions between the metal d-orbitals and the ligand orbitals make the value of Δ_o fluctuate, and thus influence the spin state.

To summarise the previous paragraphs, in the case of π-donor ligands, the Δ_o decreases, the ligands are then called “weak-field ligands”. On the contrary, the π-acceptor ligands make the Δ_o increase and are then called “strong-field ligands”. Since the electronic configurations are heavely dependent on the value of Δ_o, we can say that the π-donor ligands tend to encourage the high spin state and oppose the pairing of electrons. While the π-acceptor ligands tend to encourage the low spin state and the pairing of the electrons.

Nevertheless, a ligand π-donor ligand does not necessarily induce a high-spin state, this is why it was essential to establish an order relation based on the strength of the ligands.

[3] LUMO (Lowest Unoccupied Molecular Orbital) in opposition to HOMO (Highest Unoccupied Molecular Orbital), this is the lowest-energy vacant molecular orbital.

The spectrochemical series was created with this goal in mind. This is a ligands classification according to the value of Δ_o, which they induce. In 1938, the spectrochemical series was established on the basis of comparisons of absorption spectrum of several cobalt complexes. In fact, the value of Δ_o is accessible at the start of these spectrum. A part of the ligands has thus been defined as weak, they are not able to force the pairing of the d electrons, leading to a state of high spin. Whereas the ligands defined as strong are able to do it, leading to a state of low spin. Obviously, the π-donor ligands are considered weak, among those there is the majority of the halide, water and the hydroxides. The ligands presenting only a σ-donor effect are considered as intermediate, it was the case, by example, for the ammoniac and the ethylenediamine. Finally, the π-acceptor are considered as strong, notably cyanide or carbon monoxide. It is interesting to note that there is also a metal spectrochemical series following the same concept. It turns out that the value of the crystal field splitting increases with the oxidation state and the period of the metal. In general, the metals of the first row of the transition metals are high spin if they are not heavy on positive charges, while the metals of the two other rows are low spin. De facto, two aspects favour the low spin configuration: strong bonds inducing an increasing of Δ_o; and more spread orbitals, which reduces the energy gain when two electrons are paired. In the case of iron, it is high spin the majority of the time when it is Fe(II) while the Fe(III) is often low spin.

Tanabe-Sugano diagrams [17-23]

These diagrams allow us to observe the energetic evolution of the electronic states from weak-field to strong-field. In fact, it gives us a better approximation of the reality, which is often intermediate. We can take a lot of information from those diagrams, such as the wavelength of the absorption peaks in UV, visible and infrared. The value of the crystal field splitting can be approached by an octahedral or tetrahedral coordination complex based on the spectroscopic data [17].

To take into account the electronic repulsion effects in the coordination complexes, special parameters have been introduced: Racah's parameters A, B and C [18]. The parameter A is assimilated to an average of all the repulsions between electrons. More generally, for electrons of the same nature (meaning d), this parameter is stationary, which means it is not required to show it in the Tanabe-Sugano diagrams. The B and C parameters are related to individual repulsions for the d electrons and are linked by a mathematical relationship. It is then often approximated to a fraction of B. The parameter B determines the strength of the metal-ligand bond. In addition, for the value of B for a free ion which has a non-identical

coordination complex, we generally use the ratio β. It is called the nephelauxetic parameter and is the division of B for the B complex by B if the free ion. In this manner, it defines the increasing in size of the d-orbitals and thus the reduction of the electronic repulsions when a transition metal forms a coordination complex [20,21]. In fact, the volume in which the electrons position themselves increases under the influence of two effects. Firstly, it can result from the creation of a bond of a covalent nature. The overlapping of the orbitals is responsible for this and, at the same time, enlarges those orbitals. The second effect is that the introduction of negatively charged ligands allows for a diminution of the actual electrical load of the metal core, which leads to orbitals to expand.

Regarding the resulting value of this ratio β, it can only be inferior or equal to 1. The strength and the nature of the bond can be studied according to it. Indeed, when $\beta = 1$, the bond is strictly ionic since the coordination did not have any impact on the size of the orbitals. The more the value decreases, the more we tend toward a covalent bond. It happens when there is a delocalisation of the electron cloud of the metal towards the ligands. Since this nephelauxetic is of different importance depending on the ligand's nature, it generates an ascending order of the effect [22,23]. There is the same type of classification for transition metals. It is noteworthy that this effect also exists for lanthanides via their f-orbitals but is insignificant in relation to the d-orbitals one of the transition metals.

The Tanabe-Sugano diagram (see figure 31) represents E/B in relation to Δ/B, in which E is the energy, B a Racah's parameter and Δ the splitting of the crystal field. Curves are starting at the spectroscopic terms at the level of the y-axis and represent a degenerated electronic state each. The minimum E/B of the graph corresponds to the spectroscopic term of the fundamental state. For the configurations from d^4 to d^7, a vertical line is added and divide the diagram in two parts corresponding to the low spin and high spin state. It is positioned at a particular value of Δ/B, meaning that the pairing energy of spins equalise the crystal field spitting energy. To be precise, the left part defines the high spin situation, and the right part defines the situation of the low spin complexes. Moreover, this straight line represents a breaking in the curves, thus loses of various energy levels.

There are also Orgel's diagrams (see figure 32), which are strictly qualitative and can be used only for weak-field, in other words: for high spin. Their specificity is that they show only the symmetry states with the highest multiplicity, only the states possible through the

rule of Laporte[4]. This is not the case for the Tanabe-Sugano diagrams, in which the complex is also considered as low spin. Orgel's diagrams show the states for a certain configuration (d^n and d^{n+5}) for a tetrahedral complex on one part and for an octahedral complex on the other part. The Tanabe-Sugano diagrams of a kind of combination between Orgel diagrams, Russel-Sanders terms and the low spin state.

In our case, we are studying the coordination compounds of the Fe(II). Therefore, we can refer to the d^6 diagram. It is good to keep in mind that the value of Δ_o can be guessed to exploit it, including in the absorption wavelength calculation [19]. This diagram can also be useful to determine in which state a compounds of Fe(II) is, by comparing it to the diffuse reflectance spectrum. Indeed, the compound's nature can be found by establishing a connection between the number of peaks in the spectrum and the number of possible transitions starting from the fundamental state. In the case of the Fe^{2+}, only one transition is allowed in the high spin state ($^5T_{2g} \rightarrow {}^5E_g$) and two in the low spin state ($^1A_{1g} \rightarrow {}^1T_{1g}$, $^1A_{1g} \rightarrow {}^1T_{2g}$). It should also be noted that there is third transition possible for the latter case, but it is so energetic that the wavelength associated is not in the visible range, but in the UV. Only one peak will be visible in the first case while two will be visible in the second. Furthermore, we can note that the possible transitions in low spin have E/B values far more important than the high spin electronic transitions ones. The crystal field in the low and high spin states can be determined and we obtain an interval in cm^{-1} so we can know if we are in the high spin state below a defined value, in the high spin state above the other, or if there is a coexistence with two intermediate values for Δ_{HS} and Δ_{LS}, which would mean there are transition spin properties.

Magnetism [24,25]

It is here described as characteristic property of a material that can be attracted or repulsed by a magnet. In the everyday life, it is mainly through permanent magnet that we speak about magnetism. Nevertheless, there are several types of magnetism. We will develop on the subject for a bit because the spin crossover study is based on it.

[4] Laporte's rule is one of the selection rules that determine when an electronic transition is possible or not. It states that a transition can only happen between different parity states, in other words if electrons are distributed from one orbital towards another. Transitions are allowed if $\Delta l = \pm 1$, the transitions d→d are then forbidden. The other selection rule is the rule of the multiplicity of spin in which transition only happen if they respect $\Delta S=0$.

Diamagnetism [24,25]

The diamagnetism is the more universal magnetism form. In fact, as soon as baryons are involved, it is there. Which means that it is all that contains protons, neutrons or electrons that is to says all atoms and molecules. Even if it is omnipresent, it is not always perceived because it is often shadowed by other magnetism types effects that are of greater size.

The diamagnetism results in the creation of a weak magnetic field in the material subject to a magnetic field. In this case, it means that the magnetic moments of the material's electrons direct themselves in the opposite way of this external magnetic field. The result is a weak magnetization opposing the applied magnetic field. If the external field is not applied anymore, then the magnetic moments orient themselves randomly again. It is a quantum phenomenon.[25]

The χ_m magnetic susceptibility was introduced to study the size of the resulting magnetic field. It characterises the capacity of a material to magnetize itself after the application of a magnetic field. In the case of the diamagnetism, it is around -10^{-5} or -10^{-6}. The minus sign highlights the opposition to the external magnetic field and its size shows the weakness of the induced magnetic field. Furthermore, the magnetic susceptibility of the diamagnetic material is not impacted by temperature changes. This is not true for all kinds of magnetism. [24]

When the Fe^{2+} (d^6) is in an octahedral geometry and in the low spin state, the pairing of the six electrons leads to an annulation of the spin and a diamagnetic compound. Since S = 0 for the Fe^{2+} (d^6) which is d^6 low spin, the product $\chi_M T$ is null too.

Paramagnetism [24,25]

It characterises the materials in which the magnetic moments are randomly oriented initially, but, once subject to an external magnetic field, align themselves on the applied magnetic field. The magnetization then induced allows to strengthen the applied magnetic field. It notably shows by a positive magnetic susceptibility and a superior order of magnitude compared to the diamagnetism (10^{-5} to 10^{-3} in this case). If the external field is not applied anymore, then the magnetic moments orient themselves randomly again. The paramagnetism is typical of the compounds in which the atoms have a permanent magnetic moment but are not coupled. The induced polarisation is weak since the thermal agitation takes over and thus oppose the magnetic moments orientation. [25]

The paramagnetism is not an inherent property of a material but is induced by an exposition to a magnetic field. Therefore, it is not constantly present, it depends on the conditions. It appears in a ferromagnetic or ferrimagnetic material once the Curie temperature is reached. In the same manner, an antiferromagnetic material becomes paramagnetic once the Néel temperature is reached. [24]

It is important to highlight that the high spin (S =2) Fe^{2+} (d^6) is paramagnetic because of its four lone electrons in an octahedral geometry.

Ferromagnetism [24,25]

As previously, the materials are able to magnetize themselves when they are subject to an external magnetic field. The slight difference here is that they keep their magnetization even when they are not subject to a magnetic field (remanent magnetisation) anymore. [25]

The magnetic susceptibility associated is around 10^5, meaning that the introduced field is big. The magnetic moments aligned and parallel once the magnetization is done and the magnetic susceptibility obey to the Curie-Weiss rule. Under the Curie temperature, the material is ferromagnetic, otherwise it is paramagnetic [24]. It is again due to the thermal agitation. Among the ferromagnetic substances, there is the iron (Nickel, Cobalt and some derivatives) which is the subject of our research.

Antiferromagnetism [24,25]

The magnetism type characterises the materials in which the equivalent magnetic moments align themselves as antiparallel so that they cancel themselves. In addition, they are strongly bond. The resulting magnetization is null. However, if the temperature increases, the antiparallel alignment deteriorates which leads to the magnetic moments being more impacted by the effect of an external magnetic field. Consequently, there is a temperature below which those materials are antiferromagnetic and above which they are paramagnetic: the Néel temperature. The antiferromagnetism is very often considered to be a particular case of ferrimagnetism. [24,25]

Ferrimagnetism [24,25]

There is a magnetism type in which the magnetic susceptibility is big and positive: the ferrimagnetism. Without any magnetic field applied, the magnetic moments are aligned in the individual Weiss domains, but since are antiparallel and from different magnitudes, they do not counterbalance each other. Since each domain is oriented differently, the whole does not have any resulting magnetic moments. [24]

The ferrimagnetism is a type of magnetism appearing when the materials are constituted of two atoms of different natures. There is a strong antiferromagnetic coupling between two different spins because attributed to atoms of non-identical nature. The result is that the spin is not null and that there is a magnetisation without magnetic field applied. [25]

However, when there is an external magnetic field, the magnetic moments align according to the magnetic field (in one direction or another, in order to obtain a non-null magnetic moment). Below the Curie temperature, the material is ferrimagnetic, it is otherwise paramagnetic in accordance with the same thermal agitation than before.

Spin crossover complexes [1, 26-38]

History [1, 26-38] (see figure 1)

In the early thirties, Cambi et al. have noted a magnetic behaviour in Fe(III) dithiocarbamates complexes [26]. The first SCO phenomenon has just been identified. From there, it was deduced that the spin states were heavily impacted by the nature of the amine substituents. Thirty years later, the first SCO complex based on CO(II) was discovered [27]. In 1964, W.A. Baker and H.M. Bobonich have noted a spin transition that had been induced in the complex of Fe(II): $[Fe(phen)_2(NCS)_2]$ [28]. Between 1965 and 1985, complementary researches on the Fe(II) complex show that the transition between two spin states can be induced by pressurising [29] or by light exposition [30]. In the eighties a way to identify spin transition for other transition metals was found. The ones that had been discovered are compounds of Mn(III) [31] and Cr(II) [32]. A particular phenomenon on the chez $[Fe(ptz)_6](BF_4)_2$ has also been noted [30]. In fact, they were able to induce the spin transition through light irradiation. It is more commonly called the LIESST[5] effect. Depending on the transition being made from the low spin complex toward the high spin one or the other way around, the wavelengths change.

The possibility to trigger the change of spin state boosted the interest in those compounds. Nevertheless, the research in this domain goes through the roof in 1992 as a result of a publication of O.Kahn et al [33] that highlighted the practical potential of the compounds. There were, in particular, possible applications in detection, memory or display. Even if these complexes are initially from the coordination inorganic chemistry domain, the conception and use possibilities opened research in other domains. Currently, the transition spin compounds are still at the core of research. Although the knowledge is getting better with

[5] LIESST : Light-Induced Excited Spin-State Trapping

time, there is still a lot of possibilities in terms of research and conception. Moreover, a large task of optimisation and research must be continued to transition spin compound at room temperature, among other things. More generally, the transitions must be done under some conditions specific to the application, which often leads to a lot of difficulties.

Among the publications that enabled the progression of chemistry on the transition spin compounds, we can point out some publications linked to our project. First of all, the work of Haasnoot et al regarding SCO two-dimensional array [35] as well as SCO one-dimensional chain [34]. More recently, Real et al [36] have first created interpenetrated SCO two-dimensional arrays, then contributed to the obtention of SCO nanoparticle. Finally, other documentations from Professor Garcia [37,38] inform us on the crystal structure of SCO one-dimensional chain and on the conception of three-dimensional arrays.

With each discovery, the interest over the spin crossover phenomenon only grew larger, thanks to the numerous possible applications. From technologic point of view, research are made to be able to use them as captors, molecular magnet, in the catalysis of transition metals or in molecular electronic. [1]

Iron and SCO are very closely connected since this is the more exploited atom in the transition spin compounds and in the research for magnetic properties materials.

Metal-Organic Frameworks

Origin of our research [39]

During this project we mainly used here identified by their respective IUPAC names: the 4-[4-(4-pyridin-4-ylphenyl)phenyl]pyridine and the 4-(2-pyridin-4-ylethenyl)pyridine. These molecules have been chosen based on the publication of Zhao-Ping Ni et al [39]. Indeed, this publication seemed very interesting to us since it covers on one hand transition spin properties, and on the other hand it aims to integrate them in MOFs (metal-organic framework) materials. Which would be a very appealing exploration route regarding large scale applications. The reference publication for this project aims to inform on the production and on the conception of Hofmann type MOFs presenting transition spin properties, and more precisely on the amplification of those through a guest molecule effect. An investigation has also been made to determine which factors were key and to what extent regarding SCO properties of those materials.

Brief history of Hofmann type coordination polymers [40-48]

Initially, they were known as the Hofmann clathrates. Discovered in 1897, they are coordination polymers able to contain guest molecules. The first known compound is the $[Ni(CN)_2(NH_3)].C_6H_6$, also called the benzene clathrate of Hofmann (see figure 33) [40]. Its synthesis was then realised from an aqueous solution of ammoniac and nickel cyanide to which benzene was added.

Following this, this compound family has extended with similar materials, but with another aromatic guest incorporated. Hofmann and his colleagues have then synthesised compounds in which pyrrole, pyridine, thiophene, phenol or aniline were contained in the pores [41,42]. In addition to this, their research has made it possible to determine that it was impossible to get the same property for hindered aromatic guest molecules, meaning that the pore's volume is restrictive and does not allow the incorporation of all molecules [42]. This factor must thus be taken into account when we try to create polymers of this type and can be studied more in-depth.

In 1949, Rayner and Powell were able to determine the particular structure of the clathrates [43,44]. As a matter of fact, two two-dimensional frameworks constituted of parallel layers separated by a distance of 8 Angströms in the case of original clathrate to create cavities between the layers where the guest molecule can position themselves. Those sheets are formed by octahedral Ni^{2+} ions, two ammoniac ligands axially positioned relatively to the metal core and square plan linkers $[Ni(CN)_4]^{2+}$. In fact, the Ni(II) core are of two types, depending on their environment: $[Ni(CN)_4]^{2+}$ and $[Ni(NH_3)_2]^{2+}$, the azote cyanide do binding between themselves, cyanide are thus bridging ligands. While the ammoniac defines the cavities occupied by the benzene molecules.

From those basics, the Hofmann type coordination polymers family has developed with compounds of the formula : $[M(L)_nM'(CN)_4].G$ in which M is a metal cation such as Fe^{2+},Ni^{2+},Co^{2+},Zn^{2+} ,Mn^{2+} ,Cd^{2+} or Cu^{2+} , L a ligand uni- (n=1) or bidentate (n=2, bridging), M' is a Pd^{2+}, Ni^{2+} or Pt^{2+} cation and finally, G represents the guest molecule incorporated in the framework [45,46]. Depending on denticity of the ligand, it can lead to creation of coordination two- or three-dimensional frameworks. It should be noted that there is a formula adapted to some cations charged one time, which is $[Fe(L)_n\{M''(CN)_2\}_2].G$, it uses the same code as previously, except for M'', that represents Ag^+ or Au^+.

A few years before 2000, the first polymer of this type having SCO properties was synthesises by Kitazawa et al [47]. It is a compound similar to the previous one, but in which the NH_3 have been replaced by axial pyridines on octahedral cores of Fe^{2+}. The layers now being represented by $[Ni(CN)_4Fe]_\infty$. The adjacent sheets being non-aligned, small cavities were created. This polymer shows a cooperative spin crossing and a thermal hysteresis loop from around 9 K.

In 2001, the same type of behaviour was observed by Real et al. With hysteresis loops of 5 and 8 K each in the case of similar polymers, but in which Ni^{2+} was replaced by Pd^{2+} and Pt^{2+} [48]. Furthermore, the hysteresis appeared at higher temperatures, around 210K compared to 190K before.

Before that, the SCO behaviours were limited to two-dimensional polymers. The revolutionary idea was to introduce bridging ligands such as the pyrazine instead of the pyridine. This is how the first three-dimensional spin transition polymer of this type has been created. In fact, it is very close to Kitazawa's compound, but the pyrazine ligands act as pillars, thus enabling the formation of a 3D equivalent. This material presents a bigger hysteresis loop and is at far higher temperature than its two-dimensional counterpart. It was also possible to create similar polymers with Pd(II) and Pt(II) replacing the Ni(II), the aforementioned tendency has then been confirmed.

Considering the conclusions drawn from the transition of those polymers from two-dimensional to three-dimensional, it appeared that the synthesis of those compounds was very attractive for research on SCO properties materials. On one hand the hysteresis is bigger and on the other hand, they are closer to room temperature. It is obviously very interesting for the technologic development.

The spin crossover and the MOFs: emphasis on the interest for three-dimensional Hofmann type coordination polymers

Previously, we highlighted two structures capable of containing guest molecules having the following formulas: $[Fe(L)_nM'(CN)_4]\cdot G$ and $[Fe(L)_n\{M''(CN)_2\}_2].G$. (see figure 2) Since ligands act as pillars in the material's structure, their nature obviously has an impact on the size of the cavities created. At the same time, it influences the possibility to incorporate a molecule rather than another, which means that not all molecules can be guest molecules in those structures. Therefore, the volume of the pores is a decisive factor. Of course, the guest molecule is also determined by the modus operandi chosen. It does not seem odd to think

about the possibility of an eventual replacement of this guest molecule by another one that we have chosen. It would then be very rewarding to study this mechanism and the key-points associated to it. Depending on the molecule inserted in the pore, other properties could be explored and other eventual materials of interest could be found.

Previously, we introduced the two-dimensional polymer of Katazawa et al. To have a better understanding of the importance of this research, we will go through its results as well as through the conclusions related to it. Starting from now, we will call the compound pyNi to facilitate the comprehension. First of all, let's take a look at the cooling (186K) and heating (195K) transition temperatures, which induce a thermal hysteresis loop of 9K. The compound shows a cooperative transition. We will now compare those results with the ones obtained by Real et al. for the same type of polymers, but with Pd(II) and Pt(II). It appears that the spin transition was of the same type in the case of the pyPd and pyPt.

Compounds		Transition temperature (K)		Width of the hysteresis loop (K)
		Cooling	Heating	
PyM	PyNi	186	195	9
	PyPd	208	213	5
	PyPt	208	216	8

Table a. Table representing temperature associated to the SCO phenomenon as well as the hysteresis loop width for two-dimensional compounds based on pyridine and a metal M = Ni, Pd or Pt

It was then noted that the nature of the metal core influences a bit the size of the hysteresis and its temperature range, we will get back on that subject later.

To establish the interest of the three-dimensional Hofmann type coordination polymers, we will discuss the results for compounds similar to the previous ones, but in which the pyridine has been replaced by pyrazine (bridging ligand). In addition, water molecules are associated with the compounds as guest molecules. Let's observe the cooling transition temperatures of each of those compounds:

Compounds		Transition temperature (K)		Width of the hysteresis loop (K)
		Cooling	Heating	
PyM	PyNi	186	195	9
	PyPd	208	213	5
	PyPt	208	216	8
PzM	PzNi.2H_2O	280	305	25
	PzPd.2,5 H_2O	233	266	33
	PzPt.2H_2O	220	240	20

Table b. Table representing temperature associated to the SCO phenomenon as well as the hysteresis loop width for compounds based on pyridine or pyrazine and a metal M = Ni, Pd or Pt, with the quantity of guest molecules (H_2O) incorporated

Compared to their 2D counterparts, it clearly appears that there is a shift of the transition temperatures towards higher values as well as an increasing of the hysteresis. However, it raises some questions, in particular about the factors impacting this evolution. There is no similar order of compounds based on the same metal cores in 2D and 3D. Besides, the pzPd compound incorporated more guest molecules than the rest, so there could be an effect on SCO properties. More generally, the rigidity brought by the three-dimensional coordination explains the increasing if the T_c and of the size of the hysteresis, even if it is, in principle, partially mitigated by the effect of the ligand field (less significant for the pyrazine than for the pyridine).

This aroused interest on the possibility to obtain an hysteresis at room temperature. In 2020, the impact of the synthesis conditions, and thus of the morphologies associated to the final compound of $[Fe^{II}(C_5H_5N)_2Ni^{II}(CN)_4]$ on the SCO properties has been thoroughly demonstrated [49]. Particularly in terms of cooperativity and of hysteresis size with 22K for the "nanoplates" and 2K for "nanosheets", this emphasises a dependency of the SCO properties to morphology of particles.

Preliminary study of some SCO properties factors

In order to discover other Hofmann type coordination polymers, several possible modifications have been implemented on the basis of the previously synthesised polymers. There are four main types of modifications that have been implemented:

1) The use of new ligands having the respective denticity of the pyridine and the pyrazine
2) The introduction of cyanometallate linkers of different nature, including $[Au(CN)_2]^-$ and $[Ag(CN)_2]^-$ or square plan units
3) The extension of the guest molecules to the aromatics or the protic solvent by example, to study the impact on the magnetic properties of the compound
4) The shaping: nanoparticles or thin film to determine the future applications more precisely.

We will discuss those four changes and their influence on the compounds properties. This part aims to enlarge the avenue of research and take into consideration all of the essential factors.

Influence of the choice of the ligand [50-56]

Previously, we noted the evolution of the SCO properties according the ligands changes. A comparison of 2D polymer properties with similar polymers, but in which pyridine is replaced is a good start to understand the influence of the ligand choice. This has been done in particular with pyridine in position 3 replaced by fluor [50], an amine NH_2 [51] or a phenyl (here in position 4) [52]. The following results have then been obtained:

Compounds		Transition temperature (K)		Width of the hysteresis loop (K)
		Cooling	Heating	
PyM	PyNi	186	195	9
	PyPd	208	213	5
	PyPt	208	216	8
3-FpyM	3-FpyNi	206	234	28
	3-FpyPd	214	248	34
	3-FpyPt	214	240	26
3-NH_2pyM	3-NH_2pyNi	148	173	25
	3-NH_2pyPd	169	206	37
	3-NH_2pyPt	183	213	30
PhpyM	PhpyPd	163	203	40
	PhpyPt	172	221	49

Table c. Table representing temperature associated to the SCO phenomenon as well as the hysteresis loop width for two-dimensional compounds based on pyridine or a derivative and a metal M = Ni, Pd or Pt

It shows that whatever the function of the ligand, it tends to increase the width of the hysteresis. Regarding the second case, it would seem that the additional interactions increase the cooperativity. In fact, there are hydrogen bonds adding up, but also a weak Ni-N_{amino} interaction involved. In a quite spectacular way, hysteresis loops from 40 to 49 K have been obtained with phenyl functionalizing the pyridine. This has been attributed to double π-π interactions working once again in favour of cooperativity. Moreover, there is a water molecule incorporated in the platine compound, it could have an impact on SCO properties, as we will see later.

According the science literature, a link can be established between the size of the pillar ligand and the SCO properties. As a matter of fact, it has an impact on the available volume for the guest molecule and also influences the width of the hysteresis. Indeed, Hofmann type three-dimensional polymers with SCO properties have been made based on organic ligands of larger size. Consequently, two 3D compounds have been synthesised then compared: bpacPt.0,5bpac.H_2O [53] and bpebenPt.0,5bpeben [54]. The first ligand is long and rigid, the

final compound had cavities capable of hosting molecule of a volume of 294 angströms³. It has an hysteresis of 21 K which starts at a temperature of 301 K. While with the even longer second ligand, the pores could contain molecules of angströms³. Even if the volume available for the guest molecules has drastically increased, there is no hysteresis anymore. It was deduced that the longer a ligand is, the worse the transition of the SCO cooperativity is. Meaning that the hysteresis decreases or even disappear for compound using longer pillar ligands. Thus, it seems essential to select the used ligand adequately to maximise the hysteresis that would be associated with the final materials.

Furthermore, other cyanometalate linker scan be used. In this case, it is the nature of the metal center that changes. In a $[Fe(L)_n\{M''(CN)_2\}_2].G$ compound, the M'' now represents a metal cation one time positive, more precisely: Au^+, Ag^+ or Cu^+ [55]. This project iniated by Real and his team bore its fruits in 2002 when they synthesised a doubly interpenetrated three-dimensional complex on the basis of pyrazine and silver pzAg.pz [56] (see figure 3 and 3 bis). The $[Ag(CN)_2]^-$ linkers allowed the binding to the Fe^{2+} ions in the two-dimensional sheet then created. The organic ligand had two roles: link the iron atoms of different sheets as well as ensure the interpenetration of the layers. There are similar structures with gold despite having incorporated longer bridging ligands[6], they are also interpenetrated. However, large cavities are available in it to host eventual guest molecules.

Influence of the choice of the guest molecules [57-65]

Scientific literature is more and more well-furnished regarding the role of the guest molecules in the capability of Hofmann type three-dimensional MOFs in the associated SCO and magnetic properties [57, 58]. In fact, all kinds of molecules have been tested as guest molecules and the polymers created have then been studied. Among them, there are firstly the organic solvents, the gas compounds that have been incorporated as well as the CS_2, aromatic molecules or the thiourea. It leaves a large panel of possibilities and paths of exploration in the future. Depending on the chosen molecules, numerous characteristics fluctuate, like the hysteresis width, the temperatures associated to the transition and the spin state in which the polymer is initially.

The comparison of two polymers based on platinum and pyrazine (pzPt.G) in which only the guest molecule has been changed speaks for itself. Indeed, if we consider the polymer containing the benzene and the one containing the CS_2 at room temperature, the first

[6] More precisely : bipytz [56a], bpmp [56b], bpp [56c] or dpb [56d]

one is in the high spin state while the latter is in the low spin state. The nature of this molecule is not the only thing impacting those properties, its presence or absence has an impact as well. De facto, for the previous empty polymer or whose cavities are filled by thiourea molecules, we noted a strong impact on the temperatures $T_{1/2}$ specific to the transition as well as the hysteresis width. In the case, once the pores have been filled by the thiourea, the transition is the room temperature range.

Compounds		Transition temperature (K)		Width of the hysteresis loop (K)
		Cooling	Heating	
PzPt.G	PzPt empty	285	309	24
	PzPt with thiourea	213	277	64

Tableau d. Table representing temperature associated to the SCO phenomenon as well as the hysteresis loop width for compounds based on pyrazine and platinum if there is no guest molecules or if thiourea has been incorporated

Additionally, very particular facts have been described by Ohba and his team regarding the absorption/desorption of guest molecules [60]. About ten years ago, they showcased memory effects in the range of temperature associated to the transition. The idea was to study the absorption of benzene in the form of steam for the platine and pyrazine polymer (pzPt) whose cavities are empty. It is then in the low spin state at a tempature included in the hysteresis ($pzPt^{LS}$). The low spin state has then been converted into a high spin state after the benzene was incorporated ($pzPt^{HS}$.bz). But the interisting phenomenon appears once the the vacuum desorption has been done: the empty polymer is still in the high spin state ($pzPt^{HS}$).There was no reversibility of the phenomenon, this highlights the memory capacity associated to the host polymer. Indeed, the latter remembers in a way the spin state induced by the guest molecule. However, it is possible to cancel the information retention by cooling down the compound. The other point of interest is that the temperature corresponds to the room temperature since the hysteresis is centered on it.

However, if the CS_2 is adsorbed then desorbed on the same empty polymer, the memory effect is present, but the spin states are reversed for the whole processus. The polymer is initially in a high spin state ($pzPt^{HS}$), and then the metal centers enter in a low spin state once the CS_2 has been adsorbed ($pzPt^{LS}.CS_2$) and stay that way after its desorption ($pzPt^{LS}$).

At the same time, Kepert and his colleagues verified this phenomenon with a nickel and pyrazine polymer with acetonitrile being the molecule guest [61]. However, they

discovered new information: the desorption memory (see figure 4). Indeed, if the same absorption then desorption process is realised, it is the sorbed phase that keep the adsorbed state in memory. Once the guest molecule is adsorbed ($pzNi^{LS}$.Acn), then desorbed ($pzNi^{HS}$) and finally readsorbed ($pzNi^{HS}$.Acn), the polymer is the opposite spin state of the one having only adsorbed the guest molecule. It means that an absorption following a desorption does not lead to the same spin state that if there was only an absorption of the guest molecule. This double property allows to imagine the use of this kind of materials for solar captors. C'est-à-dire que l'adsorption consécutive d'une désorption ne mène pas au même état de spin que si il y a seulement eu adsorption de la molécule invité. Cette propriété double permet d'imaginer utiliser ce genre de matériaux dans le cadre de capteur moléculaire.

In order to determine the effect of the size of the guest molecules, Kepert and his group have used the same system as previously as a base: pzNi which presents little cavities and whose transition temperature is close to room temperature [61]. They used different common solvents as guest molecule. They established a correlation between the Tc observed and the volume of the guest molecules. In the majority of the cases, the more the guest molecules were voluminous, the more the Tc observed were little. It would in fact be an "internal pressure" effect, reflecting the fact that the bigger the molecules are, the more they induce high spin state. Nonetheless, the T delta associated to the spin transition could not be linked by any effect to the size of the molecule in the pores.

The same polymer, with platine centers (pzPt) has also been submitted to the introduction of molecules of more diverse nature in the structure this time [60]. It led to the observation of high spin states at room temperature. But after the absorption of the CS_2, the low spin state prevailed. Moreover, when the benzene is the guest molecule, whatever the temperature, it is only possible to observe the high spin state. It could mean that the transition may be impossible if the guest is of sufficient size and presents a steric hindering which disadvantages the polymer's contraction.

Some years later, Ruiz and his colleagues also studied the question [62]. It led to interesting observations. Indeed, the same material with a platinum base: pzPt has shown different SCO properties depending on the guest molecule. This made it possible to confirm the impact of large-sized guest molecules on the value of critical temperatures. In fact, for the guest molecules with increasing volume, in this case furane, pyridine, thiourea and benzene, the critical temperatures observed are decreasing and are inferior to the ones of the desorbed network. This confirms the idea that the high spin state is more stable for large-sized guest

molecules. The opposite tendency has not been observed for guest molecules of small volume, the two spin states would have energies in the same range. Since the volumes attributed to those compounds fluctuate depending on the calculation method used, it was decided to agree on a calculation [63] of volume of van der Waals described by A.Bondi in 1964 [64]. So that to take into account the atomic contributions and the bonds. This is done using this formula:

$$V_{vdW} = \Sigma \text{ all atom contributions} - 5.92N_B - 14.7R_A - 3.8R_{NA},\ N_B = N - 1 + R_A + R_{NA}$$

In which N_B is the number of figures, N is the total number of atoms, R_A and R_{NA} correspond respectively to the number of aromatic and non-aromatic cycles.

Nevertheless, it is important to precise that there are exceptions that do not abide to the effect of the size of the guest molecule previously observed. It is the case for acetonitrile or water in the previous example with nickel metal centers [61] or the CS_2 [60] and SO_2 [65] for the previous platinum compound. It tends to show that there are other factors involved, such as other effects or interactions. This last hypothesis has been made in the case of hydrogen bonds in the MOF having adsorbed water, preventing the rule from applying. In the case of acetonitrile, pi interactions between this molecule and the pyrazines would be responsible for the favouring of low spin states over high spin states. While in the case of CS_2 and SO_2, the S-Pt interactions are the cause of the modulation of the magnetic properties.

Influence of the shaping [66-78]

The shaping under thin MOF films in the scale of nanometres was an important concern to be able to imagine nanotechnology applications [66-70]. This is why in 2006, Molnar et al. Developed thin films made of pzM: a Three-dimensional MOF having SCO properties [71]. It was possible to obtain micro- and nano-patterned films through two methods: electro-beam lithography and the layer-by-layer method in the case of pzPt. This provided routes of creation for nano-devices, but also exploration ones in order to understand the connection between the size and magnetic properties [72].

Ten years ago, the influence of the guest molecule on thin SCO nano-patterned films of bpacPt has been investigated by Salmon et al. They noted favourable results for host-guest interactions as well as the spin crossover in those films. That's why MOFs in the form of thin films drew attention in the applicative domain of microsensors [73]. Later, the same compound shaped into micro-patterned grattings has been exploited in order to quantitatively determine the gas captation a gas [74]. This sensor has numerous positive points, such as a

good reversibility, hi slow detection limit (up to thirty ppm) and the process can happen at room temperature.

A bit later, Otsubo et al. observed a dynamic response from a structural point of view on thin nanometric films of pyPt, which is a two-dimensional MOF with SCO properties for little-sized guest molecules, such as acetone, water, methanol and ethanol [75]. Furthermore, when the compound is in the form of particles around of 135nm, no incorporation of guest molecules has been noted: the compound stay in closed form (see figure 5). Whereas there is a dynamic incorporation for little-sized guest molecules for the same compounds in thin film. Consequently, it appears that shaping the two-dimensional SCO coordination polymers is essential for detection applications. Beside that, other researchers tend to highlight the influence of the morphology and the nature of the host on SCO properties [76-78].

Other factors [60,62,79-83] (see figure 6)

Scientific literature approaches the effect of the polymer through the characteristics of the guest molecule, a point of view that is the opposite of the one seen above. In fact, we are discussing dielectric interactions. To understand this, we will take a look at the ε dielectric constants [79,80]. However, the interactions between the host and the guest are assumed to be reciprocated, the compounds should thus mutually affect each other.

Kepert and his colleagues have studied the impact of the solvent on the properties of a Hofmann type MOF with large cavities $[Fe(bpbd)_2(NCS)_2]$ and on the SCO properties [81]. To this end, five solvents with different dielectric constants (protic or aprotic) have been used. When the guest molecule having the weaker dielectric constants values have been adsorbed, the low spin state was observed. In fact, an empirical rule making the connection between the critical temperature and the dielectric constant has been established. The hypothesis is that there is a polarisation effect impacting the energy of the ligands fields, and thus the SCO properties.

However, Cortés and his collaborators [82] have noted an opposite rule for a another Hofmann type MOF having a different organic ligand. The guest molecules were also different and based on an aromatic cycle this time. It is difficult to determine the source of this opposite tendency. It is interesting to note that the effects linked to the dielectric constant on the critical temperature can be reduced or even hidden by other effects in the case of frameworks having cavities of small volume occupied by large-sized guest molecules. Indeed, the external pressure effect applied by the guest molecule takes over eventual effects caused

by the dielectric interactions. Accordingly, this effect can be neglected or at least does not require an in-depth study for materials with small pores. It is better to investigate it in the case of frameworks presenting large cavities and in which the guest molecules are small and not very limited in space.

The effects linked to the volume of guest molecules and to the electronic interactions are thus in competition. This has been particularly explored in a gold polymer with biphenylpyridine (bppAu) ligands [83]. Strong interactions with gold have been observed and tend to strengthen the stability of the framework. There are large pores in this material presenting a gradual spin transition at a critical temperature close to 150 K if there are no adsorbed molecules. When the protic solvents or cyclohexane fill those cavities, the width of the hysteresis is globally increased and the range of temperature associated to it is moving toward room temperature, except for the cyclohexane. The critical temperature's increasing would be connected to the interaction between the alcohol function of the guest molecules and the azote of the organic ligands used in the framework. When volume of van der Waal is large, the steric effect is obviously more significant. The guests molecules on which this effect is less impactful respect the tendency to have a higher critical temperature the more their dielectric constant is weak.

As a direct consequence of the introduction of organic ligands in the structure, the existence of π-π interactions with the aromatic guest molecules must be taken into account. This is a particularly important subject of study in supramolecular chemistry. Here, the goal is to find a causality regarding SCO properties and to understand which modulations are beneficial to the material. The impact of those interactions in a platinum and pyrazine polymer (pzPt) has been studied for the following aromatic molecules: benzene, thiourea, pyrrole, pyridine and furan [60,62]. In the case of thiourea, two Fe^{2+} sites having different distances with azote have been observed. It is then easy to imagine that it can have an impact on the symmetry of the frame and thus create local perturbations. Those two Fe^{2+} sites were initially in a high spin state, they saw their bond with azote shorten so that they were in an intermediate spin state at far lower temperature. They behave differently because of the asymmetry, which results in the sites having each a different critical temperature. With pyrrole and furan, there exists only one type of Fe^{2+} site. However, the π-π interactions with the guest molecules seem to create perturbations that are at the source of the varying nature of the iron sites and thus of a transition spin by steps. It would then be possible to optimise the

nature of the transition through π-π interactions for a framework having large cavities in order to reduce the steric effect.

The value of our research in the MOFs applications domain [84-124]

We can highlight the interest of this research by emphasizing the major advantages of the MOFs, that is to say the adaptability and the malleability associated to their structures, compositions and porosities, among others. The fact that their conception can be relatively easily modulated allows to conceive a lot applications answering diverse and varied needs. We have in mind the exploitation of the cavities in those materials which can be used in gas storage [84-91] or even in the molecular separation process [92-98] in which they would be considered as selective adsorbents. As a matter of fact, the structure of the polymer offers large surfaces which are interesting to maximize the contact and thus the adsorption. The adaptability is another interesting factor because it allows to select the volume of the pores, hence to control the associated characteristics. Other technologies could be developed based on specific properties such as magnetism [99-102], chirality [103,104], conductivity [105,106], catalytic activity [107-112] or luminescence [113-118], by example. The idea is to modulate the different constitutive elements of those MOFs or guest molecules in order to obtain the desired properties. As a result of those characteristics, we can picture using those materials for detection [116-118], catalysis [107-112] and energy storage [119-124], among other things.

More generally, Hofmann type MOFs are considered very attractive in the context of applications related to detection, thereby as chemical captors. In fact, they present several advantages such as: the possible modulation of the transition spin temperatures, allowing them to be brought to room temperature; the influence of the guest molecules on the magnetic properties which supports the adaptability of these properties; the cooperativity associated with SCO is common and there are shapes that allow to keep the bistability; the choice of the bridging ligands and cyanometallate units influences the properties associated to the materials. In scientific literature, few connections have been made regarding the interactions between the material, the guest molecule and the properties associated to the spin transition. On a conceptual level, some factors should be involved: the structure and composition of the polymer, the size of the cavities created and in parallel the shape and size of the molecule inserting itself as well as its functions, and thus the type of interaction with the material and the strength associated with it. There are seemingly numerous factors being able to influence the properties. Some of them will be discussed hereafter.

For our part, our main ambitious is to develop MOFs that may present spin crossover properties. The point of this phenomenon is the possibility to induce the change between the spin states following an external perturbation which we could control. What makes this phenomenon attractive is the bistability of the molecules and the fact that this property is controllable. In our case, it mainly concerns variations of the temperature or pressure, of the light exposition or even of the guest molecule. Research in this domain focuses on d^4-d^7 transition metals, consequently to the « crystal field theory » and in particular on the first period of those metals. Among those, we can note the iron, which will be at the core of our research. It is also good to precise that the geometry of the complexes based on those metals is octahedral and the metal centers are coordinated six times. Iron has been extensively studied in this domain, we can mention the $[Fe(phen)_2(NCS)_2]$ or even the $[Fe(btr)_2(NCS)_2]\cdot H_2O$ complexes.

Spin transitions are usually brings significant physical changes that can be detected. In particular, we think about the colour changes which can be useful as a detection tool. Another identification tool is the structure of the compound. Indeed, structural changes are noticeable between two spin states. The polarisation is also simultaneous to this phenomenon.

Methodology

As previously mentioned, we followed a simple method, but one that has already proved to be successful in the context of the investigations led by our colleague Li Sun. Since it is easy to put into use, this technic was a particularly attractive choice. Of course, it did not lead to results for each and every compound, be it in the previous works or during our project. Therefore, we should not consider the production or the absence of crystals as an absolute truth. In fact, it is important to call into question the method in its capability to crystallize or the experimental conditions. It is essential to not overlook the existence of some coordination polymers following the results here presented. Most of the compounds are accessible via synthesis routes which can involve conditions that are more or less restrictive and easy to put into effect.

The idea here was to synthesise crystals in a restricted volume system by involving small quantities of reagents and solvents. The tube is filled gradually by three solutions prepared beforehand. Two solvents are used during the operations. They were chosen to be miscible, but of different densities. Solvents of very different densities were favoured when possible. Indeed, the density factor is essential to the diffusion principle. Nevertheless, it will

be possible to note that 1 : 1 type intermediate ratios are not necessarily the more favourable to crystallization. Regarding the composition of those solutions, they are partly determined by the compound to dissolve, meaning that the solvent is chosen according to its capability to dissolve partially or entirely the reagents. Since our goal is to crystallize, it is also critical that the mix resulting from the solvents does not dissolve crystals of the compounds of interest. This would oppose the crystallisation and would prevent us from observing crystals that could be formed.

The solution at the bottom of the tube is made from the most dense solvent and the desired quantity of ligand in our case, before being distributed in the tubes. The intermediate solution is in fact a mix of two solvents with a ratio going from 1 : 5 to 5 : 1, depending on the desired composition of the buffer. More generally, the five solutions were made and distributed then, in the case of a crystallisation, the buffer giving the best crystals was chosen. Considering the nature of the process, it was necessary to be very careful during the addition of the solutions in the tubes. For this reason, the use of a syringe was recommended as well as a slow flowing on the tube wall. Finally, the last solution was made from a Fe(II) compound, a linker with cyanide ends and ascorbic acid (see figure 7). The ascorbic acid stops the oxidation of the Fe^{2+} into Fe^{3+}.

The buffer's presence favours a slow contacting of the two solutions and consequently the crystallisation. In fact, we use the reaction kinetics through this method. A quick contact of the solutions and thus of the reagents leads to a precipitation in the form of powder, not to crystals. If we try to put the reagents together in a single reaction medium, the precipitation will be instantaneous. The same scenario happens we do not use a buffer, even if density can be used to obtain a slower mix, it will not be slow enough to allow the crystallization. However, the diffusion only favours the crystallisation in the case of an efficient reaction happening. It can happen that the contacting in a reactional medium does not produce any precipitate and then the method here presented would lead to a similar result.

Several factors seem to influence the crystallisation and its quality. Amongst those: the width of the tubes. As a matter of fact, the width of the tube is an important factor since it impacts the contacting of the solutions and species. When the contacting surface between the solutions is reduced, it seems logical that less species meet at the interface. In addition, a there is kinetic factor since for the same volume of solutions introduced in tubes of different width, the layers height is also impacted. The result is that a shorter and larger test tube, species will encounter quicker than in a higher and thinner test tube. This is the reason why during the

experiments we began by using larger tubes before using the thinner ones. There is practical interest to using the least effective approach first. Indeed, there are two main arguments justifying this approach. On one hand the time and on the other hand the ease of use. De facto, time is a key element in a scientific research. Since we could not afford a crystallisation taking weeks, using larger tubes was a good alternative. Thanks to this approach, we were getting results, positive or negative, in a few days. If we got powder then we moved to thin test tubes and noted or not the presence of crystals. In the case we obtained crystals in larger tubes, if the quality of those were sufficient we determined the composition of the buffer leading to optimal crystals and repeated the experiment in order to collect them for deeper analyses. Besides, our colleague, Li Sun, had previously established through similar experiments that some crystals can only be obtained by using thinner tubes, confirming those hypotheses.

Another factor that influences the crystallisation is the solubility of the initial reagents in the solvents. It has an impact via the solvents available at the dissolution, and consequently the corresponding densities of those solvents. Since, as precised previously, a great disparity in densities is better between the two solvents in order to favour the crystallisation. Further, you will be able to notice that we encountered difficulties to dissolve one of the organic ligands and that it led to resounding failures while using this method. Nevertheless, it was possible to synthesise a few crystals of unique composition by an alternative method taken from literature, but in which the compound was only partially solubilized.

Finally, a last factor was considered: the concentration in reagents of the solutions. In this case, it contains two sub-points. First of all, since the three-dimensional structure had to be established, it is necessary to add sufficient but most of all stoichiometric quantities to the expected final result. Depending on the nature of the cyanide compound introduced to link the metal centres, one or two equivalents of the Fe(II) compound were needed. Indeed, in the case of a compounds presenting two nitrogen atoms at its ends, thus bridging, such as the sodium dicyanamide, we could not have more of this compound than we had Fe(II) centres. On the contrary, when the compounds with a single cyanide end was introduced, it was in double the equivalent of the Fe(II) compound to which it had to bind itself. It is notably the case for $NaBH_3CN$, KSeCN, KSCN or NH_4SCN.

The use of the term “ligand”

Over the course of this project, we used the term “ligand” for the organic molecules acting as pillars in the MOFs as well as for the molecule with cyanide groups, associated as

well to the iron atoms. However, it would be more correct to use the term “coligand” regarding organic molecules called L_n (n depends on the reagent) and the molecules with cyanide groups. It is kind of an abuse of language to define both types of molecules by the term “ligand”.

One of the objectives of this project was to study the effect of the coligand on material properties. In the same way, it is here a matter of the influence of the choice of the L_n organic molecule as well as of the influence of the choice of the cyanide molecule. Even if at first sight the second part of the research is less approachable, as you will notice further.

Characterisation

Once the crystallisation conditions have been established and the crystals quantity is sufficient. The experiments are repeated for around thirty tubes and fresh crystals are synthesised to be analysed. Since we are searching for transition spin properties on materials, a lot of methods can be used, be it magnetic or optic measures, the Mössbauer, vibrational spectroscopy, etc. In fact, the spin crossover comes with a numerous changes of the physical properties of the compounds. We can notably mention changes in terms structural, magnetic, electric, optic, elastic and vibrational properties.

We wanted to follow the following analyses pattern:

1. Single-crystal X-ray diffraction
2. X-ray diffraction analysis
3. Fourier transform infrared spectroscopy
4. Thermogravimétric analysis
5. Elemental analysis
6. Superconducting quantum interference device
7. Mössbauer spectroscopy
8. Differential scaning calorimetry

Complementary analyses such as DFT, UV-vis-DRS, analyses of optic properties, DES or spectroscopy Raman are also possible.

Relevant analysis methods to study the properties associated to the compounds

This part of the thesis will aim to establish an analysis pattern through known and relevant technics regarding the compounds. We will attempt to set up the plan of the

necessary and complementary analyses in order to determine with precision the different characteristics of the synthesised compounds.

However, this also partially aims to do an in-depth study. Indeed, a part of the technics was used during this project while the other part will be set up in the future with the purpose of studying those compounds the more accurately possible. In fact, we choose to focus our efforts on the formation of the crystals of different compounds. Furthermore, some compounds have shown a weak stability, which led to major challenges during the analyses. This is the reason there are few data related to a part of this work. Since there is a strong time constraint, we will try to offer solutions to those problems. However, this will be purely theoretical. The use of those alternatives could end in failure, thus taking us back to the starting point and to the search of new conditions of formation and study of those compounds.

In this section, you will be able to catch a glimpse of the relative contributions of these technics to the characterisation of the obtained compounds. This revising of the basics will be non-exhaustive and will allow for a better comprehension of the expected results and of the associated interpretation.

Single-crystal X-ray Diffraction.

Contribution to the characterisation of the compound

This method mainly informs us on the crystal structure and on the disorder associated with the compound. When it is possible, an analysis is done at room temperature and 100 K to note eventual changes to the unit cell. The formula can be deduced from the analysis along with the presence of solvents or counterions. This information will be particularly interesting in the context of the study of coordination compounds. In particular to establish a possible effect of the solvent on the material properties. As a matter of fact, if we compare a solvated material to a partially or entirely desolvated material and some properties change, it can then be attributed to the solvation. It would be easy to verify the characteristics of those compounds via a “single-crystal” analysis and to note changes related to variation in the unit cell. We would also be able to deduce the spatial group associated to the compound. Indeed, a drastic change linked to the measure conditions (the temperature) would show variable properties and thus a behaviour to comprehend, explain or even exploit. It is also possible to highlight an ordinary symmetry. This method would allow to know the different parameters of the unit cell, such as its dimensions (through a, b, c), its angles (through α,β,γ), the volume. We can also get information on the distance between the metals centres and other atoms. From there, we can deduce the spin state of those metal centres. (for atoms capable of

presenting different spin states). In fact, in the case of iron, the distances between the iron atom and the ligand are characteristics of a high or low spin state. There of around 2,2 Å in high spin and around 2 Å in low spin. Therefore, the determination of the spin state of the metal atoms is done, among other things, through the determination of this distance.

This method allows to identify new compounds based on their structure. Any structure unknown to the date base can be considered as new and added to it. It offers the possibility to have a better understanding of the existing coordination and of the interactions between non-coordinated molecules (counter anions or solvent) in a material. Under certain conditions, high pressure or thermal phase structures can be known. More generally, since the spin transition is accompanied by more or less significant variation of the compound's properties, it would be in our interest to compare the different mentioned parameters at different temperatures.

X-ray diffraction analysis (XRD)

Contribution to the characterisation of the compound

Generally, this method is used in the investigations of unknown crystal compounds in order to identify them. It is also a characterisation tool appreciated in the domain of crystal compounds research. It is also possible to deduce information regarding the purity of the sample from it.

More globally, this method shows benefits in terms of time and efficiency of the analysis. It does not need a lot of preparation of the sample and gives data which can be interpreted easily when the necessary precautions have been respected. However, it needs to have a sufficient quantity (tens of milligrams) of the sample and that there is only one phase of the compound, homogenous and pure. Comparing the obtained results to the ones from the reference files would be ideal. But this is not always possible in the context of the study.

This technic can be interesting to compare easily and quickly different samples of a same compounds having been subject to diverse conditions (temperature, solvent, time, etc.).

Fourier Transform Infrared Spectroscopy (FTIR)

Contribution to the characterisation of the compound

The FTIR allows to identify a chemical compounds by identifying functional groups and chemical bonds in a molecule on the basis of an infrared absorption spectrum. Each spectrum is specific to a chemical compound, meaning that the spectrum's profile is specific to it. It acts as a fingerprint. The studied samples produce a spectrum that is analysed and compared in order to attempt to define the present functional groups and the nature of the

bonds involved. It has its origin in the fact that a majority of molecules absorbs infrared light. It is generally used to identify the groups or the organic compounds. It is possible to exploit this method from a quantitative point of view. Nevertheless, it is mainly used qualitatively, in detection.

In addition, it presents some logistical advantages such as the non-destruction of the sample, the speed of the measurement and the increased sensibility and precision. There are reference tables that allow to attribute peaks to the bond and the vibrational mode according to the number of waves associated to it and the shape of the peak.

As its counterpart in vibrational spectrometry (FT-Raman), the ST-IR spectroscopy is also an excellent technic in the context of the study about transition spin compounds. Indeed, vibration bands corresponding to Fe-L are discovered. They are shifted toward inferior wave number values or even disappear during the transition from the low spin state to the high spin state [138,139]. This is why those technics are particularly indicative of a spin state change and thus of a transition. Consequently, they have to be integrated to the analysis plan.

Furthermore, the use of types NCX^- (X = S, Se, etc.) ligands results in specific stretching bands of cyanide around 2200-2100 cm^{-1}. It was noted that the spin transition (high spin into low spin) results in a shift towards higher frequency [2].

Thermogravimetric Analysis (TGA)

Contribution to the characterisation of the compound

The TGA is a complementary analysis giving information about the loss of mass in the sample relatively to the temperature. Since the sample is subject to a constant heating level, it is important to choose it accordingly to the information we want to get, but even more importantly to the necessary precision. The TGA can be done in special atmosphere, obviously this impacts its result since it can be oxidizing, inert or reactive. This can lead to particular mass variations of the sample. Consequently, it must be chosen adequately in an effort to measure the mass changes attributed only to the loss of components.

There are therefore numerous factors influencing the loss or gain of mass of the sample. Among those, there are: the oxidizing of the metals or the oxidative decomposition of some organic compounds under oxygen or air; the thermal decomposition and the formation of gas under inert conditions; the water losses by crystallization; the drying; the evaporation of volatile solvents; the adsorption or desorption of gas; the heterogeneous chemical reactions induced by the atmosphere such as condensation or decarboxylation, etc. Moreover, it is good

to remember that the properties of some types of compounds evolve with temperature. Notably the ferromagnetic materials, which become paramagnetic once the Curie temperature is reached. A signal can thus be created in TGA if the measure is realized under a non-homogeneous magnetic field. There are a lot of possible sources behind each peak, and thus a lot of factors to verify to achieve a determination of the phenomenon associated to the mass variation. There is also the possibility to understand some changes of properties by highlighting particular phenomenon in TGA. Phenomenon of physical and chemical natures can be demonstrated.

Elemental Analysis

Contribution to the characterisation of the compound

This method can inform qualitatively and quantitatively on the elemental composition and even the isotopic composition. Through the studying of those results, we will try to establish the proportion of each element in the sample. From, there, i twill be possible to deduce a chemical formula. This method allows us to assert or invalidate that the sample is the product of interest and also to evaluate the purity associated. It is a more general term that is often assimilated to the CHNX analysis in organic chemistry and highlights mass fractions in carbon, hydrogen, nitrogen and heteroatoms: very often halogens or Sulphur. It is generally used to characterise unknown compounds.

In our study, we can also confirm the presence of solvent in the studied compound as well as highlight an eventual "contamination" due to the reagents or the solvent by example.

Superconducting Quantum Interference Device (SQUID)

Contribution to the characterisation of the compound

The SQUID analysis enables a sensible measure of the magnetic fields. A lot of information regarding the magnetic properties and thus a spin transition can be deduced from this analysis. The $\chi_M T$ spectrum based on the temperature shows the evolution of the magnetic susceptibility according to this parameter. It is thus possible to deduce the spin state from it, as well as the transition's profile (gradual or sharp, complete or incomplete) if there is one. More specifically, it is possible to determine the magnetic susceptibilities at the low and high spin states. It should be null or close to null at the low spin state and around 3-3.5 at the high spin state of the Fe^{2+}. In fact, the high (S=2, $t_{2g}^4 e_g^2$) and low spin (S=0, $t_{2g}^6 e_g^0$) states present very different magnetic characteristics: The first being strongly paramagnetic while the second is diamagnetic. It is also possible to define the molecular fractions of each spin state associated to any temperature. As well as information regarding the transition

temperature ($T_{1/2}$ or T_c depending on the profile), enthalpy and entropy variations attributed to them, the spin state of the material at room temperature and the molecular fractions (of the spin states) present.

Mössbauer Spectroscopy

Contribution to the characterisation of the compound

In our case, it gives information on the local environment of the iron atom. This method presents a very strong sensibility and an outstanding energy resolution. This analysis generates numerous data through the study of the hyperfine structure of the energy levels of the atomic core. It is also possible to observe the perturbations which can be generated by the electric, chemical and magnetic environment of the atom, the oxidation stage, the ligands,… Even if the induced energetic variations are very weak, they can perceived thanks to the excellent resolution of the Mössbauer. The main information that we can take from it are the ones we take from the so-called hyperfine interactions, that is to say: the isometric movement δ, the ΔE_Q quadrupolar pairing and the hyperfine structure.

The isometric movement δ (mm/s) are reflected into a movement of the spectrum in relation to the speed corresponding to 0 mm/s. It is good to known that the isometric movements of the Fe^{3+} are inferior to the ones of the Fe^{2+} ions, as a consequence of the better screening induced by the additional electron, the charge density is, for its part, decreased. This parameter represents the plating effect existing for the d electrons (in other word the electrons involved in the coordination bond in a complex) towards s electrons (which are directly affected by the charge of the nucleus). Its value gives relative indications regarding the oxidation stage and the associated state of the metal-ligand bond.

The quadrupolare pairing represents the fact that the quadrupolare moment of the core and the gradient of the electric field interact together, which induces the addition of an energetic term. This can lead to the loss of the degeneracy of the energetic levels of the core when in presence of an asymmetric electric field. It is reflected by a doublet in the Mössbauer spectrum. This is the ΔE_Q (mm/s) quadrupolare splitting. The value of the quadrupolare splitting can be taken from the spectrum by measuring the distance between the two peaks composing the quadrupolare doublet. Its value gives information concerning the electronic configuration of the Fe(II) ion, the spatial distribution of the ligands, its charge and allocation as well as information about the reactivity (acceptor or donnor) associated to the ligands.

Finally, the Zeeman effect is attributed to the fact that, under the influence of a surrounding magnetic field, there is a loss of the degeneracy of the electric levels of the core. By following the selection rules, a transition can be done from the fundamental state towards an excited state where the spin is increased. In addition, for a core which has a S spin, there are 2S+1 energetic sub-levels. As a result, a certain number of peaks are observed by Mössbauer according to the number of possible transitions.

It is possible to identify a compound on the basis of those parameters by comparing it to a data base. However, most of the time, this is not the desired goal. We can also interpret the intensity of the peaks in a semi-quantitative manner by extrapolating the relative concentrations into species contained in the sample.

In general, the Mössbauer spectrometry gives information regarding the nature of the iron atom's bonds and highlights the spin states for a range of temperature. In this continuity, it is possible to determine or confirm the transition spin temperature by observing the fractions of high and low spin states present depending on the temperatures. As previously mentioned, the two spin states of Fe(II) present different electronic distribution properties, strength and bond length. Following those basics, it appears that the Mössbauer spectrums fluctuate depending on if there is a low spin state, a high spin one or both states in variable proportions. One of the main indicators is the number of peaks and the ΔE_Q value associated. In fact, in the low spin state, a singlet or even a quadrupolare doublet of low splitting is observed. Whereas in the high spin state, a quadrupolare doublet of much higher ΔE_Q is noted.

Differential Scanning Calorimetry (DSC)

Contribution to the characterisation of the compound

Thanks to this method, particular phenomenon can be shown such as the crystallisation, the fusion or glass transition. Another interesting aspect of this method is the possibility of deducing the enthalpies and the transition temperatures, and thus being able to build the phase diagram. More generally, depending if the peak is positive or negative we can determine if the phenomenon associated is exothermal or endothermal and by deduction try to explain it. Furthermore, the enthalpies that are specific to those peaks act as an indicator of the type of phenomenon according to the energy released or consumed. This energy can be attributed to changes of chemical or physical nature. However, the heating level is a key element to obtain a good quality spectrum and thus an analysis leading to precise results. It is

also possible to extract form them information regarding the stability and the thermal degradation of the compound.

In the context of the study of spin crossover compounds, this technic is useful to determine the data of the thermodynamic enthalpy and entropy variations associated to the spin transition and therefore to the transition temperature. On its own, it does not necessarily provide the temperature attributed to this phenomenon and is very often done along with other complementary analyses. It fact, it also depends on the complexity of the spectrum thus obtained and of the different effects that can complicate the analysis.

Optical Measurements

Contribution to the characterisation of the compound

Previously, we mentioned that each spin state presented a particular electronic distribution in the d-orbitals. In fact, there are d-d transitions that are specific to each spin state and that can be noticed through the recording of the absorption spectrum via UV-visble spectroscopy. In a similar way, it is also possible to realise a diffuse reflectance spectroscopy (DRS).

If the high spin state is present, only one band close to the infrared range noted and corresponds to the transition $^5T_2 \rightarrow {}^5E$ (see figure 31(2)). On the opposite, if the low spin state is observed, you will be able to see two bands. The first is visible ($^1A_1 \rightarrow {}^1T_1$) and the second one in the UV ($^1A_1 \rightarrow {}^1T_2$). It should however be noted that the latter is not necessarily observed, it depends on the presence or absence of a transfer between the metal ion and the ligands.

In the case of a spin transition which may be thermoinduced, the thermochromism phenomenon, meaning the colour changes of the compound with temperature, is interesting. As previously specified, this is one of the properties affected by the spin transition. Consequently, the observation of crystals at different temperatures allows to easily see the tradition and the colouration of the compounds in the two spin states are an obvious indication of the spin state present. It can also be useful in applications directly linked to this phenomenon.

Experimental Part

Reagents Table

Reagents: name	Formula	Molar mass (g/mol)	Aspect
4,4'-Di(4-pyridyl)biphenyl	$C_{22}H_{16}N_2$	308.38	Off-white solid
1,2-di(4-pyridyl)ethylène	$C_{12}H_{10}N_2$	182.22	White crystals
Iron(II) Perchlorate Hexahydrate	$[Fe(ClO_4)_2.6H_2O]$	362.84	Light green crystals
Iron(II) tetrafluoroborate hexahydrate	$[Fe(BF_4)_2.6H_2O]$	337.55	Light green crystals
Sodium dicyanamide	$NaN(CN)_2$	89.03	White solid
Potassium thiocyanate	KSCN	97.18	White crystals
Potassium selenocyanate	KSeCN	144.08	White solid
Sodium cyanoborohydride	$NaBH_3CN$	62.84	White solid

Here, we did not specify the purity of those compounds since we did not take them into account during the experiments. As a matter of fact, the exactness of the masses was not necessary because of the nature of the reaction process and the desire to determine the possibility or not to crystallise the faux polymers. Moreover, the purity ranged from 97 to 99% depending on the compound.

Regarding the solvents, we mainly used chloroform or dichloromethane for the solution at the bottom of the tube and methanol for the one at the top. However, you will notice that some solvents were later used in the case of the solutions of L_4 ligand: 4,4,'-Di(4-pyridyl)biphenyl to make an attempt at dissolving it.

Realisation of the Experiments

In the methodology of this work, we explained the global approach used initially. In this part, we will first go into details by explaining the process of the first experiment. We will then detail the quantities of compounds and solvents, as well as some points that can change for the other experiments since the procedure is the same.

As you previously noticed, we have studied the synthesis by a method of crystals based on two ligands with pyridine ends (L_4 et L_5), two compounds of Fe(II) ($[Fe(ClO_4)_2.6H_2O]$ and $[Fe(BF_4)_2.6H_2O]$), and finally four compounds with cyanide groups (Nadca, KSCN, KSeCN and $NaBH_3CN$). According to this, there are in total eight synthesis

plans to follow (four for each ligands). Indeed, we have considered that the synthesis plans were identical for the two Fe(II) compounds.

First Plan : L_5 , Nadca

Frist, we will discuss the first plan of the L_5 since few modifications have been done. In fact, putting the first plan into practice was particularly simple for this ligand.

First of all, we take two containers of 10 mL and in each of them we put a small-sized magnetic agitator. We also take five vials of 4 mL which will contain the buffers of different ratios. Using plastic pipettes, we begin by introducing 5mL of the solvent 1 (the densest, here the chloroform) in the first containers and 5mL of the solvent 2 (the least dense, here the methanol) in the second container. We place a parafilm on top those solutions to limit the loss of solvent. In the solvent 2, we introduce a spatula tip of ascorbic acid and place the whole on a stir plate in order to homogenise the solution. Then, we measure to necessary quantity of ligand and we introduce it in the solution 1, the solution is put to be agitated. In the same way, we quickly measure the cyanide compound (here Nadca) and the Fe(II) compound and we introduce them into the solution 2 and we homogenise it. The quickness of the measurement and incorporation aims at limiting the oxidation of the Fe(II) into Fe(III). While the solutions are being agitated, we introduce, with a syringe of 1mL, precise quantities of solvent 1 and 2 in each vial so that to obtain five buffers of different compositions. More precisely, the volumes of solvent 1 respectively introduced are: 0.2 mL, 0.4 mL, 0.6 mL, 0.8 mL and 1 mL; We introduce the same volumes of solvent 2, but in the opposite order so that the total volume is always of 1.2 mL. It corresponds to ration ranged from 1 : 5 to 5 : 1 in a volume point of view. Finally, we introduce the densest solution, meaning the one of the ligand at the bottom with a volume of 0.8 mL in five test tubes of a width of 3 mL. We then homogenise the buffers individually with a syringe by repeated pipetting before introducing respectively 0.8 mL of them with delicacy by emptying slowly the syringe on the tube wall. Finally, 0.8 mL of the Fe(II) solution are also introduced in the same way in each tube. Besides, traits corresponding to the frontiers can be drawn to keep a reference and note the place where the compounds are appearing in the tube. Lastly, the openings of the tubes are hermetically closed with a parafilm in order to not interfere with the interfaces and risk a mixing of the solvents. The impermeability is essential so that to avoid a solvent loss. Moreover, the mixing of the solutions would lead to a quick pooling of the reagents and thus to the apparition of powder. The tubes are finally placed in the crystallisation room and daily observed to note the evolution of the synthesis.

In order to establish the nuances between the different plans, we will characterise them each by a table similar to the one hereafter:

			Solution 1	Buffer	Solution 2
Solvent			$CHCl_3$	$CHCl_3$: MeOH	MeOH
Volume (mL)			5	0,2 : 1 to 1 : 0,2	5
n (mmol)	L_5		0,1	/	/
	Nadca		/	/	0,1
	Fe(II)		/	/	0,1
m (mg)	L_5		18,2	/	/
	Nadca		/	/	8,9
	Fe(II)	$[Fe(ClO_4)_2.6H_2O]$	/	/	36,3
		$[Fe(BF_4)_2.6H_2O]$	/	/	33,8
$V_{solution/tube\ large}$ (mL)			0,8	0,8	0,8

Table 1. Table showing the theoretical quantities and volumes for plan 1

In this case, it was not necessary to repeat the experiment in thin tubes which would have produced the same table, but where volume of solution per tube would have been decreased. In fact, since the thin tubes are of smaller volume, it is not necessary to adapt the concentration in thin tubes at first, because the physical separation induced by the buffer is then greater for a similar volume. In addition, if powder is still forming, we begin by decreasing the volumes of the solutions 1 and 2 and/or by increasing the one of the induced buffer (up to 1.2 mL) in order to note if the reaction results in crystals. On the contrary, if no reactions happen after a few days (no powder, nor crystals), then we try to decrease the quantity of buffer or to increase the concentrations in solution 1 and 2. It always failed, probably due to a mistake in the choice of solvent. Indeed, we have noted by experimentation that the concentration does not have the same impact on the process of crystallisation than the reaction kinetics. Over the course of the different plans, we have tried decreasing the concentration down to a factor 10 when the crystallisation was not effective, without success.

Regarding the Fe(II) compounds, we have consistently tested the two compositions since colleague, Li Sun, had previously observed that some crystals could be obtained with only one of them.

In this case, we obtained bright red crystals after a day. Those crystals revealed to be of better quality for the 5 : 1 ratio in $CHCl_3$: MeOH by observation. This is the reason we repeated this composition to produce enough samples for the experiments. In addition, even if red crystals gathered on the tube's edge, there was also a white powder at the bottom.

Those crystals were tested in liquid nitrogen in order to observe a potential spin transition through a colour change. As a matter of fact, that was the case; the red crystals became very dark if not black in a spectacular way (see pictures 1 and 2). However, it is important to point out that this effect tends to disappear after a few minutes. De facto, we hypothesise that the solvent escapes from the unit cell, causing the properties to disappear. It would thus an effect to study more in-depth.

Furthermore, it should be noted that those crystals are relatively stable since once they have been collected and accumulated in a vial containing a mix of the two solvents, they keep their crystallinity for a few days. Nevertheless, this can cause trouble when some exams must be done in external labs. In order to collect the crystals, we used two containers topped by a folded paper filter. We realised a solution of the same nature than the buffer and introduced some of it in a vial. We have used two pipettes, one to draw from the bottom the white residues that constitute an impurity and must not be in our sample. We evacuated this waste in a first paper filter. Once it has been entirely removed, we scratch the tube edge with the second pipette and we collect the crystals, then we place them on the second paper filter. When the solution has gone through this paper, we humidify the crystals with the buffer solution and transfer hem in the vial. Finally, when all the crystals have been collected, we draw a maximum of the vial's solution to replace it by the clean buffer.

Later, those crystals will be called LS6.

Second Plan : L_5, KSCN

			Solution 1	**Buffer**	**Solution 2**
Solvent			$CHCl_3$	$CHCl_3$: MeOH	MeOH
Volume (mL)			5	0,2 : 1 to 1 : 0,2	5
n (mmol)	L_5		0,05	/	/
	KSCN		/	/	0,1
	Fe(II)		/	/	0,05
m (mg)	L_5		9,1	/	/
	KSCN		/	/	9,7
	Fe(II)	$[Fe(ClO_4)_2.6H_2O]$	/	/	18,1
		$[Fe(BF_4)_2.6H_2O]$	/	/	16,9
$V_{solution/tube}$ (mL)			0,8	0,8	0,8

Table 2. Table showing the theoretical quantities and volumes for plan 2

It is essential to understand that the synthetic routes have really been realised in that order. Indeed, we first spend a great part of our time trying to react the L_4 ligand, as you will

see further. This has not been very successful and sometimes prevented an in-depth analysis of the crystals obtained for the L_5 ligand.

In this case as well, we obtained dark red crystals (see picture 3) and a white precipitate at the bottom. The 1 : 5 methanol composition: chloroform has been chosen based on the observation of the crystals. Once repeated for a few tens of tubes, we collected the crystals while being cautious to separate them from the precipitate. However, it would seem that crystals are quite unstable since they become powder in a matter of hours. This gave us some trouble. Indeed, when we wanted to analyse the crystals by single-crystal X-ray diffraction, they were not stable enough for the period of time necessary to the collect then the consecutive analysis. Given the instability previously observed at room temperature, we decided to analyse them at low temperature. But the problem was elsewhere. In fact, the disintegration of the crystals in crystallites of inferior size is done in a few seconds. This would lead to negative consequences on the measurement since almost no efficient diffraction has been obtained. We tried to prevent this phenomenon by taking numerous measures, such as: putting mineral oil or paraton on the crystals, their transfer towards THF, the use of polymer to cover them. Nonetheless, none of those precautions has enabled an in-depth analysis of the crystal structure since they were not sufficient to conserve the crystals. As you will have understood, the unstable nature of the compound has been a set-back to their characterisation. This is why have few information regarding the structure and composition. We have thus mainly based the analysis on the empirical observations made during the experiment's process. Besides, the stability of this compound will be studied later, in the discussion part.

We decided to realise a similar composition with $FeCl_2$ and also similar compositions based on NH_4SCN with the same Fe(II) compounds than previously (see picture 4). Several interesting phenomenon have been noted. Firstly, when using $FeCl_2$, little or no powder has been observed at the bottom of the tube in comparison to the other Fe(II) compounds. This confirms that the precipitate is directly linked to the choice of the Fe(II) compound and the counterion associated to it. Moreover, when the NH_4SCN (buffer 1 :2 methanol : chloroform) was used, the precipitate at the bottom of the tube was not white, but yellow/khaki. Again, this confirms an already established hypothesis. However, it should be noted that NH_4SCN is a compound of yellow colour. Consequently, it is possible that the precipitate at the bottom of the tube is white, but coloured by impurities or residues of the reagent. Thus, it may not be

non-reacted NH_4SCN, but the same compound than initially that has had its colour altered by the presence of NH_4SCN.

We also observed orange crystals at the top of the tube, thus higher than what we previously noted. In fact, we often observed the final crystals in the part initially corresponding to the buffer. In addition, when we started to collect those crystals, they seemed to have deliquescence in air (see picture 4). Indeed, they seemed to surround themselves with liquid and became redder. This a bit surprising and led us to make some hypotheses. On one hand, it could indeed be a deliquescence in air and the Fe(II) compound would then oxidise which would explain its colour change. In addition, it could then be the $FeCl_2$ compound and not a compound of interest. On the other hand, it could be the result of a very low stability in air, and thus a decomposition of the crystal. However, it would seem that, again, it was not the compound of interest, but another Fe(II) compound since were able to collect the final crystals present at the middle of the tube without any degradation due to the air contact. Finally, we could also consider a particular phenomenon of solvent escaping in favour of water molecules present in the air. But it would seem quite surprising that the crystals were the same of those of interest since there would be heterogeneity in their behaviours.

Additionally, the synthesis using $FeCl_2$ led to another observation. In fact, the parafilm closing the tube was generally partially marked by red colour and was not dry. Since, in theory, there was no contact with the solutions, we made the hypothesis of a diffusion of the superior solution through gas. This would lead to an potential red residue attributed to the Fe(II) compound used in this superior solution. Furthermore, if the parafilm is removed a few minutes in order to collect the crystals, sometimes a thick red liquid covers the top of the tube. At first sight, it seems to be an oxidising of the Fe^{2+} into Fe^{3+} in air.

We realised an analysis by XRD powder of the compounds based on $Fe(BF_4)_2.6H_2O$ and $FeCl_2$, unfortunately the data obtained was unusable for one of the two samples. This prevented thus from if comparing their spectrums and thus to determine of the compounds were similar.

Third Plan : L_5 , KSeCN

	Solution 1	**Buffer**	**Solution 2**
Solvent	$CHCl_3$	$CHCl_3$: MeOH	MeOH
Volume (mL)	5	0,2 : 1 to 1 : 0,2	5

n (mmol)	L_5		0,1	/	/
	KSeCN		/	/	0,2
	Fe(II)		/	/	0,1
m (mg)	L_5		18,2	/	/
	KSeCN		/	/	29,0
	Fe(II)	$[Fe(ClO_4)_2.6H_2O]$	/	/	36,3
		$[Fe(BF_4)_2.6H_2O]$	/	/	33,8
$V_{solution/tube}$ (mL)			0,8	0,8	0,8

Table 3. Table showing the theorical quantities and volumes for plan 3

This time, we repeated the same method than before, except for the fact that we changed the cyanide ligand (KSeCN here). Nonetheless, it did not led to any results. We later tried the experiment again but with thin tubes, without success.

Fourth Plan : L_5, $NaBH_3CN$

			Solution 1	**Buffer**	**Solution 2**
Solvent			$CHCl_3$	$CHCl_3$: MeOH	MeOH
Volume (mL)			5	0,2 : 1 to 1 : 0,2	5
n (mmol)	L_5		0,05	/	/
	$NaBH_3CN$		/	/	0,1
	Fe(II)		/	/	0,05
m (mg)	L_5		9,1	/	/
	$NaBH_3CN$		/	/	6,3
	Fe(II)	$[Fe(ClO_4)_2.6H_2O]$	/	/	18,1
		$[Fe(BF_4)_2.6H_2O]$	/	/	16,9
$V_{solution/tube}$ (mL)			0,8	0,8	0,8

Table 4. Table showing the theoretical quantities and volumes for plan 4

Ultimately, the last plan for the L_5 ligand was to put it into contact with a solution of Fe(II) and $NaBH_3CN$. It was not a success since no crystals could be observed, be it in large tubes or in thin tubes. There is a very thin orange precipitate on the tube wall at the buffer's level as well as yellow agglomerate in solution at the top of the tube.

Fifth Plan : L_4, Nadca

			Solution 1	**Buffer**	**Solution 2**
Solvent			$CHCl_3$	$CHCl_3$: MeOH	MeOH
Volume (mL)			5	0,2 : 1 to 1 : 0,2	5
n (mmol)	L_4		0,05	/	/
	Nadca		/	/	0,05
	Fe(II)		/	/	0,05
m (mg)	L_4		15,4	/	/
	Nadca		/	/	4,5
	Fe(II)	$[Fe(ClO_4)_2.6H_2O]$	/	/	18,1
		$[Fe(BF_4)_2.6H_2O]$	/	/	16,9

$V_{solution/tube}$ (mL)	0,8	0,8	0,8

Table 5. Table showing the theoretical quantities and volumes for plan 5

Following the same process as before, we have decided to realise the same experiments for the four-cycle L_4 ligand. The procedure has proven to be a lot more difficult to put into practice in an efficient way this time. In fact, we decided to dissolve the L_4 ligand in chloroform, just as before. The dissolution appeared to be incomplete since the obtained solution was cloudy. Still, we continued the experiment, guessing that a part of this ligand was in solution and thus that it could react. For this reason, we decided to only filter the solution before distributing it in the tubes. Despite the solvent wetting of the paper filter, a few millilitres of solvent were lost in this phase, impacting the final concentration of the inferior solution. We did not consider this prohibitive given the nature of the experiment and the final goal of reaction and crystallisation instead of performance.

We quickly realised the impossibility to obtain crystals. In addition, we have globally noticed the presence of yellow or dark yellow precipitate at the level of the buffer and of the solution at the bottom of the tube. We made the hypothesis of precipitation of the L_4 ligand, and thus of the inefficiency of this method. This was also observed when we used thin tubes.

Taking into account the difficulties associated to the dissolution of the pyridine ends reagent, we attempted to solubilise it in dichloromethane. We have thus used the following similar quantities:

			Solution 1	**Buffer**	**Solution 2**
Solvent			CH_2Cl_2	CH_2Cl_2 : MeOH	MeOH
Volume (mL)			5	0,2 : 1 to 1 : 0,2	5
n (mmol)	L_4		0,05	/	/
	Nadca		/	/	0,05
	Fe(II)		/	/	0,05
m (mg)	L_4		15,4	/	/
	Nadca		/	/	4,5
	Fe(II)	$[Fe(ClO_4)_2.6H_2O]$	/	/	18,1
		$[Fe(BF_4)_2.6H_2O]$	/	/	16,9
$V_{solution/tube}$ (mL)			0,8	0,8	0,8

Table 5 bis. Table showing the theoretical quantities and volumes for plan 5

However, this did not solve the previously mentioned problem. In parallel, the results were the same as when the chloroform was used. Despite that, we note a clear improvement in the size of the agglomerates produced.

Accordingly, we tried approaches that were a bit different: we kept the two solvents used to dissolve L_4, but added external actors to it with the aim of influencing the solubilisation. To do this, we heated the solution (while preventing the solvent to escape) up to fifty Celsius degrees in the case of the chloroform. It did not work, the dissolution was not better and after the filtration we tried putting it into tubes again, but no crystals appeared with time, only powder. After this we decided to introduce a few drops of DMSO in the dichloromethane in order to facilitate the dissolution. Even if it is known to be an excellent solvent, adding DMSO did not show any improvement. Following this, we tried to replace the dichloromethane by the DMSO, still without success since it did not lead to a total dissolution and the previous result repeated itself.

Despite the unsuccessful attempts, we repeated the same experiments, then alternative ones for the other established plans. It allowed us to verify on a case by case basis the failure of this procedure and to search other improvements capable of changing the situation. Indeed, putting those different alternatives into practice did not lead to a crystallisation in any of the plans for the L_4 ligand. As a consequence, the several tables of quantities are more indicative than instructive.

Sixth Plan : L_4, KSCN

			Solution 1	**Buffer**	**Solution 2**
Solvent			$CHCl_3$	$CHCl_3$: MeOH	MeOH
Volume (mL)			5	0,2 : 1 to 1 : 0,2	5
n (mmol)	L_4		0,1	/	/
	KSCN		/	/	0,2
	Fe(II)		/	/	0,1
m (mg)	L_4		30,8	/	/
	KSCN		/	/	19,4
	Fe(II)	$[Fe(ClO_4)_2.6H_2O]$	/	/	36,3
		$[Fe(BF_4)_2.6H_2O]$	/	/	33,8
$V_{solution/tube}$ (mL)			0,8	0,8	0,8

Table 6. Table showing the theoretical quantities and volumes for plan 6

		Solution 1	**Buffer**	**Solution 2**
Solvent		CH_2Cl_2	CH_2Cl_2 : MeOH	MeOH
Volume (mL)		5	0,2 : 1 to 1 : 0,2	5
n (mmol)	L_4	0,1	/	/
	KSCN	/	/	0,2
	Fe(II)	/	/	0,1
m (mg)	L_4	30,8	/	/

	KSCN		/	/	19,4
	Fe(II)	$[Fe(ClO_4)_2.6H_2O]$	/	/	36,3
		$[Fe(BF_4)_2.6H_2O]$	/	/	33,8
$V_{solution/tube}$ (mL)			0,8	0,8	0,8

Table 6 bis. Table showing the theoretical quantities and volumes for plan 6

Seventh Plan : L_4, KSeCN

			Solution 1	**Buffer**	**Solution 2**
Solvent			$CHCl_3$	$CHCl_3$: MeOH	MeOH
Volume (mL)			5	0,2 : 1 to 1 : 0,2	5
n (mmol)	L_4		0,1	/	/
	KSeCN		/	/	0,2
	Fe(II)		/	/	0,1
m (mg)	L_4		30,8	/	/
	KSeCN		/	/	29,0
	Fe(II)	$[Fe(ClO_4)_2.6H_2O]$	/	/	36 ,3
		$[Fe(BF_4)_2.6H_2O]$	/	/	33,8
$V_{solution/tube}$ (mL)			0,8	0,8	0,8

Table 7. Table showing the theoretical quantities and volumes for plan 7

			Solution 1	**Buffer**	**Solution 2**
Solvent			CH_2Cl_2	CH_2Cl_2 : MeOH	MeOH
Volume (mL)			5	0,2 : 1 to 1 : 0,2	5
n (mmol)	L_4		0,1	/	/
	KSeCN		/	/	0,2
	Fe(II)		/	/	0,1
m (mg)	L_4		30,8	/	/
	KSeCN		/	/	29,0
	Fe(II)	$[Fe(ClO_4)_2.6H_2O]$	/	/	36,3
		$[Fe(BF_4)_2.6H_2O]$	/	/	33,8
$V_{solution/tube}$ (mL)			0,8	0,8	0,8

Table 7 bis. Table showing the theoretical quantities and volumes for plan 7

Eigth Plan : L_4, $NaBH_3CN$

		Solution 1	**Buffer**	**Solution 2**
Solvent		$CHCl_3$	$CHCl_3$: MeOH	MeOH
Volume (mL)		5	0,2 : 1 to 1 : 0,2	5
n (mmol)	L_4	0,05	/	/
	$NaBH_3CN$	/	/	0,1
	Fe(II)	/	/	0,05
m (mg)	L_4	15,4	/	/
	$NaBH_3CN$	/	/	6,3

	Fe(II)	$[Fe(ClO_4)_2.6H_2O]$	/	/	18,1
		$[Fe(BF_4)_2.6H_2O]$	/	/	16,9
$V_{solution/tube}$ (mL)			0,8	0,8	0,8

Table 8. Table showing the theoretical quantities and volumes for plan 8

			Solution 1	**Buffer**	**Solution 2**
Solvent			CH_2Cl_2	CH_2Cl_2 : MeOH	MeOH
Volume (mL)			5	0,2 : 1 to 1 : 0,2	5
n (mmol)	L_4		0,05	/	/
	$NaBH_3CN$		/	/	0,1
	Fe(II)		/	/	0,05
m (mg)	L_4		18,2	/	/
	$NaBH_3CN$		/	/	6,3
	Fe(II)	$[Fe(ClO_4)_2.6H_2O]$	/	/	18,1
		$[Fe(BF_4)_2.6H_2O]$	/	/	16,9
$V_{solution/tube}$ (mL)			0,8	0,8	0,8

Table 8bis. Table showing the theoretical quantities and volumes for plan 8

Reasearch of Solutions and Alternative Methods for the Crystallisation of L_4 Compounds

Until now, we did not find the correct modification to solve our problem. One of the direct paths was to search for another solvent among the most common solvents. However, it was crucial to take into account the restrictions on density and miscibility imposed by our method.

Accordingly, our first idea was to try to swap the solution solvents, that is to say using the methanol for the ligand solution. But this idea was quickly discarded. Indeed, on one hand it caused problems of solubility of the ascorbic acid at the level of the Fe(II) solution in the chloroform and thus it did not prevent the oxidising of the iron. On the other hand, we observed that the dissolution was again inefficient and that a blurred solution was appearing.

This method had been quite effective when using L_5 ligand partly because of the density difference between the two solvents ($d_{chloroform}$ = 1,49 and $d_{méthanol}$ = 0,792). A difference of that size will be difficult to obtain when we replace the chloroform. This is why if a solvent with a higher density than methanol is found, we will have to cautiously put down the solutions in order to keep the interfaces. With this in mind, we have tried dissolution in high density and miscible solvents with methanol, such as DMSO (d=1,1) or the DMF (d=0,944). But they were not very effecient at room temperature. However, it should be noted that once the temperature is increased, the dissolution is possible. In fact, in the case of the DMF, it was possible to solubilise the L_4 ligand by putting the plate at 75° Celsius. en réglant

une plaque à 75°C. Mais cet effet disparait dès que la solution n'est plus chauffée. We have attempted to repeat the process under heat by heating the solution and putting the desired quantity in a tube put in a recipent dipped into an oil bath heated in the same manner than before. We realised the procedure with a Fe(II) solution and Nadca in propan-2-ol. This choice of solvent is based on the fact that the density of the propanol (d = 0,786) is slightly lower than methanol's (d = 0,792). We realised three tubes to verify the results. After two days the tubes were removed from the oil bath and cooled in air, without results. No precipitate or crystals appeared. We then repeated the experiment using an ice bath to cool the tube down. The result was the same.

Regarding the usage of other solvents, we also tried to solubilise the ligand via benzene, toluene, formamide or mesitylene, again without success. We then used a specific solvent on the basis of a publication stating that it succeeded in dissolving this ligand: the orthoxylene. We tried to put the first plan into practice changing only the solution solvent and we also made an attempt using a propylene glycol as solvent (d = 1,03) because of its qualities in term of toxicity. Once again, we did not perceive a complete solubility in solution and the final result was not conclusive. Nonetheless, given the scientific literature, we persevered.

This led us to try an indirect approach; we kept the diffusion principle, but this time with gas diffusion. To be precise, we introduced ascorbic acid, around 0,03 mmol of L_4 and the same quantity of Fe(II) compound, $Fe(BF_4)_2.6H_2O$ or $FeCl_2.4H_2O$ in a recipient containing 4,5 mL of hot DMF. Indeed, the whole process is realized in an oil bath on a plate at 75°C. In total, there are 6 tubes in two closed recipients containing methanol (some millilitres). In one recipient the 4,5 mL of $Fe(BF_4)_2.6H_2O$ (blurred white solution) distributed into 3 tubes and in the other one the 4,5 mL of $FeCl_2.4H_2O$ (blurred yellow solution) solution distributed into the 3 other tubes. In each container, a spatula tip of Nadca, KSCN or $NaBH_3CN$ has been added in one tube since the associated quantities fluctuate between 0,86 mg and 1,94 mg, the measurement would have been too big of an error source and the cyanide ligands are here necessarily excessive. The containers are closed and kept into the oil bath in an attempt to diffuse quickly and above all to allow for a better solubility of the ligand. However, it did not result in the synthesis of crystals. This DMF attempt did not give any precipitate. In the case of the orthoxylene replacing the DMF, we have noted powder of similar colour for the tubes of two containers having the same cyanide ligands: khaki-brown, green and purple for Nadca, KSCN and $NaBH_3CN$. This implies that it might be possible to make the L_4 ligand react in orthoxylene, even if the dissolution in not complete. We must

however keep in mind that these colourations are probably due to the formation of iron having integrated only the cyanide ligands or in any case to an impurity.

We finally had a conclusive result based on a publication of Biradha et al. [125], we have adapted the modus operandi. The method used in this one is quite similar. In fact, the reaction is also done in tubes, but without buffer. Initially, it allowed for a reaction between a L_4 ligand solution in orthoxylene and a $Ni(NO_3)_2.6H_2O$ solution in methanol. The solution were around 10^{-3} mol/L, ten time less concentrated than the ones we used until then. We have thus tried to adapt the modus operandi by keeping the same quantities of L_4 ligand solution and distributing it in three different tubes in which the composition will vary. We tested in one go the synthesis based on $Fe(BF_4)_2.6H_2O$ with the Nadca, and with the $NaBH_3CN$. In the third tube, we added a $FeCl_2.4H_2O$ solution and KSCN. Depending on the composition, a variable volume of L_4 ligand has been introduced while the superior solution has been established on the basis of this factor.

			Solution 1			**Solution 2**	**Solution 3**	**Solution 4**
Solvent			o-xylène			MeOH	MeOH	MeOH
Volume (mL)			15			2,5	2	2
n (mmol)	L_4		0,04			/	/	/
	Nadca		/			0,02	/	/
	$NaBH_3CN$		/			/	0,03*	/
	KSCN		/			/	/	0,03*
	Fe(II)		/			0,02	0,02**	0,02**
m (mg)	L_4		12,6			/	/	/
	Nadca		/			1,8	/	/
	$NaBH_3CN$		/			/	2,1	/
	KSCN		/			/	/	3,2
	Fe(II)	$[Fe(ClO_4)_2.6H_2O]$	/			/	/	/
		$[Fe(BF_4)_2.6H_2O]$	/			6,9	5,5	/
		$FeCl_2.4H_2O$	/			/	/	3,3
$V_{solution/tube}$ (mL)			**2**	**3**	**4**	2	1,5	1,5
			6	4,5	4,5			

Table 9. Table showing the theoretical quantities and volumes for one of the alternative plans. Note: the final box for solution 1 shows the volumes of solution 1 introduced at the bottom of the respective tubes, while the solution 2, 3 and 4 werer added by the top. *: 0,03 is in fact 0,033 while **: 0,02 is in fact 0,016 mmol

We determined the quantities based on equivalences in L_4, Fe(II) and cyanide ligand previously used. For the solutions 2, 3 and 4, we used more solvent than has been put into

tube in order to limit the losses since the masses and volumes are small; we did not take this precaution for L_4 ligand solution. Besides, despite the smaller concentration in L_4 ligand, the complete dissolution at room temperature did not happen. The solution was thus blurred.

We sealed the tubes with parafilm and kept them at room temperature for a week. Thin orange crystals (see picture 6) have been observed for the composition involving the solution 2, but not in large quantity. We then repeated this composition with around ten tubes of a composition similar to the one above. It was then possible to collect the crystals in the same manner than before. However, the crystals were too small for a structure analysis. Moreover, the collected quantity was very small. In order to collect enough product for an analysis (a few or even tens of millilitres), a hundred of tubes should have been realised. In this case, it would consume a lot of solvent and reagent for a procedure that can probably be optimised.

Despite the small quantity of crystals, we decided to test qualitatively the crossover spin properties. To achieve this, we plunged the crystals into liquid nitrogen. No colour change and thus no transition have been noted. Nonetheless, we do not exclude this type of properties since the test is purely indicative and does not cover the whole range of temperature. In addition, the experimental conditions can also interfere with the demonstration of these properties (solvent escaping the framework by example).

Results and interpretations

Single crystal analysis for LS6

Following the analysis of our compound, we have observed red crystals. We were able to repeat those by experiment. This is why we decided to study them further. We began by a microscope analysis to confirm their crystal nature and thus determine if it was relevant to make an X-ray diffraction single crystal analysis on them. The answer was positive and we started synthesising fresh crystals in order to analyse them with this method. The compound was only tested at 100 K, we have no result at room temperature. This is due to an underestimation of the crystal stability at this temperature. However, optimal measurement conditions still have to be determined. The cif file that resulted from this test was then processed using the program Mercury (version 3.8) (see figures 8a-10c).

We could then observe the unit cell associated to the synthesised compound. According to this model, it appears that metals centres (iron) are coordinated to 6 nitrogen atoms (see table 1). Four of these atoms belong to ligand molecules, which means that pyridine forming the ends of this ligand are linked to the iron following two of the three axis

of the cell. Whereas the two other nitrogen atoms correspond to the dicyanamide used, thus linking the iron atoms between them according to the last direction. It differs from the usual structure of Hofmann type coordination compounds since the L_5 ligand does not take into account the pillar role, but build in two dimensions, not one. On the contrary, the cyanide coligands seem to bind better with pillar ligand by linking the plans formed by the L_5 ligands.

An interesting point comes from this analysis when we take into account the "packing", the structure of a larger scale than the unit cell: there are solvent molecules inside the cavities. This is important to note since during the preliminary work done with the same purpose, it was demonstrated that the presence of molecules had an impact on material properties. In fact, it was previously shown that a reduction of the solvent quantity inside the framework decreased or even inhibited all effects associated to the initial spin transition. In this molecule's case, the chloroform is inserted in the structure.

The composition has only been researched when the solvent was introduced in the material. We can imagine doing another analysis by X-ray diffraction of a single crystal with a sample having been dried up beforehand this time. However, it would be necessary for the compound to be stable enough to withstand the test this time. In an empirical way, we have been able to observe a decreasing then an extinction of the transition spin properties in a few minutes once the compound was in contact with air. In fact, we demonstrated an obvious colour change once the compound was subject to low temperatures through a wetting in a liquid nitrogen bath. The initially red crystals became very dark after being cooled. This thermochromism disappeared once the crystals were subject to ambient conditions.

Among the data given by the structure and its processing on Mercury, we could note its C 2/m space group, which corresponds to a monoclinic system. De facto, it presents similar cellular lengths accordingly to a and c while the length of b is inferior. The angles α and γ are 90° while the angle β is around 105°. We can also note the volume of the cell (11724 A^3).

According to the representation, it is possible to imagine an interaction between the perchlorate molecules and the ligand at the level of hydrogen of the double bond and the pyridine. There are also interactions between perchlorate and chloroform molecules, which probably contribute to the stabilisation of the structure.

Thanks to the enCIFer (version 1.5.2) software and the cif file, we obtained some complementary information. First of all, we learned about the different atoms present as well as their proportions and the potential molecules or functional groups observed via

"chemical_formula_moiety". From this, we deduced that it corresponded to C_{26} H_20 Fe N_7. 6(C H Cl_3). Cl O_4 [+ solvent]. We can also deduce the molar mass associated to the compound, in this case 1302 g/mol (division of the total mass by two to get to mass related to only one iron atom). As for the crystal system, we already know that it is monoclinic with a space group C/2m, but we can go a little further in terms of precision by qualifying it of –C 2y. The type of radiations used is also indicated, a MoKα source of a wavelength of 0.71073 Å. The calculated density can also be found by reading the data of the cif file; it corresponds to 1,475 g/cm³. In the same way, it is also possible to understand to exactness of the model by examining some information related to the "restraint" data and parameters engaged as well as the goodness of fit. However, we will not dwell on this data.

It is also interesting to take a look at the interatomic distances in order to define the strength of the bonds. Here, we will be specifically interested in the Fe-N distances since they give us information about the spin state. Via the cif file and Mercury, we were able to notice that those values range from Å to 2,00 Å (see table 1). This indicates that there is a low spin state. This is to be expected since we have a structure at 100 K and we previously perceived a spin transition when the crystals were plunged into liquid nitrogen, thus at under 77,36 K (boiling point of the liquid nitrogen) starting from room temperature. Consequently, it means that the transition happens at a temperature between 100 K and room temperature (around 293,15K).

Furthermore, the observation of the N-Fe-N angles shows an octahedral symmetry of the centres with almost no distortion since the angles range from 88,8° to 91,2° for the four nitrogen atoms in relation to the nitrogen atoms at the summits and the summits form an angle of 179,3° between them (see table 2). The angles between the two nitrogen face-to-face vary between 178,9° and 179,3°, which is very close to the expected 180°.

We also noted a distortion in the tetrahedral geometry of perchlorates for some molecules (see table 3) with angles fluctuating between 93° and 127° instead of the expected 109,4°. This tends to show a disorder. We can observe distorted perchlorates presenting two oxygen atoms interacting with two hydrogen from L_5 ligand (on from the ring and one from the double bond) as well as a chloroform. When the perchlorate interacts with only chloroform molecules, only a slight distortion is noted (106 à 112°).

We were able to establish the estimated volume of the pores and the distance between the adjacent metal centres. To achieve this, we noticed that the distances varied between two

values when they are separated by the dicyanamides (8,447 Å and 8,456 Å), by the ligands following the c axis (13,402 Å and 13,456 Å) while a unique distance has been observed by following the a axis (13,420 Å separated by the L_5 ligand too). For a pore, only the distance between two iron atoms separated by dicyanamides are different. Therefore, we have considered the average of those two values to obtain a pore volume of 1520,016 $Å^3$ (Fe-Fe by L_5 =13,402 Å) and 1526,168 $Å^3$ (Fe-Fe separated by L_5 = 13,456 Å). We did not attach any image showing this because of the reading complexity in the hindered structure. There is thus an asymmetry in the structure. The variations of the distances are caused angle differences between the metal centres and the dicyanamide groups, the Fe-N-C angle is of either 174,53° or 169,30° for the external nitrogen and its neighbours. In addition, there are also C-N-C angle variations (central nitrogen of the dicyanamide): 123,60° and 127,76° that lead to a bond shorter of 9 Å in the first case.

Furthermore, by observing the ellipsoid on Mercury, it was possible to imagine the scale of the disorder. In this manner, we noticed that the ones vibrating are mainly the molecules incorporated by solvent (chloroform) and the perchlorate anions, that is to say the freest molecules. In addition, the central nitrogen of the dicyanamide is probably prone to vibrating because it kind of acts as a pivot. This seems coherent since by modulating its position, it allows to favour its interaction with the chloroform (see figures 19a-20).

Given the values of R_1 ($I>2\sigma(I)$) and R_1 (all data) which are respectively 14,11% and 22,31%, we have to admit that the structure presents a part of uncertainty. However, we assume that this is probably consecutive to molecules present in the network.

FT IR LS6

We realised an infrared analysis on our compound LS6. To do this, we collected the compounds a few minutes before its analysis. Indeed, given the relative stability if the compound and the presence of solvent in the framework, it was crucial to do the analysis quickly. We hoped that way we would be able to witness the presence of chloroform and perchlorate in the spectrum, which would imply their presence in the framework. However, it is important to note that the sample had to be collected by a paper filtration, which did not allow it to be selective to the product. In fact, since the compound was not the only precipitate in the tube, it was difficult to obtain a pure sample. We could notice that the sample was a mix of two compounds, a red one in crystal form (the interest output) and a white powder. We made the hypothesis of the latter one was in fact the non-reacted ligand that would have precipitate one time the three environments together (two solvents and the buffer). Regardless

of the nature of this precipitate, it distorts the spectrum's peaks. In addition, we decided to compare this spectrum to the one of only the ligand so that to observe if potential characteristic peaks would prove its presence in the compound structure. However, if this compound is the non-reacted ligand, peaks associated to it will obviously be noted. Consequently, it seems difficult to attempt an interpretation of the spectrum in this context and to draw conclusion from it regarding the integration of the ligand in the final compound.

However, when comparing the spectrum of the sample and the one of the corresponding ligand, we note an intense peak at 2170 cm^{-1} that does not appear at all in the case of the ligand. Therefore, it seems that we have to find the source of peak elsewhere. In order to determine the origin of the peak, we decided to compare this spectrum to the spectrums of other reagents initially present and those of solvents used during the synthesis. Since we did not have the corresponding spectrums at our disposition, we decided to base our comparison on spectrums coming from data bases as well as on tables including the characteristic peaks in infrared according to the chemical functions. According to the latter, there are few possibilities for this peak, thus making it characteristic of a specific group. We could deduce that it is in fact the stretching of the "carbodiimide" function of the sodium that is responsible for this. In general, the wavenumber ranger associated to it is slightly lower: 2145-2120 cm^{-1}. Nevertheless, several factors confirm this hypothesis. Firstly, the shape and the intensity of the peak correspond to the date of the infrared table. As a matter of fact, the peak is intense and not large nor sharp. In addition, a hardly marked peak is visible at 2235 cm^{-1}, at first sight it is not very instructive. But when we observe the existing spectrum for the dicyanamide sodium, we can notice a series of three consecutive peaks at 2170 cm^{-1}, 2230 cm^{-1} and 2290 cm^{-1}. We can then wonder about the presence of those peaks in the final spectrum. We can assume that the third peak is in the larger range around 2320 and 2365 cm^{-1}. According to the publication [140], We should note a shift toward higher frequencies for the bands between 2150-2350 cm^{-1} when the Nadca is coordinated to the metal and in particular when it is bidented: $\nu_{as} + \nu_{sym}$ (C≡N) = 2304 cm^{-1}, ν_{as}(C≡N) = 2240 cm^{-1} et ν_{s}(C≡N) =2180 cm^{-1} , meaning a shift of 6-17 cm^{-1}. In our spectrum, we effectively observe 3 peaks in this part of the graph, but at 2170 cm^{-1}, 2243 cm^{-1} and 2324 cm^{-1}. However, there is also a peak at 2363 cm^{-1}.

Regarding the peak at 1085 cm^{-1}, we assume it is also characteristic of a reagent. Based on the known spectrums, the more relevant hypothesis is that of the iron (II) perchlorate. Indeed, it appears a peak is visible at around 1060 cm^{-1} for this compound. Its

presence in our sample is interesting since it endorses the fact that perchlorate anions are present inside the cavities of the structure. It is an interesting result in tune with the first data obtained through the single crystal diffraction. Concerning the chloroform, we cannot confirm it is in the framework via this analysis. In fact, no known peaks of the chloroform appear in an obvious manner in the spectrum of the final compound. Moreover, there are no traces of one of them in the interest areas, around 750 cm^{-1} and 1200 cm^{-1}. Since the first one is very intense, if there was at least a remnant, we should be able to notice it. This does not infirm the hypothesis we made. All the facts until now show that we were right. Be it following the results of the x-ray diffraction analysis on a single crystal of our compound, or be it the empirical observation of the disappearing of the transition spin properties in a few minutes in air. All of this seems to point toward a difficulty of the material to retain the chloroform in its cavities once taken out of its environment. It would be appropriate to try to determine the exact conditions and the implications that it could have on the potential usage of this compounds in ulterior applications. Or le premier étant très intense, si il y avait ne serait qu'un restant, nous pourrions espérer l'observer. In addition, it would be interesting to exploit this capture property with other less volatile solvents than chloroform and with cavities of the right size. This would be a significant path toward the comprehension of this phenomenon.

According to [141], The CH stretching of the ligand corresponds to the average peaks noted around 3030 and 2895 cm^{-1}.

DSC LS6

Via this analysis, it is possible to determine the different phenomenon happening in the compound during its heating and its cooling. Estimating the energy involved in those allows to guess their nature.

In the case of the DSC analysis of our compound, we can find out the reversibility of the phenomenon happening by highlighting a symmetry of the two curves (see figure 21). In addition, there is a conjunction between them and the transition.

The measures have been taken at 2K/min, a certain degree of precision can be expected from the data deduced from it.

By processing the peaks on Origin, we were able to establish that the area of the first one is approximately two times smaller than the area of the second one (for the heating curve) for two curves approximated by Gaussian or Lorentzian (see figure 22a,23a). The best approximation is the one done by Gaussian since the value of R^2 is the highest (see figure

25a). Furthermore, an approximation has been attempted by Voigt (see figure 24a), with a better correlation to the graph by the amount of the peaks, but a R^2 a bit lower than the Gaussian one. In the same way, for the cooling curve, the Gaussian approximation was the closest one (R^2) (see figure 25b). Here, the area of the second peak is around 2,5 times larger than the first peak's one. Nonetheless, this does not confirm that the phenomenon is of different nature when heating and when cooling. Indeed, we still favour this hypothesis since the wo curves are very close from a profile point of view and the peaks are also almost perfectly identical in temperature during the heating and the cooling.

Since $\Delta H = nC_p\Delta T$, we can calculate the enthalpy variation associated to each peak according the area under the curve. In fact, the area under the curve represents ΔH. In our case, the temperatures of the phenomena are respectively at 163K (cooling)/165K (heating) and 182K (cooling)/185 K (heating), and the respective areas deduced by the Gaussian approximation are of |-4,831 ± 0,203| kJ/mol (cooling) or 5,033 ± 0,235 kJ/mol (heating) and |-12,131 ± 0,261| kJ/mol (cooling) or 10,311 ± 0,279 kJ/mol (heating). In addition, it is possible to establish the entropy variations on the basis of these enthalpies and temperatures by dividing the first one by the second one. We can then observe respective ΔS of around |-29,6 ± 1,2| J/molK (cooling) or 30,5 ± 1,4 J/molK (heating) and |-66,6 ± 1,4| J/molK (cooling) or 55,7 ± 1,5 J/molK (heating). Even if the fit is not perfect, the aforementioned values approximate the true values. We can assume that the phenomena are of two types: the spin transition for which we should verify its nature by observing the magnetic measurements (and thus the transition temperature); a disorder of the chloroform molecules. This would confirm a certain stability in their incorporation in the compound, which could be useful in the context of specific applications. Moreover, the slight temperature discrepancy between the heating and cooling curves could imply the presence of a hysteresis of around 2-3 K. However, we assume it is due to the imprecision of the measurement.

By observing the data on the variations of enthalpy and entropy measured by fit of curves, we can deduct from the orders of magnitude that the second peak (at higher temperature) seems to correspond better with the usual values related to a spin transition (see introduction). As a consequence, we can assume that the transition happens around 182,4K-184,8K if we consider the temperatures attributed to this kind of peaks in cooling and heating (see figures 25a-25b).

Additionally, it could be interesting to compare those results to the one of a zinc compound of the same type. Indeed, since it is diamagnetic, no spin transition would be perceived and only one peak should appear, confirming the nature of the peak.

SQUID LS6

First of all, we can observe the general shape of the graphs of the magnetic susceptibility multiplied by the temperature in relation to the latter. It is possible to observe different profiles depending on the sample. In fact, we obtained a crescent curve tending toward a plateau and a sinuous profile, in other words: with a step. The first case is more common profile, generally perceived for samples that stayed a bit in air contact, or even up to a day at room temperature (see figures 26b-d, f-i and 27 b-d, f-i). They were not covered in details since they do not present any spin transition. Nevertheless, we noticed by drawing the $1/\chi$ graphs in relation to the temperature that the compound without solvent freshly added had a paramagnetic behaviour. In fact, if we extrapolate the tendency curves, we observed they were linear and of a $y = ax$ shape, in which a is positive and thus the interception with the x-axis happens at a temperature of 0 K (Θ=0K). The same graphs were drawn for the second type of profile and can only be approximated by a polynomial of significant magnitude (5).While the second have been obtained for fresh samples (see figure 26e) or left at room temperature for a day (see figure 27e) that were wetted with solvent. In addition, it should be noted that it happened that a sample like that presented the previous profile (see figure 26a and 27a). It tends to show that the solvent easily escapes the framework and that it is its presence (and its quantity) which plays a part in the magnetic properties of the compound. Indeed, the sinuous profile allows to distinguish the transition spin temperature. Furthermore, two runs have been made on each sample. This quickly demonstrated a continuation of the profile in first type profiles (see figure 26b-d, 26f-i). Whereas for the second type profile, the two run curves are different (see figures 26e and 27e). This means that the magnetic properties of the compound change with time. Additionally, we can note that the profile is sharper during the first run than during the second (see figures 26e and 27e). Meaning that the profiles fluctuate depending on the moment in which the analysis is done. We then clearly imagine that supplementary runs would keep this tendency and would tend to have a plateau profile and thus to be paramagnetic. This seems to confirm the hypothesis we made regarding the role of the solvent molecules as guest molecules on the magnetic properties, in particular on the spin crossover.

Since the graphs presenting a transition stage have a specific shape, meaning that there is only a superior plateau, we encountered difficulties to analyse them. In fact, the lack of inferior plateau and the fact that the conversion is very gradual complicate the interpretation of the graph and the determining of the transition temperature.

However, by observing the spectrum we note that the spin transition temperature is in the range of 150-200 K. It would also seem that the latter tends to decrease with the second run, which probably has a value tending to stray from "truth". In all cases, the conditions are not at optimum magnetic and transition properties. This seems correlate with previous comments on the degradation of properties with time and more precisely with the supposed loss of solvent molecules.

Ideally, a graph showing the fraction in the spin state depending on the temperature should be drawn. But, given the unique look of the curve, we are not convinced to have reached a pure low spin state. In fact, in this case we should have obtained a null magnetic susceptibility. In addition, a plateau should have been noted at this value. We can thus deduce that the spin transition is gradual and incomplete. This corroborates the idea that all metal centres are not in a low spin state. There are few doubts left after observing the values of $\chi_M T$ above 250 K. A value of a range of 3,8 $cm^3.mol^{-1}.K$ is typical of a high spin state and of 1,7 $cm^3.mol^{-1}.K$ (by removing the values under 25 K to take the ZFS effect, which will be discussed later, into account we could probably have extended its influence area up to around 50K where $\chi_M T$ is of 1,9 $cm^3.mol^{-1}.K$) corresponds to a mix of both spin states. Without considering the effect that impacts $\chi_M T$ at low temperature (<25-50 K), we can deduct that half the iron centres were still in the high spin state just above 50 K by dividing the values of $\chi_M T$ at 50K by the value of the high spin state (high temperature threshold).

The first part of the graph shows a strong reduction of the magnetic susceptibility in a small range of temperature, which looks a bit like a supplementary step, in other words a transition in stages. But, it is impossible to lower the temperature even more, consequently this hypothesis seems invalidated. The specific reduction of χT is in fact due to a well-known phenomenon of the iron compounds: the zero-field splitting [133] (see figure28). In general, this abrupt reduction in the first Kelvins can be associated to two phenomena: either a spin transition; or the zero-field splitting, or even an additional antiferromagnetic effect. The more effective way to verify this is to realise a Mössbauer analysis. Indeed, it allows to establish the spin state of the metal centres and in which proportions they are present. It should be noted that this reduction is present on both curve profiles and is present below 25 K. Since the

profiles do not present the same magnetic properties, it could be useful to wonder if the same phenomenon is the cause of the reduction in both cases. Indeed, it would be possible that for the molecule non-wetted with solvent, it is the zero-field effect; while in the second of profile curve it could be due to the spin transition or a combination. However, the fact that the phenomenon happen to similar temperatures in both cases and at intermediate χT values (above 1 Kcm^3/mol) tends toward the zero-field splitting since there is at least one portion of centres in the high spin state. Nonetheless, the χT values generally increase with temperature in the curves of non-wetted samples. This leads us to consider that there is a spin transition in a part of the metal centres. There would thus potentially be a combined effect of both causes. Furthermore, it would theoretically be possible to confirm the ZFS effect by optimising the Curie-Weiss rule for paramagnetic compounds (non-wetted) and a deviation of this model should then be observed at low temperature. We could thus limit the impact of this effect on the model applicable to the second profile by omitting this range of temperature.

Furthermore, we can note that the y-axis value increased during the second run. This tends to indicate that the stability of the low spin state is very low. In fact, we can guess that the compound in which the solvent molecules would be kept incorporated could present a pure low spin state. But, since the chloroform is at least partially easily a desorbed, the magnetic properties associated to it would quickly disappear. However, in a run we note a slight fluctuation of the magnetic properties due to the heating and cooling. This questions the hypothesis of the solvent molecules desorption. Indeed, we assume that they are mostly adsorbed in the low spin state, as suggested by the structure analysis at 100 K. The high spin state should contain very few or no guest molecules. Consequently, it would mean that the desorbed molecules are adsorbed again almost perfectly given the very slight variation in the measures. Moreover, it would raise questions about the explanation of the previous increase of the y-axis values. In fact, we would thus have to assume that the solvent molecules are not desorbed anymore at room temperature without readsorption (or with less), but this would not be the case during the runs. Therefore, it would be useful to know the exact measurement conditions. De facto, we have assumed that the compound had been wetted once with the solvent before being analysed by the two runs. But, if it was, by example, wetted again, we could assume that the time before its analysis favoured a larger loss of solvent than previously; or if there is a period of time between the first and the second run that would let the sample in conditions favouring the desorption, then there would be less solvent molecules available once at adsorption temperature.

In addition, we must take into account the potential order-disorder phenomenon of the chloroforms which we supposed was the source of the second DSC peak.

The publication of S. Kolb et al. [134] gave us much to think about for several reasons. First of all, the article talk about Fe(II) compounds also synthesised with L_5 ligand, but with selenocyanate. A polymer based on it could not be created with our modus operandi. They also studied the properties associated to complexes produced by quick cis-trans photoisomerisation. In this context, they observed two known structure isomers (all-cis and all-trans): Fe(II) L_4X_2, in which L corresponds to a L_5 analogue and X to a SeCN group. The ligand is in fact similar to L_5, except that one of the pyridines at the ends is replaced by a phenyl group. What is particularly interesting is to compare their magnetic susceptibility data (see figure 29) to ours. The observation of their curves shows a complete and slightly gradual spin transition for the all-trans complex and on the contrary a low spin complex for the all-cis one. A similarity was noted between the all-cis complex curve and our non-wetted curves. Consequently, It would be interesting to investigate this further. We can also assume that the curve in which we see the spin transition could show the presence of ligand both trans and cis at the same time. It also raise the question of an potential connection between the proportion of cis or trans ligand and the number of adsorbed guest molecules. Later, it would be useful to consider a structure study of the compound for intermediate fractions of incorporated solvent molecules in order to confirm this hypothesis. However, the structure did show signs of cis ligand at 100 K (inferior spin state). But we assume that there could have been a prior chloroform loss that would have influenced the structure and thus the cooperativity.

As for the previous publication, we would like to realise a more in-depth analysis of the transition spin curve via the Slichter-Drickamer model [134] or the Domain model. This would allow us to obtain important information on spin transition, such as enthalpy variations and the entropy associated, cooperativity parameter, transition temperature or the χT value in high spin. Those data could be compared to the DSC ones by example and thus confirm the previously deduced values. Similarly, with Mössbauer analysis by example, we could verify the transition temperature.

A Sorai and Seki fit of the data has been made for the first run of LS6 that was showing a SCO phenomenon (see supporting data 3). This fit was based on 3 variables: n, ΔH and $T_{1/2}$. They have been optimised by the least square method to find the best fit for n = 2, ΔH_{SCO} = 7,31 kJ/mol and $T_{1/2}$ = 146K. This gives us a ΔS_{SCO} = 50,07 J/molK. The fit was tested for ΔH between 2 and 10 kJ/mol, $T_{1/2}$ between 50K (because of ZFS) and 300K and n =

1, 2 or 3 because a higher n gave really bad fittings. The best fit has been found for RMSE = 0,0552 (in term of high spin fraction). When we look at the fit, we observe a difference compared to the data that could be explained by the instability of the spin transition (and thus of the spin states present) when the compound is not in a bath of solvent anymore. This is why we cannot discard the values thus taken from the fit. Moreover, they are in accordance with the expected values of the enthalpy and entropy variations of a spin transition. However, the transition temperature noted fluctuates significantly compared to the one estimated in DSC (the other data too). At first sight, it is not possible that the transition is not observed in DSC; this is why we assume that the measurement conditions have had an impact on the results and affect the compound properties.

Discussion

According to the same article [125] as before, crystals synthesised from L_4 ligand and benzene could be obtained with the same procedure by simply replacing the o-xylene by benzene.

Moreover, this article shows the possibility to obtain coordination polymers from L_4 ligand with "non-interpenetrated square-grid networks". Given the size of the L_4 ligand, the resulting polymer shows a big square-grid of around 20x20 Angströms. Even if we could assume that such a polymer would have a low stability, this is seemingly not the case. In fact, it would seem that they were able to study it by single-crystal X-ray diffraction even though my molecules were not in the framework anymore. Similarly, the thermogravimetric analysis confirmed the stability by keeping the polymer's integrity up to 300°C even if guest molecules escaped between 70°C and 150°C. In addition, the structure was only slightly affected with a similar space group. In the case of the publication's crystals, the guest molecules are the ortho-xylene, which would be true for our crystals. There is great number of interactions in this polymer: between ligands and adjacent grids; between guest molecules themselves by interactions between methyl groups; those functions with adjacent cycles; interactions of the guest molecules with the host (through aromatic moieties). The layers are then very near from each other (4,5 Angströms) and draw rectangular canals. Still based on this publication, the polymers obtained from benzene would be less symmetric than their ortho-xylene counterpart. In fact, it would seem that it is due to a different occupation of the square pores. On one side the cavities would be occupied by only 5 benzene molecules; on the other side, other cavities would also contain 2 methanol molecules. This difference of cavities occupation would be the source of the slight deformation of the network. In addition, the

benzene being symmetric, the interactions between molecules are less selective than when the ortho-xylene is the guest molecule.

In contrast to the publication, we used Fe(II) compounds that did not present the same counterions than the $Ni(NO_3)_2.6H_2O$. This should have an impact on the reactivity and the stability of the final polymers.

Since we encountered difficulties solubilising the L_4 ligand, we considered other options, including the functionalisation of this compound. For this purpose, we mainly thought about three reactions: nitration, sulfonation and the addition of alcohol functions.

Previously, we have noted some difficulties to keep a certain stability for the synthesised crystals. It was not a problem in the first plan since we have been able to maintain the stability in order to realise the major part of the analyses. Whereas for the second plan crystals, it prevented us from doing a series of analyses; thus impacting the characterisation of the compound. Until then, we were able to obtain them by following the initial procedure. However, given the problems encountered, we wanted to inquire about the existence of other modus operandi and about the literature associated to this crystal. This is how we made the connection with an article of Wöhlert et al. [126]. This publication is about Fe(II) compounds and thiocyanato based on the same ligand (L_5). They developed a specific synthesis route aiming to thermally decompose the reagents with N-bonded thiocyanate anions in order to obtain coordination polymers by heating. Furthermore, it was later noted that the compounds they obtained could also be obtained by solution. It should be noted that at the time this article was published, the scientific literature had already reported the existence of $[Fe(NCS)_2(L_5)_2(H_2O)_2]$ [127]. Complementary investigations then highlighted the possibility to obtain a different compound in which there is at first the loss of water molecules by heating, then a second step to results in a composition of $Fe(NCS)_2(L_5)$. This has been demonstrated by thermogravimetric analysis even if the intermediate compounds could not be isolated. According to Wöhlert's method [126], it has been possible to observe the $[Fe(NCS)_2(L_5)_2.(L_5)]$ compound. Based on this procedure, an excessive quantity of L_5 ligand is used in order to obtain the aforementioned compound in pure stage. Whereas if an inferior quantity of L_5 ligand is used, the synthesis leads to the hydrated compound reported by Nakashima et al. [127].

An in-depth study of the $[Fe(NCS)_2(L_5)_2.(L_5)]$ compound showed by XRPD measurement that it was structurally close to the Co(II) analogue [128]. In addition,

simultaneous thermogravimetric (TG) complementary analyses and differential thermal analyse (DTA) demonstrated the existence of two endothermal peaks and mass variation. They were respectively attributed to the transformation of the rich compound into ligand (1 :3) into a deficient compound (1 :1): $[Fe(NCS)_2(L_5)]_n$; and to the of the latter at higher temperature. Unsurprisingly, the study of the $[Fe(NCS)_2(L_5)_2(H_2O)_2]$ compound indicated the presence of three endothermal stages (and mass variation). In this case, the two last ones are the same phenomena observed for the previous compound. The first peak corresponds to the compound's transformation into its anhydrous equivalent. The second peak is, as previously mentioned, due a loss of about half the L_5 ligand as from certain temperatures. It means that the composition obtained in this way is similar the one of the intermediate aforementioned in the case of the thermal decomposition of $[Fe(NCS)_2(L_5)_2.(L_5)]$. In order to confirm these hypotheses, several analyses have been realised on the sample at different moments of the thermogravimetric study. In fact, the samples have been analysed after each mass variation in an effort to establish the nature of the intermediates and of the process unfolding with the temperature increase. The infrared spectroscopy highlighted the bridging via thiocyanato anions by a shift of the vibration frequency associated to the asymmetrical stretching of the C=N group in $[Fe(NCS)_2(L_5)]_n$ in comparison to $[Fe(NCS)_2(L_5)_2.(L_5)]$ and $[Fe(NCS)_2(L_5)_2(H_2O)_2]$. Through XRPD measures and CHNS analyses on the output of the thermal decomposition of the $[Fe(NCS)_2(L_5)_2.L_5]$ and $[Fe(NCS)_2(L_5)_2(H_2O)_2]$, it has been confirmed that the compound thus obtained was identical in both cases: $[Fe(NCS)_2(L_5)]_n$. Moreover, this compound is in the same crystal stage in both cases. The elemental analysis allows to verify the previous hypotheses regarding mass losses as well as the nature of the compounds at each stage. In the continuity, a Mössbauer analysis of the $[Fe(NCS)_2(L_5)]_n$ highlighted the nature of the metal cation, a Fe(II). As a matter of fact, only one doublet was observed.

The $[Fe(NCS)_2(L_5)_2.(L_5)]$ and $[Fe(NCS)_2(L_5)_2(H_2O)_2]$ compounds are not predisposed to show a magnetic cooperativity since they are not polymeric. In fact, the magnetic properties associated to them show a paramagnetic behaviour. The magnetic data relative to each of them follow the rule of Curie-Weiss.

On the contrary, the $[Fe(NCS)_2(L_5)]_n$ compound should be able to demonstrate magnetic cooperativity phenomena due to its structure. Firstly because the metal centres are linked by the thiocyanato anions so that to form magnetic chains; but also the latter are linked by the L_5 organic ligand in order to obtain a three-dimensional structure in layers. Indeed, an

antiferromagnetic behaviour inside the chains has been highlighted as well as transition from an antiferromagnetic state into a paramagnetic one.

This analysis series could be useful to compare the experimental data that we would obtain for our KSCN and L_5 ligand to the one obtained for the different compounds of the publication. However, due to our crystals being too unstable, we could only picture the analyses plan to follow. In fact, we focused on the experimental part of the article in particular with the idea in mind that we had maybe synthesised one of those compounds. Given the similarity of the reagents used (only the solvent and the Fe(II) compound change), we wanted to explore this lead further. Even if the method is not identical, we considered the hypothesis of an alternative synthesis route. De facto, in the context of the article, the different reagents are put in common in solution in variable proportions and variable solvents during 3 days depending on the compound synthesised. They are then cleaned with water and diethyl ether before being dried in air.

First of all, let's take a look at the first compound: $[Fe(NCS)_2(L_5)_2.(L_5)]$. It was formed starting from a ration 1 : 2 : 4 in $FeSO_4.7H_2O$: KNCS : L_5 in acetonitrile. The compound thus formed was in the form of dark red polycrystalline powder. If we compare the modus operandi to ours, we can easily note that we did not use the same proportion of reagents. In fact, we used 1 : 2 : 1 in $FeBF_4.6H_2O$: KNCS : L_5 in the tubes. This also does not correspond to the composition used to synthesise $[Fe(NCS)_2(L_5)_2(H_2O)_2]$, that is to say a ratio 1 : 2 : 2 in $FeSO_4.7H_2O$: KNCS : L_5 in water. The output also corresponds to a red crystal powder. Even if both options are possible considering that the reactions were incomplete in our case; the hydrated compound seems not very coherent regarding the procedure we used. We favour another possibility. Previously, we highlighted the fact that $[Fe(NCS)_2(L_5)_2]$ was a compound resulting from the thermal decomposition of the above hydrated compound. Nonetheless, it seems unlikely that this form was obtained through our synthesis route since water is not the solvent and the reaction was realized at room temperature. Our choice fell on the compound of the publication: $[Fe(NCS)_2(L_5)]_n$. When we observe a bit more the ratio used, 4 : 8 : 1 in $FeSO_4.7H_2O$: KNCS : L_5 in a test tube with water as solvent and heated at 120°C during the period of crystallization, on note that it is very far from ours. However, the authors explained that a composition 1 : 2 : 1 in $FeSO_4.7H_2O$: KNCS : L_5 in water led to a polycrystalline red powder. It is based on this similarity that we thought it was possible that we obtained the same compound. But, given that our compound was kept in solution, it should not have

disintegrated into powder as it was the case in the article since the compound was filtered, cleaned and dried in air.

In order to verify this hypothesis, it would be helpful to realise both modus operandi and to collect our compound. Once the two compounds have been obtained, we could easily establish a potential connection by comparing their respective spectrums in XRPD.

An analysis of the magnetic properties could also be a good exploration route to infirm or confirm the hypothesis of a $[Fe(NCS)_2(L_5)]_n$ compound. In addition, a complementary research could then be realised in order to comprehend what caused the instability observed in our method. Besides, we have references at our disposition through the publication. Thanks to this, we could easily determine the nature of our compound, even if we would have to be able to stabilise the compound so that to characterise it efficiently.

It would also be useful to try to adapt our procedure by modifying the ratio to have a ratio 4 : 8 : 1 in $FeBF_4.6H_2O$: KNCS : L_5 in the tubes, in order to verify if it is possible to obtain $[Fe(NCS)_2(L_5)]_n$ crystals using our method.

We have introduced some factors impacting the structure and the properties of our coordination polymer. We will now try to verify the extent of those generalities and their application in the context of our compound.

First of all, we will focus on the compound which we have the more data on: LS6. A first approach is its composition and more specifically the reagents used. We used the L_5 ligand, which has pyridine ends. We can in a way assimilate our compound to one-dimensional Fe(II) and dicyanamide chains, which would themselves be linked by L_5 ligands in the other directions. In fact, our LS6 is truly a three-dimensional structure. A study by DFT (density functional theory) could be appropriate in order to have a better knowledge of the structural and thermodynamic properties of the polymer.

In the introduction, we highlighted that the two- or three-dimensional nature of the compound was mainly defined by the choice pf the ligand. In fact, a pyridine ligand leads to a two-dimensional compound because of its unique nitrogen atom. While the pyrazine leads to three-dimensional compounds due to its bidenticity. If we observe the structure of our L_5 ligand, it shows pyridine ends. Nevertheless, its behaviour is close to the one of pyrazine because two terminal nitrogen are available for binding with the Fe(II) metal centres. This is

why we can estimate that the formation of a three-dimensional coordination polymer is relevant in regards to the scientific literature.

However, this observation raises one question. Indeed, according to the literature, it is the organic ligand that determines if the compound is two- or three-dimensional. But, if we focus on the dicyanamide ligand, we note nitrogenous ends. Consequently, what is the factor determining to its chain binding and not in two other dimensions such as the organic ligand? In fact, we could also interpret the LS6 structure as some sort of layers limited by the zigzag L_5 organic ligands and thus non-planar bond to each other by the dicyanamides. We could also consider a difference of reactivity and kinetics that would lead to: either the one-dimensional formation of chains in the solution before the contacting and favoured by the modus operandi; either the kinetics are more favourable for the dicyanamide even once the reagents are in contact. In fact, we assume that the L_5 ligands would preferably position themselves on summits at 180° from each other and that the dicyanamides would be preferred in the square plan for hindering reasons. But the presence of four L_5 ligands around the iron atoms constrains them to make compromises. This is why we observe two L_5 ligands at 180° while the two others are positioned in opposition in the plan. In addition, the L_5 ligands orientate themselves differently from each other in order to maintain a positioning favourable to the limitation of the hindering effects. An in-depth study of the reactivity and kinetics involved would thus be instructive to understand the mechanism. The stoichiometry 1 : 1 : 1 of the reaction is not favourable to the formation of a $[Fe(L_5)_4(dca)_2]_n$ polymer, we would have expected a $[Fe(L_5)_2(dca)_4]_n$ polymer. We could also try a preliminary combining of the L_5 ligand and the Fe(II) compound (and thus a dicyanamide solution alone) to witness a potential impact on the reaction and structure. We can also consider that this positioning of different ligands in the structure is induced by an easier modulation of the distances and the hindering by the dicyanamide, which can take different configurations and adapt its angles more easily than the L_5 ligand, which is less flexible because of its double bond.

Dicyanamides are ligands heavily used in the context of perovskites synthesis. These syntheses are in general more advantageous from an energetic point of view, risks, toxicity or quickness than their counterparts for perovskites syntheses based on oxides or halides. Among the different synthesis routes, there is notably the layer-diffusion. This point emphasises the fact that the method used was more specifically adapted to the reaction dicyanamide sodium. We had thought about synthesis in tube U or H as a synthesis route and this method seems

perfectly adapted to this. This constitutes a development or even an improvement of the method that could be beneficial to the crystallisation.

If we look further at the structure of those ligands, we notice cyanides groups at the anion's ends and a central nitrogen atom that corresponds to an amide. Following this, there are thus three nitrogen atoms that lead to eight coordination modes (see figure 15). In fact, depending on the compound, it seems possible that only one external nitrogen or only the central nitrogen binds. For superior denticity modes, up to five simultaneous bonds could happen (in other words, all the nitrogen atoms). This is a ligand that demonstrated, among other things, long distance magnetic pairing between metal centres [130]. In general, the coordination is done by the cyanide groups at the ends, thus leading to a bidentate ligand. This is also true for the dicyanamide of the perovskites studied in the publication [130].

On the basis of the publication [131], we were able to get an overview of the coordination polymers based on dicyanamide as well as of the magnetic and structural properties of those compounds. At the same time, we thought about an interesting development route related to compunds derivated from dicyanamide. The publication mention coordination polymers realised from tricyanomethanide, that is to say $C(CN)_3^-$, which is without a doubt a lead to investigate. It would then only be necessary to integrate this compound to the previous experimental plans as the new ligand with cyanide ends, or even to integrate a mix of dicyanamide and tricyanomethanide ligands. As previously mentioned, in the case of the dicyanamide, the tricyanomethanide can presents different (four) coordination modes depending if one, two or three nitrogen atoms have bound (see figure 16). Contrarily to the dicyanamide, the tricyanomethanide only presents terminal nitrogen in the form of nitrile groups. In the same way, based on the publication of Shkrob [132], there are other polynitride ligands that could be interesting to test (see figure 17). Indeed, given the several branching where the cyanide groups are disposed, it could lead to the formation very unique crystal structures, which could have interesting properties.

By comparing those results to the ones previously obtained by our colleague Li Sun, a few points stuck out. In particular regarding the propensity of the sodium dicyanamide to form coordination polymers. In fact, other ligands which we will here call L_1, L_2 et L_3 had already been used during the MOFs research. These ligands each present pyridine ends and were chosen based on the publication of Zhao-Ping Ni et al [39]. Indeed, through their structures (see figure 18), they represent molecules of choice to be pillars in the Hoffman type MOFs. Using the same method, those ligands have been reacted with sodium dicyanamide

and the $Fe(ClO_4)_2.6H_2O$. The reactions allowed for the synthesis of three three-dimensional coordination polymers; among them, two showed crossover spin properties. Those two compounds are those based on L_1 and L_2 ligand, the simplest and more linear molecules. The reagent ratios were the same for each of those synthesis, 1 :1 :1 in dca^- : Fe(II) : L. In addition, the three compositions have also required methanol as a solvent for the Nadca as well as Fe(II) compound and chloroform for the L ligand. The polymers thus obtained respectively appeared in the form of orange crystals, yellow crystals and yellow/green needles for the compositions based on L_1, L_2 et L_3. It should be noted that it was possible to realise the second composition by replacing chloroform by dichloromethane, the crystals thus obtained were orange and also had SCO properties. These properties were, among other things, qualitatively observed by wetting in liquid nitrogen. Regarding compounds based on L_2, we assume that the structures are identical with the colouration being mainly impacted by the nature of the imprisoned solvent. Indeed, the powder diffraction analyses showed that the two samples were very close in terms of identity; only two peaks appeared for the chloroform compound and not for the dichloromethane one. This could also potentially be explained by the nature of the solvent. An intriguing fact, that should be explore dis that the L_2 based compounds realized with chloroform or dichloromethane do not present the same type of transition. In fact, the second is done in two stages: a first one more gradual and the second one sharper. Whereas the chloroform compound transition is gradual.

Starting from this information, we could consider an exploration route by trying to repeat the syntheses with other solvents. Trying this route on the LS6 polymer obtained from L_5 ligand and Nadca would be the most interesting. Given the already very strong transition of this compound, we can assume that if it would be synthesised again, but starting from other solvents it would have a different or even lighter colouration that could be more pronounced. However, we assume that this development would be mostly interesting in the case of compounds having a transition hardly visible to the eye. In fact, it could be useful in the context of final detection products, in which the macroscopic observation of the change could be indicative of a change and thus induce a response to this. Moreover, as we could note in the previous paragraph, the solvent's choice has a direct impact on the spin transition and its nature. This makes it a key element in the study of those compounds and future developments.

Regarding the polymer of dicyanamide and L_1 ligand, two different structures have been noted, depending on the temperature associated to the single crystal XRD analysis. This shows the two existing spin states and thus the structural change attributed to the spin

transition. At 100 K, the structure is defined as $Cmc2_1$ and as Cmca at 298K. Since this is the same space group, we can establish that the structural changes are not significant. The spin states have been established through an analysis of the bond distances between iron and adjacent nitrogen. In fact, in the structure at 100 K, those distances are all in the range of 2,0-2,1 Å, which gives an average of 2,049 Å that get closer to 2,0 Å, typical of a low spin state. While in the second case at room temperature, those distances range from 2,149 to 2,291 Å, which gives an average distance of 2,236 Å that goes over the value of 2,2 Å attributed to the high spin state. There is thus an increasing of the Fe-N bond length for the compound going from 100 K to room temperature. However, the low spin state is only partial since the given distances are mostly quite distant from the expected 2,0 Å. It is possible that a portion of the metal centres is in the high spin state while the major part is still in a low spin state. There could thus be a temperature lower than 100 K in which the polymer would be entirely in a low spin state if all the iron atoms are able to do a spin transition. Indeed, we have to consider that a part of the metal atoms could be constantly in high spin state.

Another interesting fact of this compound is that it possible to easily put it into different states in a reversible manner (see supporting data 1). To do this, the crystals have been collected, they are bright orange and contain one molecule of chloroform as a guest molecule. The solvent has then been removed in two ways: by letting the compound in air at room temperature for a week, which led to an estimated incorporation of 1,3 water molecule; by heating the crystals at 120°C for 40 min, letting 1 water molecule incorporates. Macroscopically, a colour change has been noted with on hand a light brown compound (1,3 water molecule) and on the other hand a dark brown compound (1 water molecule). This confirms the previous hypothesis according to which the solvent's choice and proportions have an impact on the compound colouration. Then, the chloroform is added (1,3 $CHCl_3$) and readsorbed in order to obtain an orange/dark brown compound. The final compound is in the form of bright orange crystals at room temperature and becomes dark red once cooled at 77 K in liquid nitrogen. In addition, previous macroscopic observations had allowed to establish a hypothetical desorption and adsorption pattern for this polymer. Indeed, the crystals initially show a spin crossover. But, if they are left in air contact for a period of time, they do not present any colour change anymore when plunged into liquid nitrogen. This is why we can consider them as being in high spin state. It is possible that it is caused by the chloroform escaping from the framework. If acetonitrile is later reintroduced in the compound by "wetting", the compound presents SCO properties again. This particular phenomenon would

confirm that the polymer is capable of incorporate a solvent or another with a certain limit size. If the compound is left in air, as previously, it does not transition at low temperature and would then be in high spin. This time, the acetonitrile would leave the cavities, thus letting the compound in a pure high spin state. Finally, if chloroform is introduced by wetting, a transition spin compound is obtained once again. This suggest possible desorption and adsorption processes for this type of compound. However, an in-depth research with strict desorption, adsorption and analysis conditions should be realised in order to the hypotheses aforementioned. In fact, it is possible that a part of the solvent is not desorbed, but that does not allow transition, or even that the water is adsorbed since the desorption has been made in room air and it impacts the properties. In the same way, it is essential to realise complementary analyses with the purpose of establishing the exact nature and proportions of the solvent incorporated in the framework.

Given the particular phenomena observed from an adsorption and desorption point of view, it would be interesting to realise the same type of research on our LS6 compound. However, in order to do this our compound must be stable enough in ambient conditions. We are not sure that is the case since it seems to decompose in a few days in tube. Furthermore, since the temperature study of its structure has not been possible, we doubt it would be possible to realise the same kind of pattern. Besides, this research would not have the same goal if it was applied to crystals that do not present transition spin properties initially. Indeed, it could then determine if guest molecules could have a positive effect on the compound's magnetic properties. Nevertheless, among the synthesised crystals, none sufficiently meets the requirements for such a research.

If we consider the fact that guest molecules are interchangeable, it would be useful to rely on a size and volume scale to determine which experiments would be appropriate depending on the volume of the cavity capable of hosting them. In the same way, the molecule's geometry also has an impact due to its hindering. A linear molecule would thus be easier to incorporate in the network than a branched molecule. In addition, we should also pay attention to the host-guest interactions that can strengthen the adsorption.

If we go back to the three crystals synthesised by Li Sun based on L_1, L_2 and L_3 ligands with dicyanamide, we notice that the third one does not show any spin transition. There is thus a lack of cooperativity in the material. Even though from a structural point of view it is quite close to L_2 ligand. We can thus assume that the presence of the central cycles would impact negatively the magnetic properties. We have no data regarding its structure;

consequently, it is hard to deduce the type of problem encountered. However, we can assume that the steric hindering induced by the fused benzene rings could have a negative impact on the volume of the MOF cavities in which the guest molecules should be incorporated. The fact that those molecules are not or hardly able to insert themselves in the pores could be at the source of the absence of SCO. Moreover, given the absence of transition, we can assume that the compound is only in a high spin state. The distances Fe-N (L_3) superior to 2,2 Å would be a consequence of this. Therefore, we can make the hypothesis that the steric hindering induced by the fused benzene rings would impact the distances by extending them in order to limit the repulsions and stabilise the structure.

In addition, the anthracene is a known compound used for its fluorescence under UV. This is why an in-depth study of light properties associated to the compounds of L_3 ligand, which has an anthracene group would be interesting. Its compounds with fluorescent properties could in fact be used as traps.

Over the course of Li Sun's previous works, it was noted that coordination polymers have been synthesised for Nadca, KSCN and BH_3CN with L_3 ligand. This endorse that this method is adequate for the formation of MOFs based on those compounds. However, we not able to synthesise the equivalent compounds with L_4 ligand and only partially with L_5 ligand. Consequently, there should be a number of possible optimisations in order to obtain them.

Regarding the coordination polymers based on L_5 ligand, it would be useful to study their optical properties. Indeed, the ligand use dis in trans conformation. Nonetheless, it is subject to photoactivation and thus to a transition from the trans form to cis form through radiation. Moreover, we have noted that in the literature [134], there were compounds close to the expected ones (except for the fact that they are in the form of complex, not of coordination polymers and that they present only one pyridine end) that present entirely different magnetic properties depending on if the ligand is trans or cis. The entirely trans compound showing a total and almost sharp hysteresis, while the entirely cis compound only showed a high spin state.

Conclusion

The spin crossover phenomena are interesting and promising in a lot of applications for the general public as well as for more specific ones. In this context, our research also took advantage of the coordination polymer research, another interest subject of chemistry.

Even if the spin transitions are always studied more, they stay prone to novelty and discoveries. The idea behind this work was to, among other things, explore the existence of a new transition spin compound family. In order to do this, we work in the continuity of the project of our colleague, Li Sun.

We encountered a certain number of procedure difficulties and the literature was lacking regarding those transitions spin coordination polymers. Consequently, we put procedures into practice based on trials and errors. In fact, obtaining crystals being a key element, we had to search for a method favouring it and easily adaptable. Due to the good results of our colleague, we continued with a similar method of diffusion in layers. It was effective for half of the compositions for the L_5 ligand. Even if an adaptation of the conditions is probably necessary for crystals formed from KSCN in order to obtain crystals with a better stability and capable of being studied efficiently.

However, we cannot obtain crystals with L_4 ligand through this method. We suspect that its solubility might be the cause and would impact its reactivity with other reagents. Even if a lot of solvents were tested, the only crystals we got were obtained through a partial dissolution in ortho-xylene. The modus operandi was almost the same than the one used here: there was no buffer and the concentrations were even lower. As a consequence, it is difficult to state that the procedure was faulty. Nonetheless, we emphasise the necessity of finding a solvent and conditions adapted to this compound.

There are still a lot of unanswered questions or that at least deserve to be explored in-depth. Among them, there is in particular the large-scale study of LS6 synthesised crystals from the point of view of adsorption-desorption process. In fact, those particular phenomena that were observed previously on other crystals could be very useful in the context of solvent capture, by example. In addition, this phenomenon has already been noted for iron crystals: $[Fe(tpa)(NCS)_2]$ [136]. There were then two crystals structures that were modulated according to the incorporation of a solvent's steam. Furthermore, the physical (notably the colour) and magnetic properties fluctuate depending on the solvent. To conduct this type of study, it would appropriate to search for the adequate stability conditions enabling these phenomena. If they are defined, then an in-depth study of molecules capable of being adsorbed-desorbed, of the compound structure at each stage and of their properties would be necessary in order to consider an application in this domain.

The structural analysis of our LS6 crystals has shown their polymeric nature and the presence of solvent's molecule in their cavities. We have also confirmed the presence of a spin transition by DSC and SQUID. Nevertheless, it is difficult to interpret the thermodynamic data associated to this phenomenon since the results change from one analysis to the other.

There are still a lot of analyses to do on LS6 crystals and other crystals if optimal conditions are established. Among them, we firstly think about the optic measures enabling a better study of the thermochromism of the LS6. And secondly, the thermogravimetric analysis would allow to explore the stability of the compound and note a potential solvent desorption with the augmentation of the temperature. The Mössbauer would be vital to confirm the data previously attributed to the transition, including the transition temperature and the molecular fractions in spin state with the temperature.

There are few materials based on Fe(II) capable of containing up to 6 chloroform molecules in their matrix as does ours. Among the compounds published in the literature that incorporate some chloroform molecules, we can mention $[Fe^{II}_2(ddpp)_2(NCS)_4]\cdot 4\,CHCl_3$ [135] which can also contain dichloromethane. The magnetic properties are then different with two stages (dichloromethane) or one stage (chloroform) transition.

Annexes

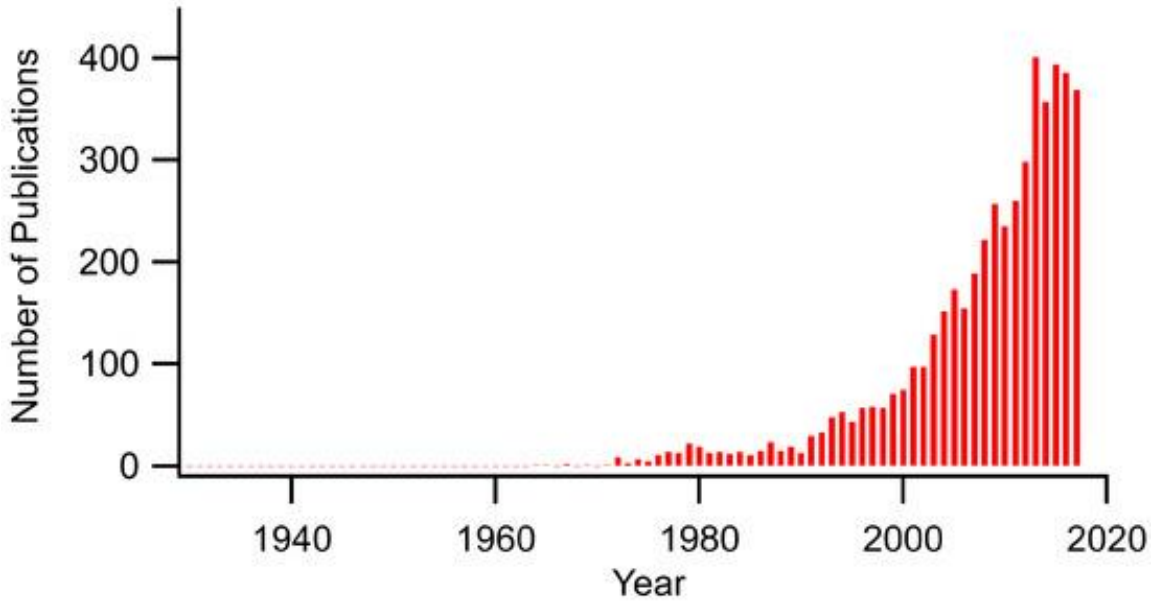

Figure 1. Bar chart representing the number of publications per year whose titles or keywords contain « spin crossover », « spin equilibrum » or derived words

Source: Spin crossover Complexes, Kazuyuki Takahashi, Inorganics, 2018, 6 (1), 32

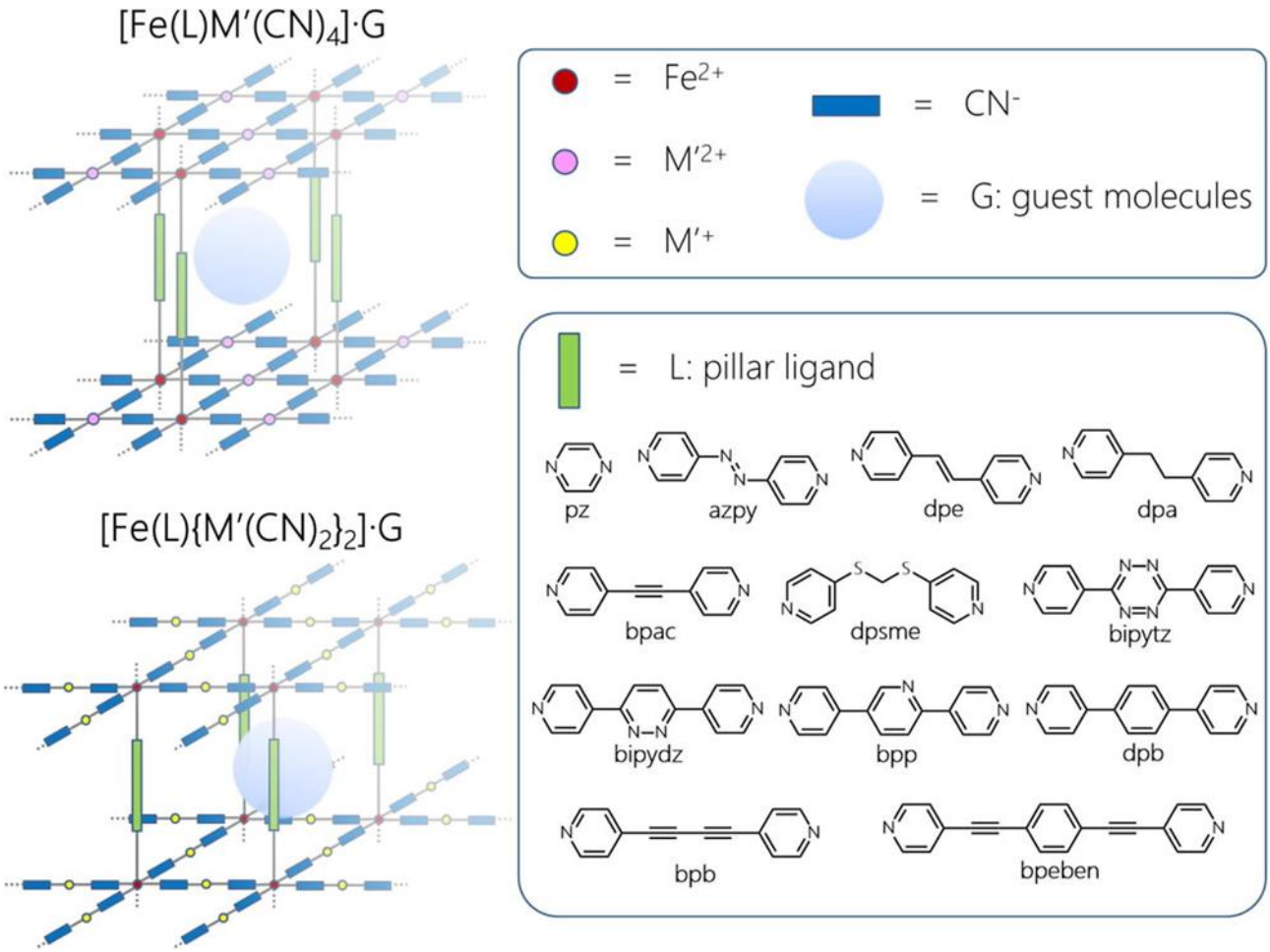

Figure 2. Schematic illustration (reported) of 3D Fe(II) SCO MOFs [Fe(L)M′(CN)4]·G (M′ = Ni2+, Pd2+, or Pt2+) and [Fe(L){M′(CN)2}2]·G (M′ = Ag+ or Au+).

Source: Coordination Chemistry Reviews, 335, 2017, 28-43

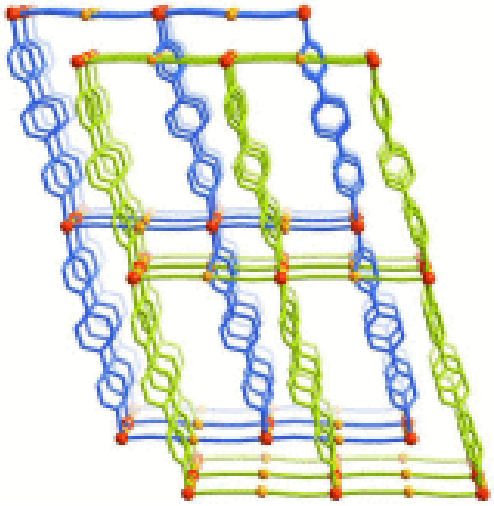

Fig 3. View of twofold-interpenetrated 3D framework of dbdAu

Source: Coordination Chemistry Reviews, 335, 2017, 28-43

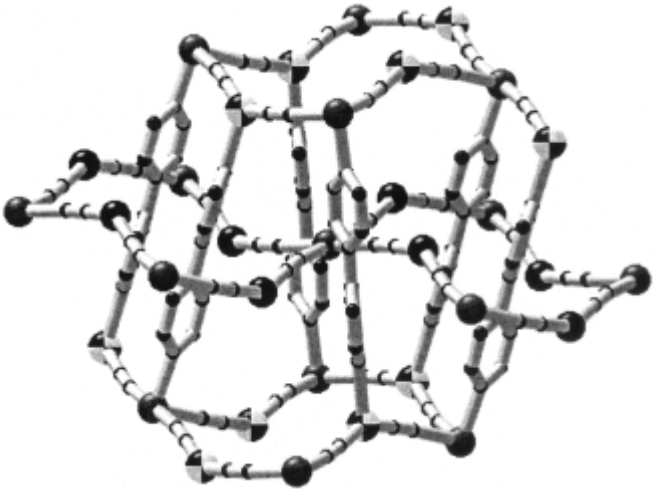

Figure 3 bis. Doubly interpenetrating three-dimensional bimetallic $\{FeL_2[Ag(CN)_2]_2\}$ networks

Source : Thermal-, Pressure-, and Light-Induced Spin Transition in Novel Cyanide-Bridged Fe^{II}-Ag^{I} Bimetallic Compounds with Three-Dimensional Interpenetrating Double Structures $\{Fe^{II}L_x[Ag(CN)_2]_2\}\cdot G$, Virginie Niel, M. Carmen Muñoz Prof. Dr.,Ana B. Gaspar,Ana Galet,Georg Levchenko Prof. Dr.,José Antonio Real Prof. Dr., 17 may 2002, Wiley

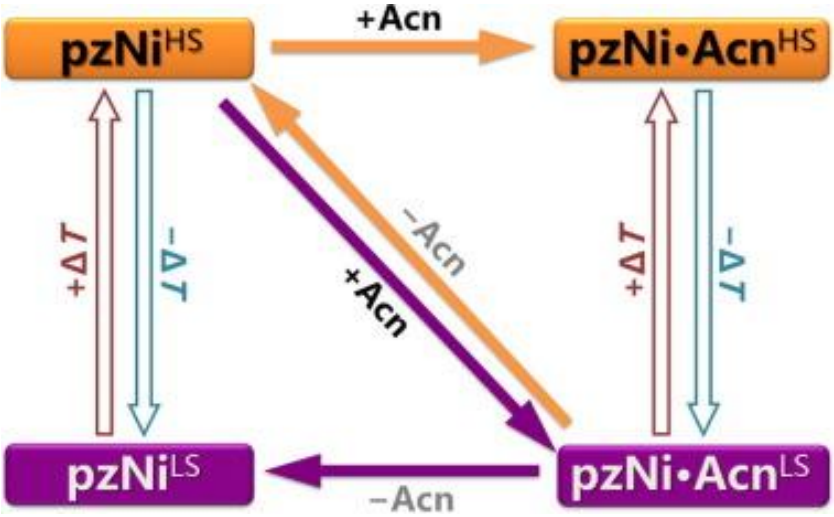

Figure 4. Schematic representation of chemical and thermal memory effects in pzNi system

Source: Coordination Chemistry Reviews, 335, 2017, 28-43

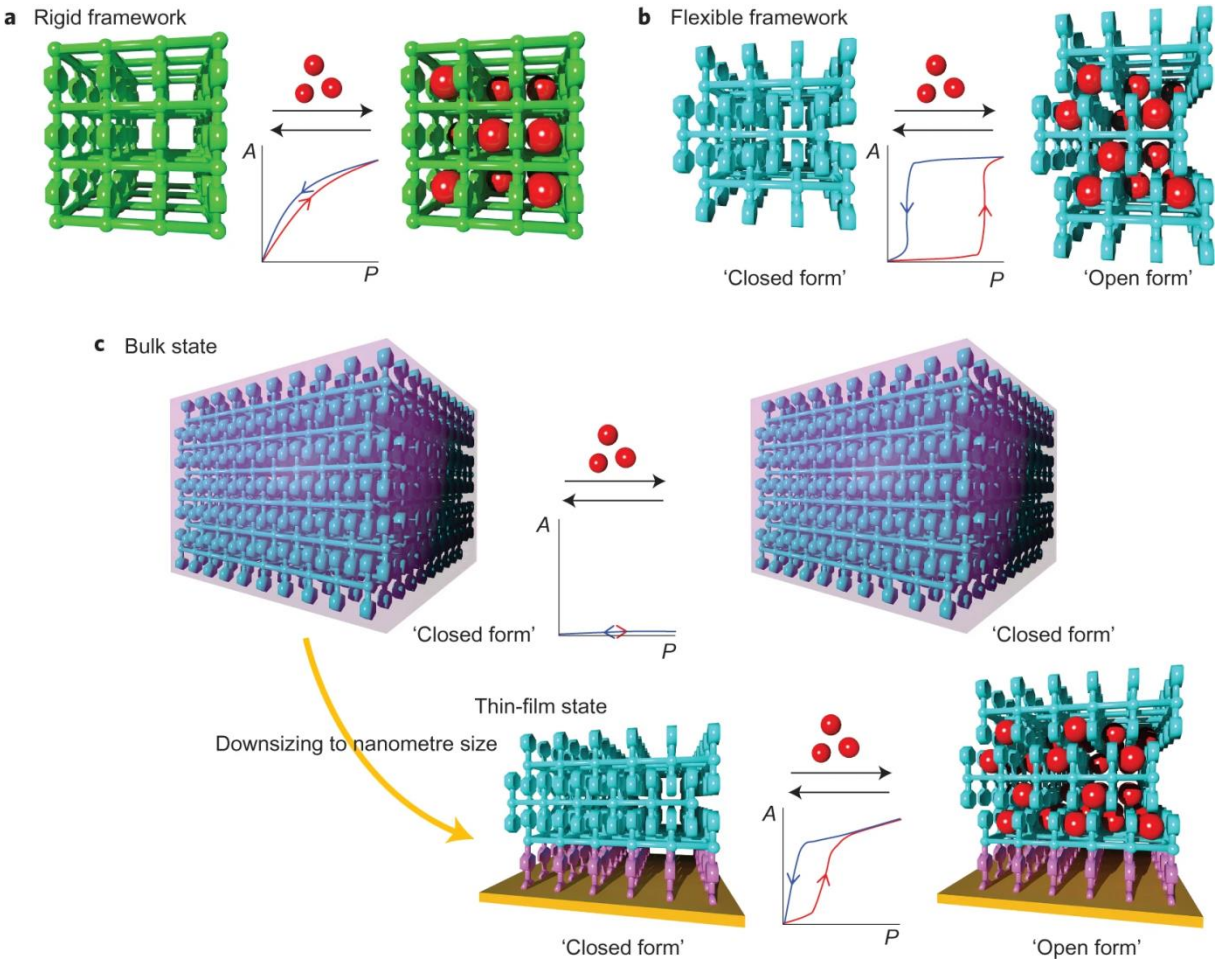

Figure 5. Schematic representation of the various structural responses in different types of coordination frameworks.

“The guest molecules are denoted by red spheres, and typical examples of the sorption isotherm are also shown in the middle parts of each panel (A, guest uptake; P, gas pressure; red line, adsorption profile; blue line, desorption profile). a, Sorption profile typically observed for a rigid 3D framework, characterized by a gradual guest uptake with little (or no) hysteretic adsorption. b, Gate-opening-type guest uptake observed in a flexible 2D interdigitated framework. Abrupt adsorption occurs at the specific pressure threshold, and a large hysteresis is observed on adsorption/desorption. c, Dynamic structural response to guests induced by crystal downsizing from the bulk state to the nanometre-sized thin film for MOF 1. In this case, the bulk material shows no significant guest uptake, whereas in a thin film, a dynamic gate-opening response to the guest is observed.”

Source : Sakaida, S., Otsubo, K., Sakata, O. et al. Crystalline coordination framework endowed with dynamic gate-opening behaviour by being downsized to a thin film. Nature Chem 8, 377–383 (2016). https://doi.org/10.1038/nchem.2469

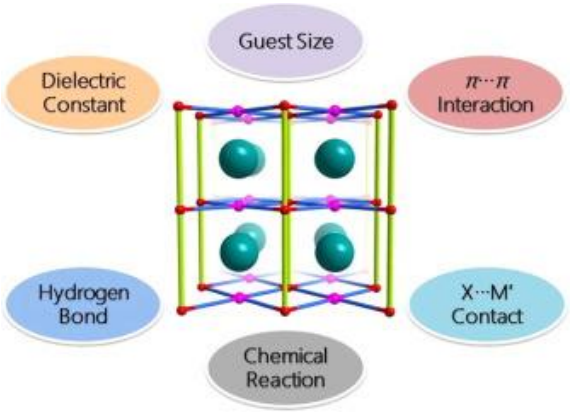

Figure 6. Summary of all the factors that could impact a SCO Hofmann-type polymer of coordination

Source: Coordination Chemistry Reviews, 335, 2017, 28-43

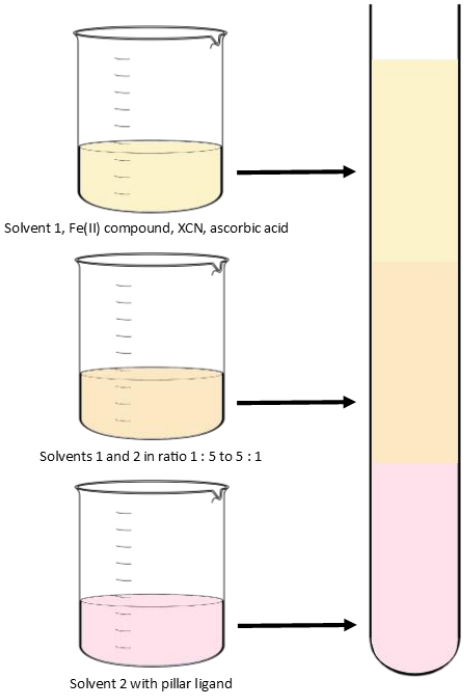

Figure 7. Schematic representation of the synthesis process. The different colours aren't the real ones, they are showing the superposition of the solutions.

Homemade

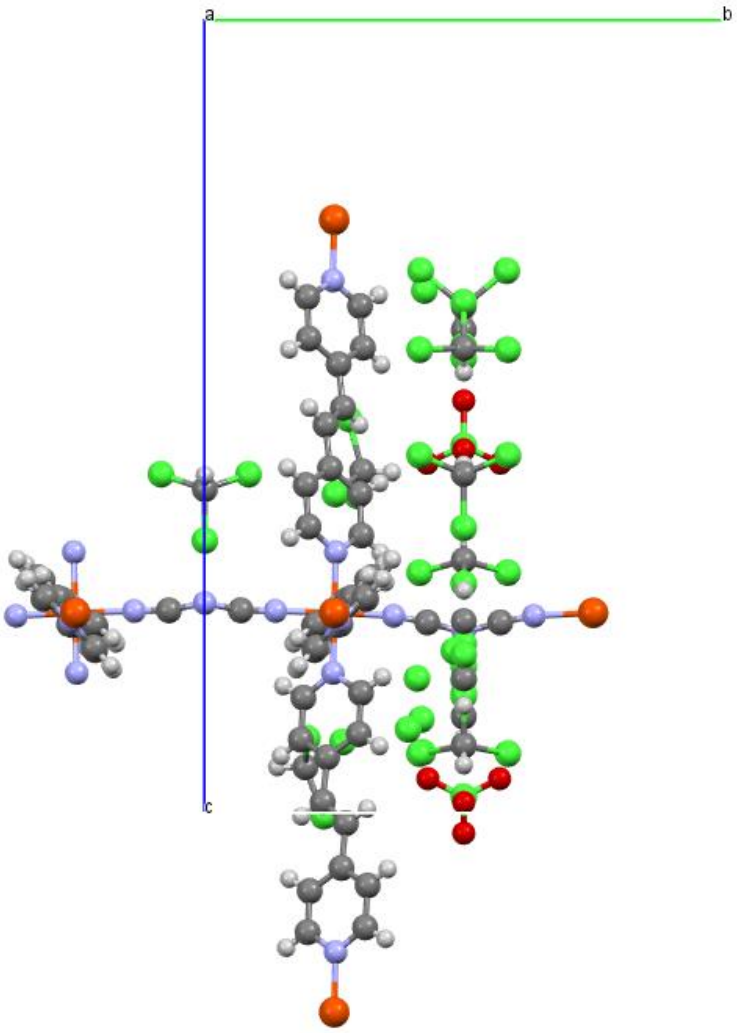

Figure 8a. Structure representation of LS6 (unit cell) following a axe's view. Atom labels: orange = Fe, light grey = H, dark grey = C, blue = N, red = O, green = Cl

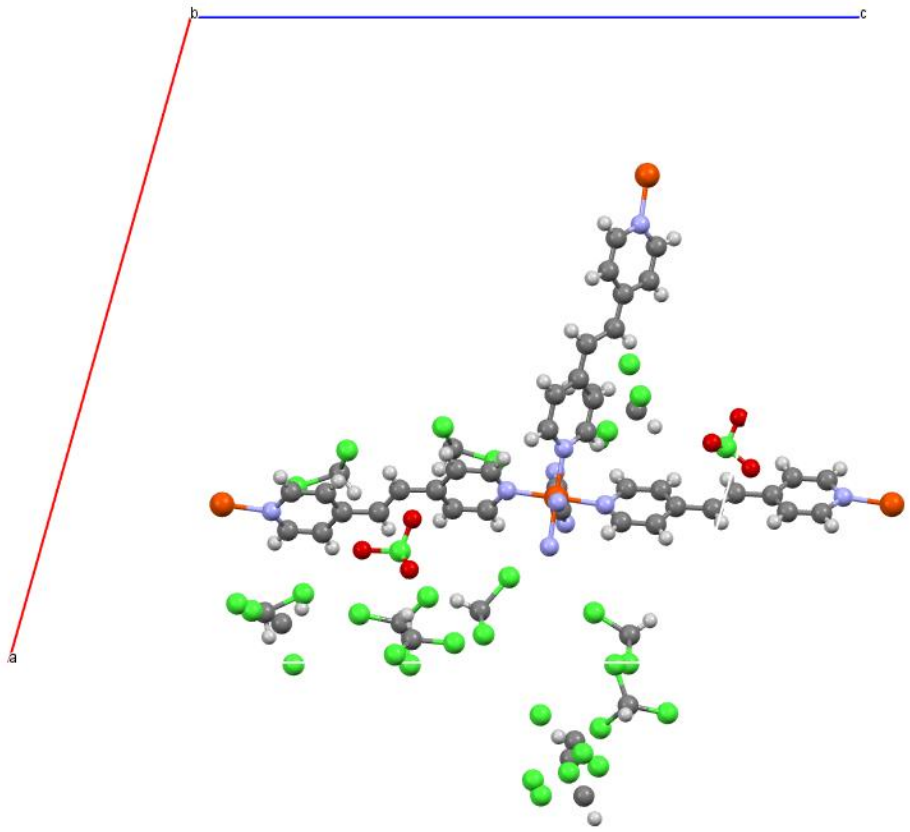

Figure 8b. Structure representation of LS6 (unit cell) following b axe's view. Atom labels: orange = Fe, light grey = H, dark grey = C, blue = N, red = O, green = Cl

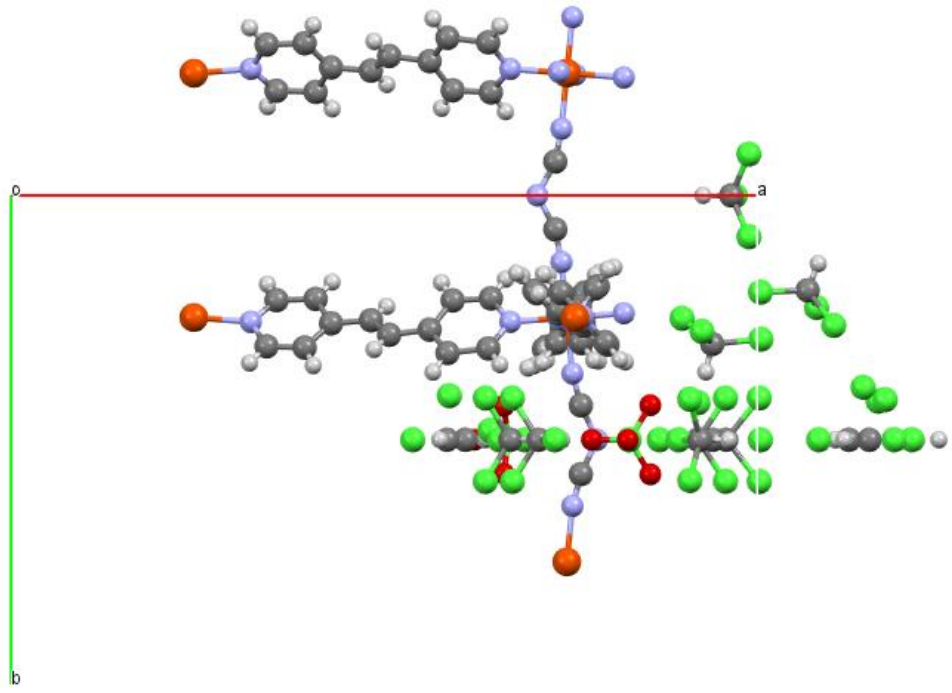

Figure 8c. Structure representation of LS6 (unit cell) following c axe's view. Atom labels: orange = Fe, light grey = H, dark grey = C, blue = N, red = O, green = Cl

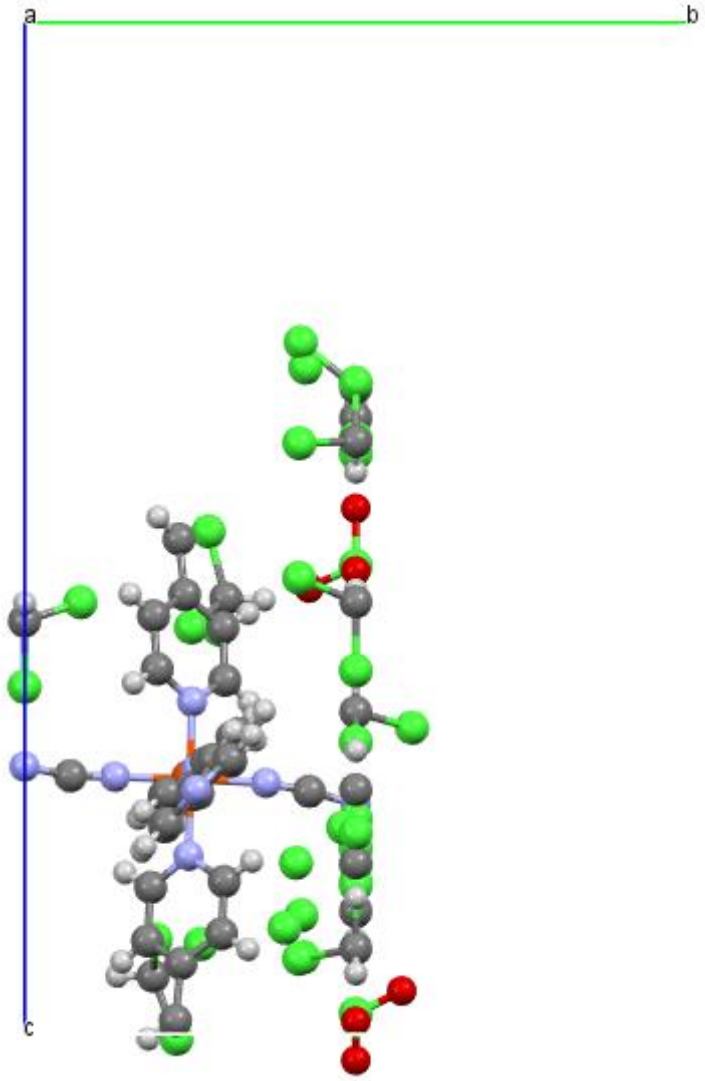

Figure 9a. Structure representation of LS6 (asymmetric unit) following a axe's view. Atom labels: orange = Fe, light grey = H, dark grey = C, blue = N, red = O, green = Cl

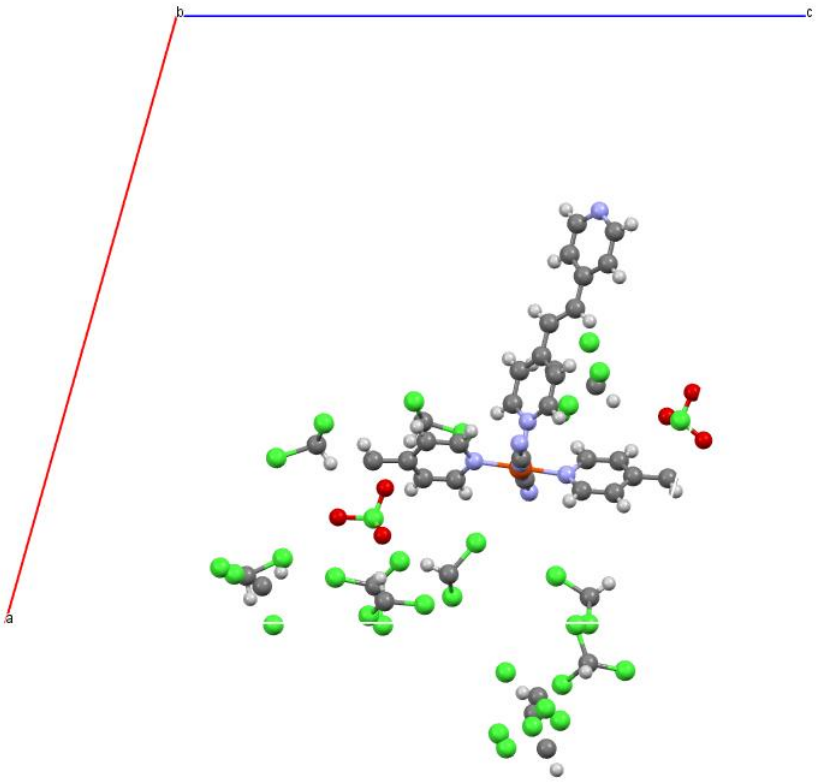

Figure 9b. Structure representation of LS6 (asymmetric unit) following b axe's view. Atom labels: orange = Fe, light grey = H, dark grey = C, blue = N, red = O, green = Cl

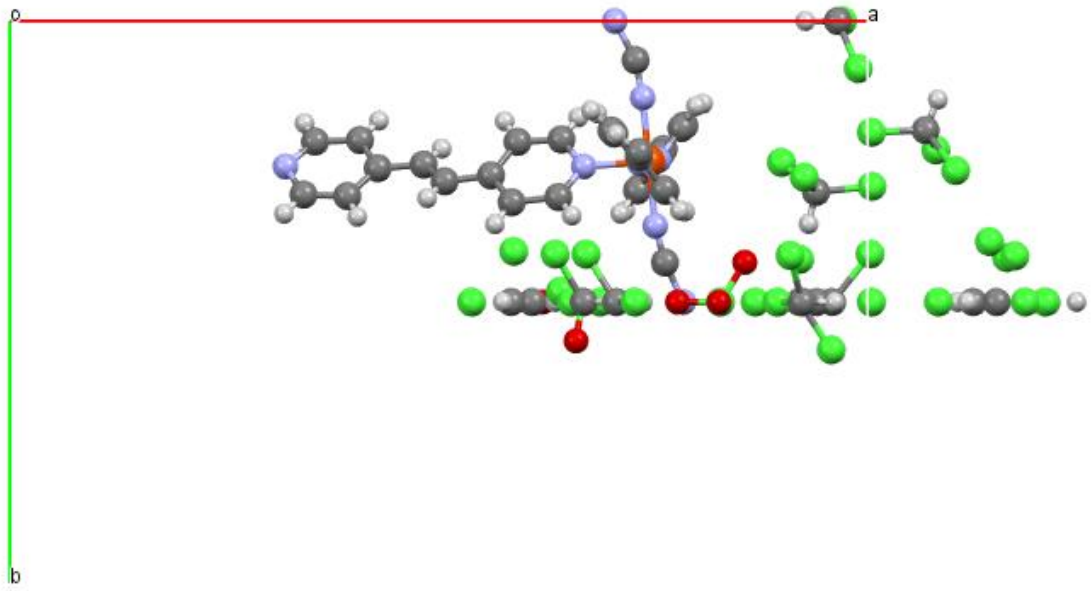

Figure 9c. Structure representation of LS6 (asymmetric unit) following c axe's view. Atom labels: orange = Fe, light grey = H, dark grey = C, blue = N, red = O, green = Cl

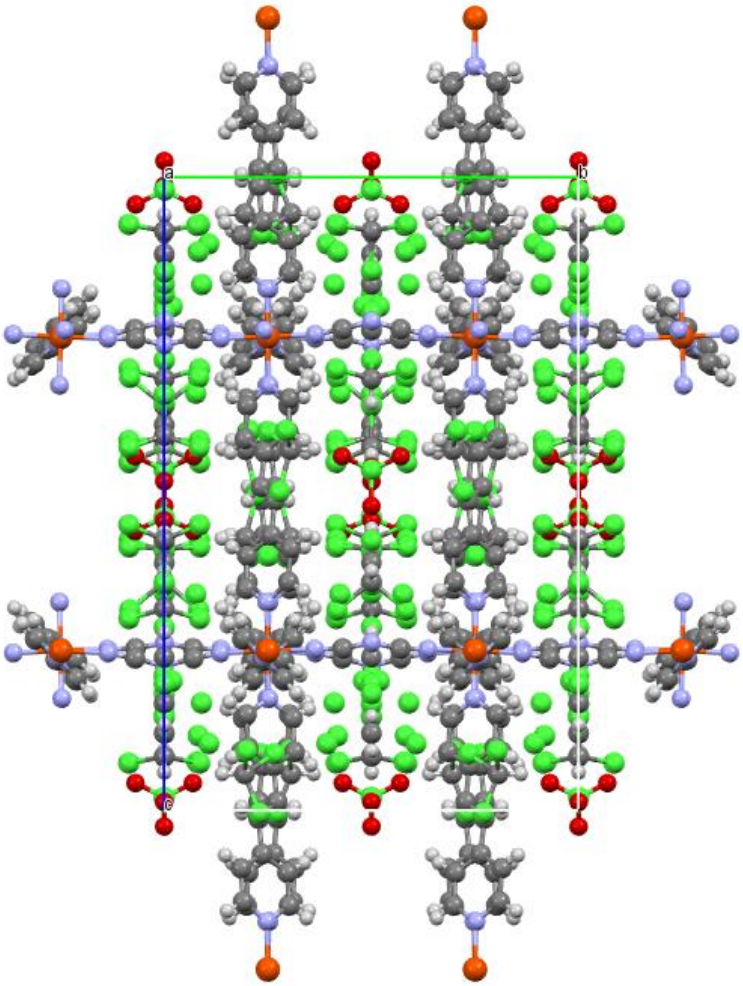

Figure 10a. Structure representation of LS6 (packing) following a axe's view. Atom labels: orange = Fe, light grey = H, dark grey = C, blue = N, red = O, green = Cl

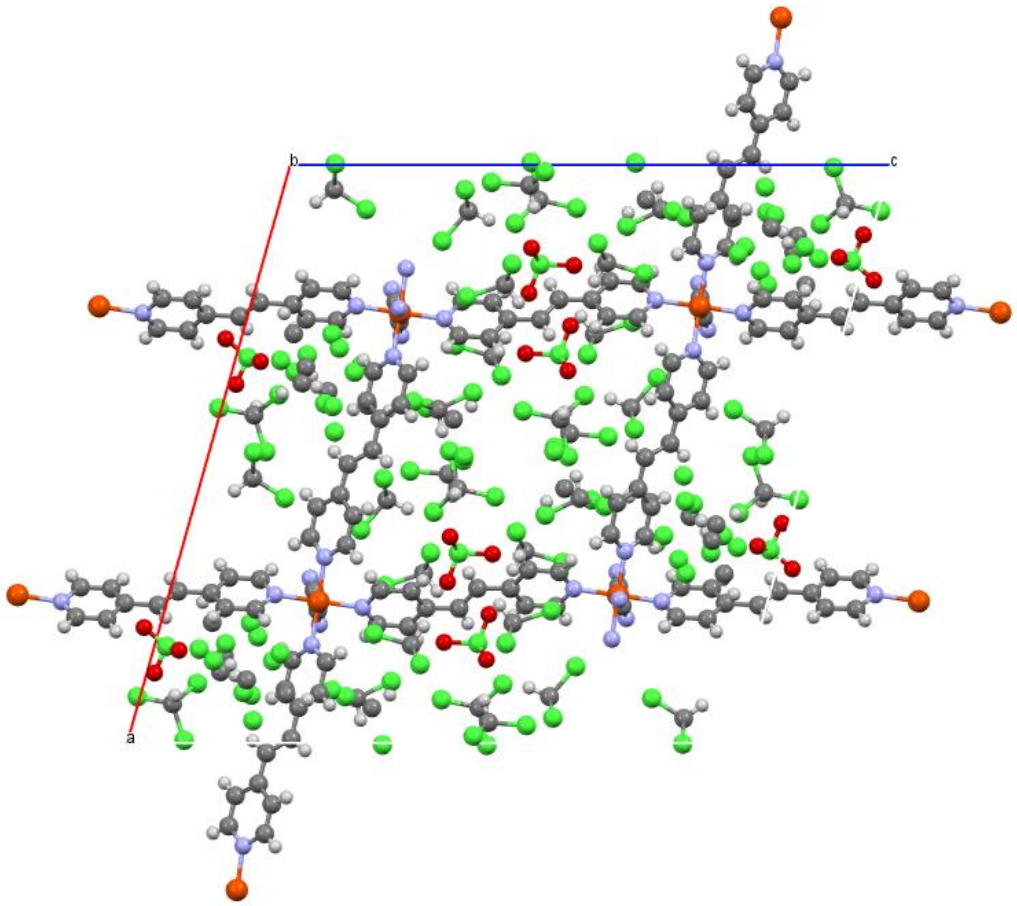

Figure 10b. Structure representation of LS6 (packing) following b axe's view. Atom labels: orange = Fe, light grey = H, dark grey = C, blue = N, red = O, green = Cl

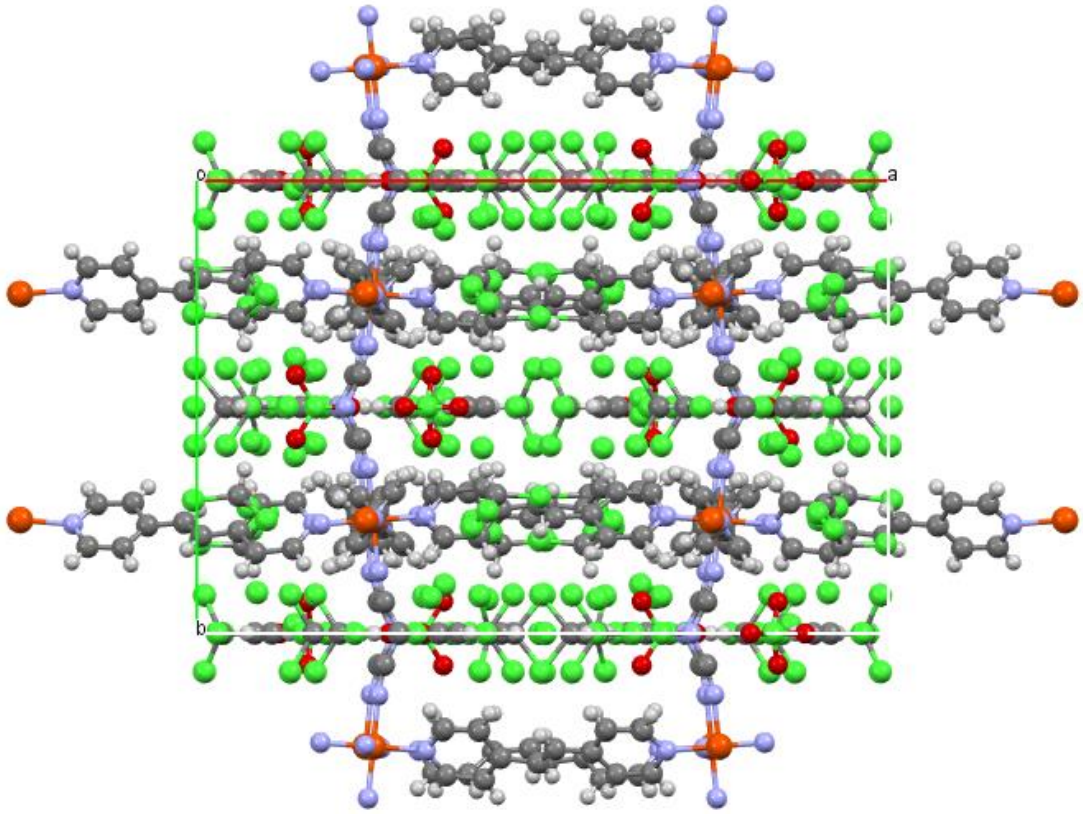

Figure 10c. Structure representation of LS6 (packing) following c axe's view. Atom labels: orange = Fe, light grey = H, dark grey = C, blue = N, red = O, green = Cl

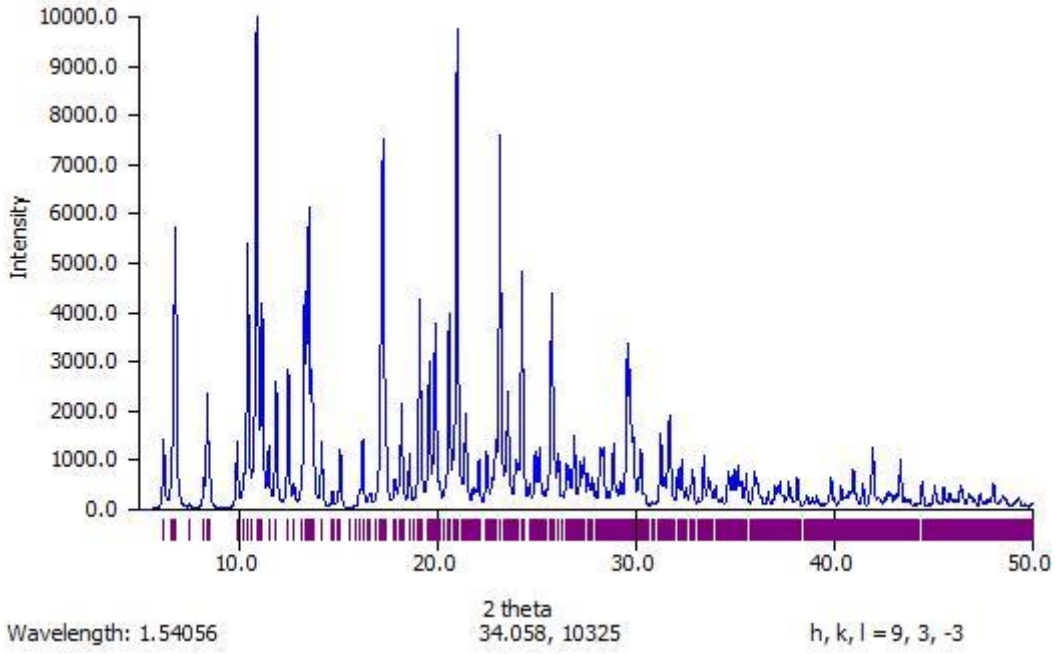

Figure 11. Powder pattern generated on Mercury based on the cif file of LS6 at 100K.

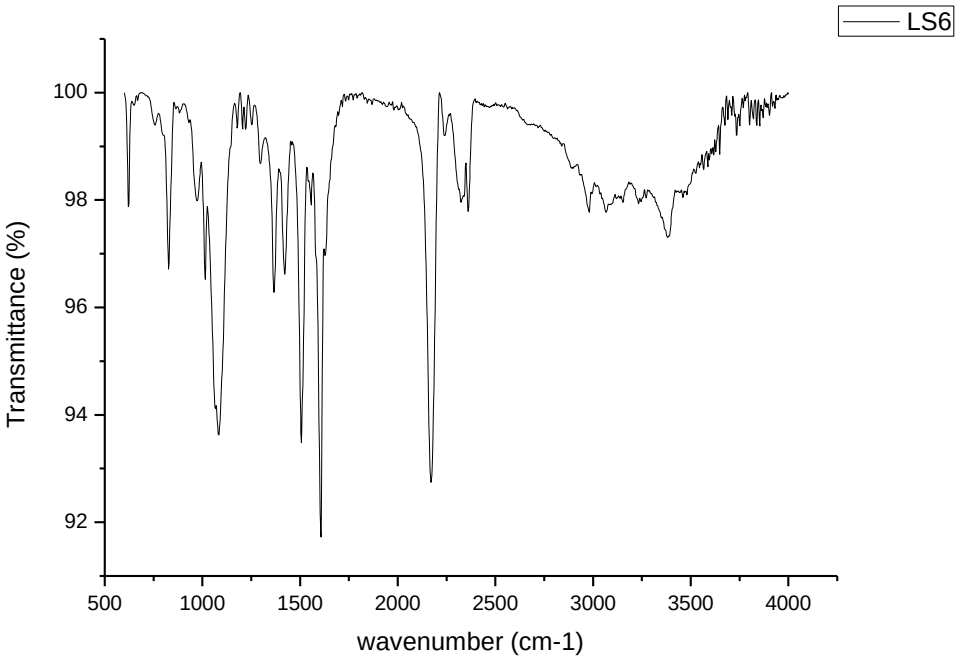

Figure 12. FT-IR for LS6 made on OriginPro. 8.5

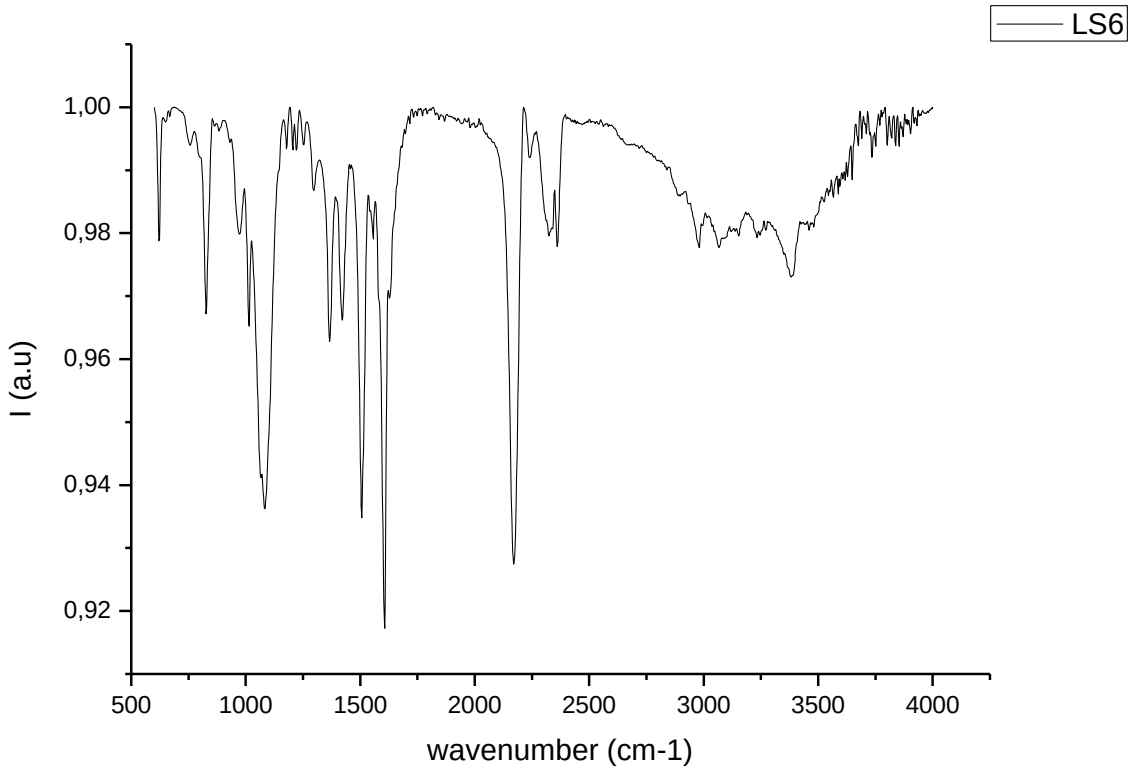

Figure 12bis. FT-IR for LS6 made on OriginPro. 8.5 with the original data

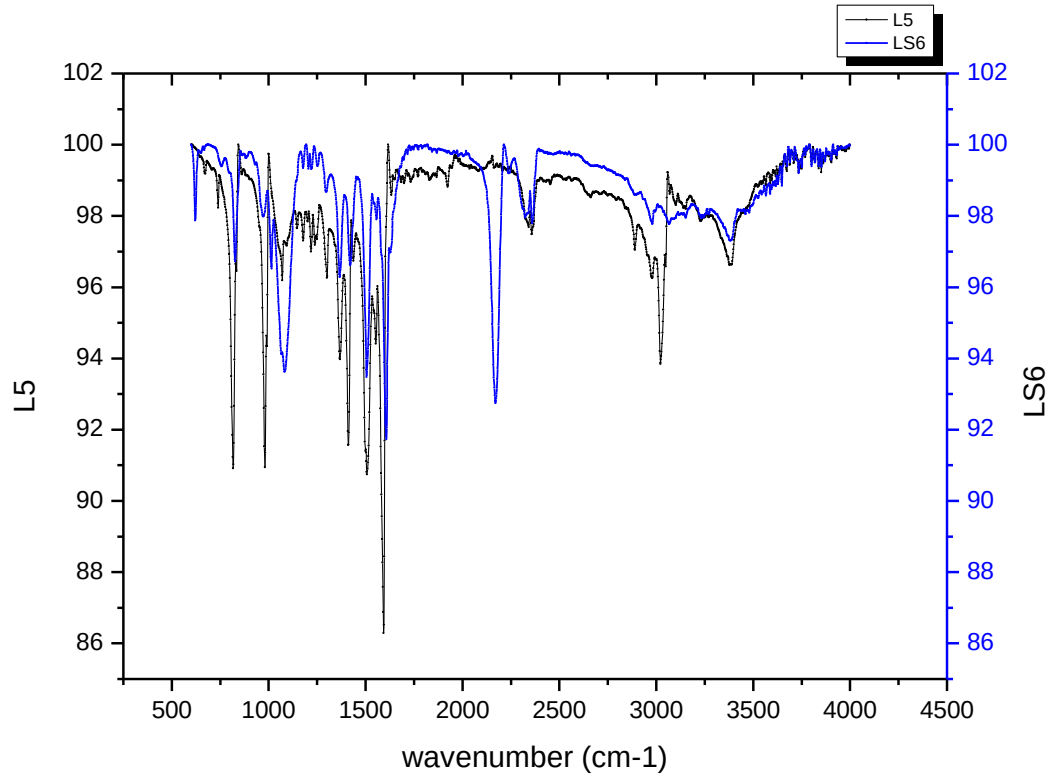

Figure 13. FT-IR for L5 and LS6 made on OriginPro. 8.5

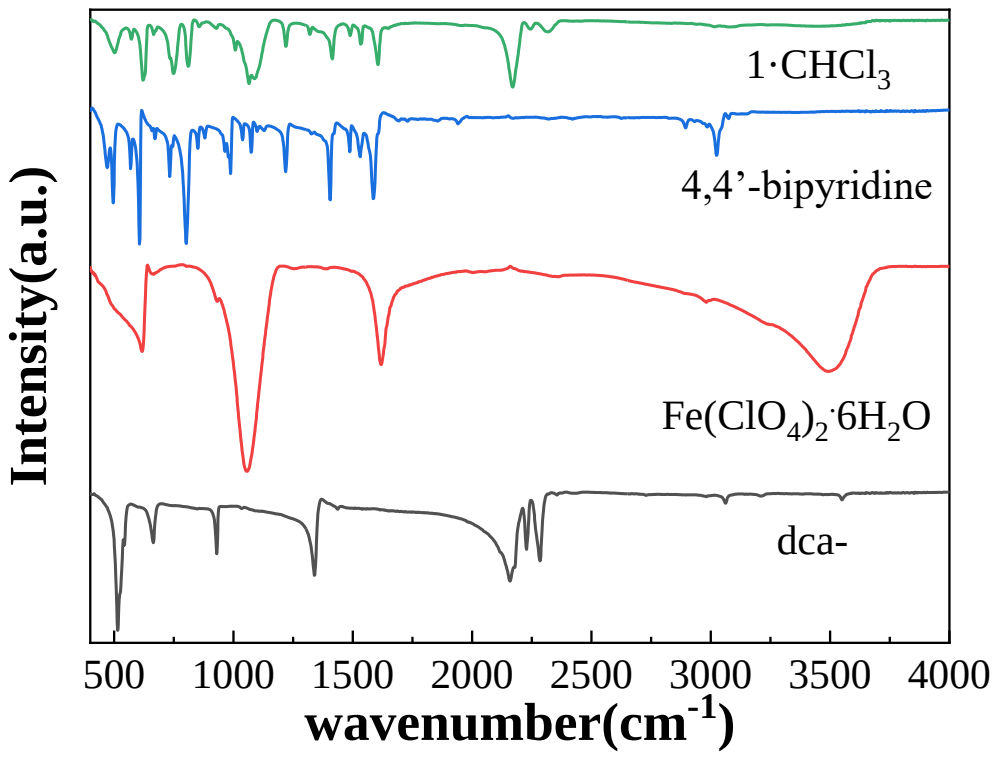

Figure 14. FT-IR for LS1 with 1 $CHCl_3$ as guest molecule and the three major reactants made on OriginPro. 8.5

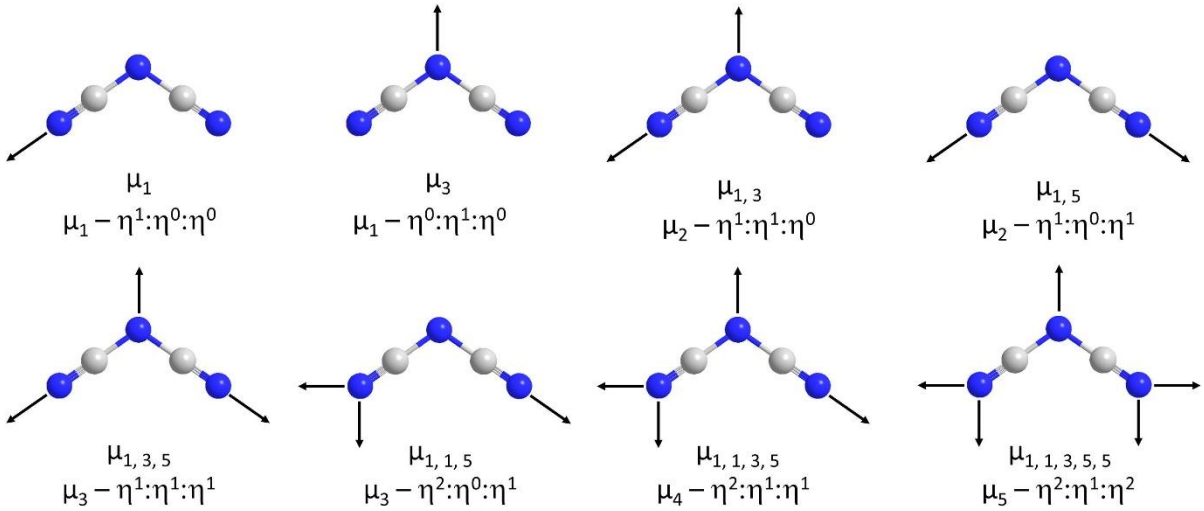

Figure 15. Coordination modes of the conjugated dca ([N≡C-N-C≡N]-) ligand observed to date. The first nomenclature is the traditional short one (most commonly used in the literature), and the second nomenclature follows the normative IUPAC recommendations. Note: N-atoms are represented in blue, and C-atoms in grey.

Source: Coordination Chemistry Reviews, Volume 455, 15 March 2022, 214337

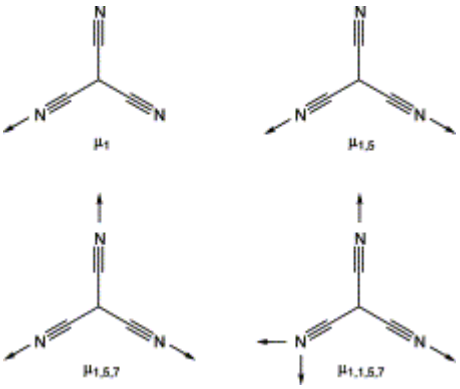

Figure 16. Tcm coordination modes observed to date.

Source : Scheme 2 Stuart R Batten, Keith S Murray, Coordination Chemistry Reviews, Volume 246, Issues 1–2, November 2003, Pages 103-130

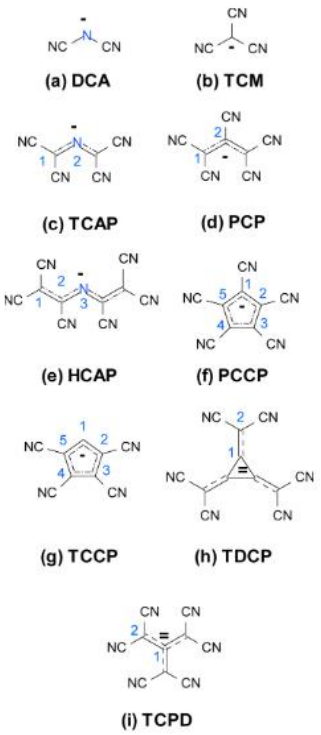

Figure 17. Polynitrile Mono- and Dianions: (a) Dicyanamide(DCA−), (b) Tricyanomethanide (TCM−), (c) Tetracyano-2-azapropenide (TCAP−), (d) 1,1,2,3,3-Pentacyanopropenide (PCP−), (e) 1,1,2,4,5,5-Hexacyano-3-azapentadienide (HCAP−), (f) 1,2,3,4,5-Pentacyanocyclopentadienide (PCCP), (g) 2,3,4,5-Tetracyanocyclopentadienide (TCCP•−), (h) 1,2,3-Tris(Dicyanomethylene)Cyclopropanediide (TDCP2−), and(i) 2-Dicyanomethylene-1,1,3,3-tetracyanopropanediide(TCPD2−)

Source : Scheme 1 Ilya A. Shkrob, Timothy W. Marin, James F. Wishart, The Journal of Physical Chemistry B, May 2013, 117 (23), pp. 7084-7094

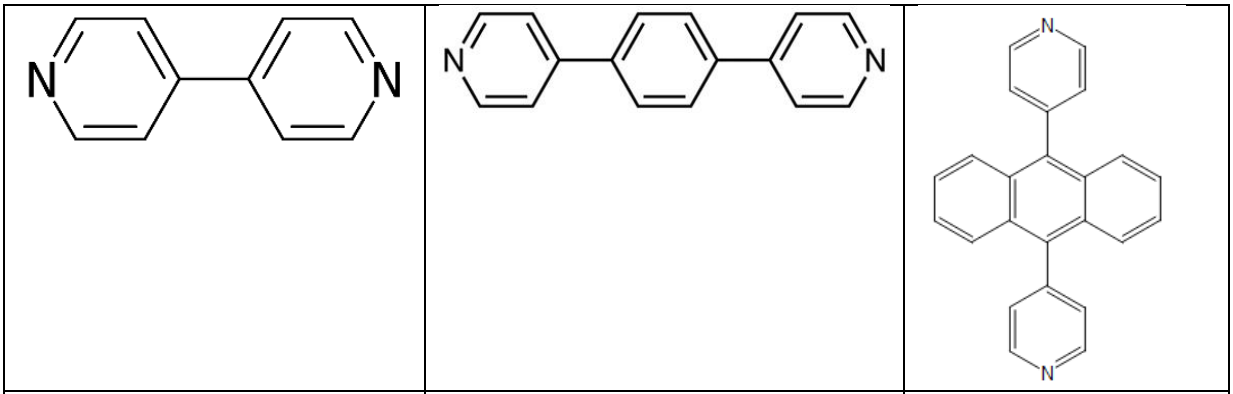

L_1	L_2	L_3

Figure 18. Structures of L_1 (4,4'-bipyridine), L_2 (1,4-bis(4-pyridyl)benzene), L_3 (4,4'-(9,10-anthracenediyl)bis-pyridine

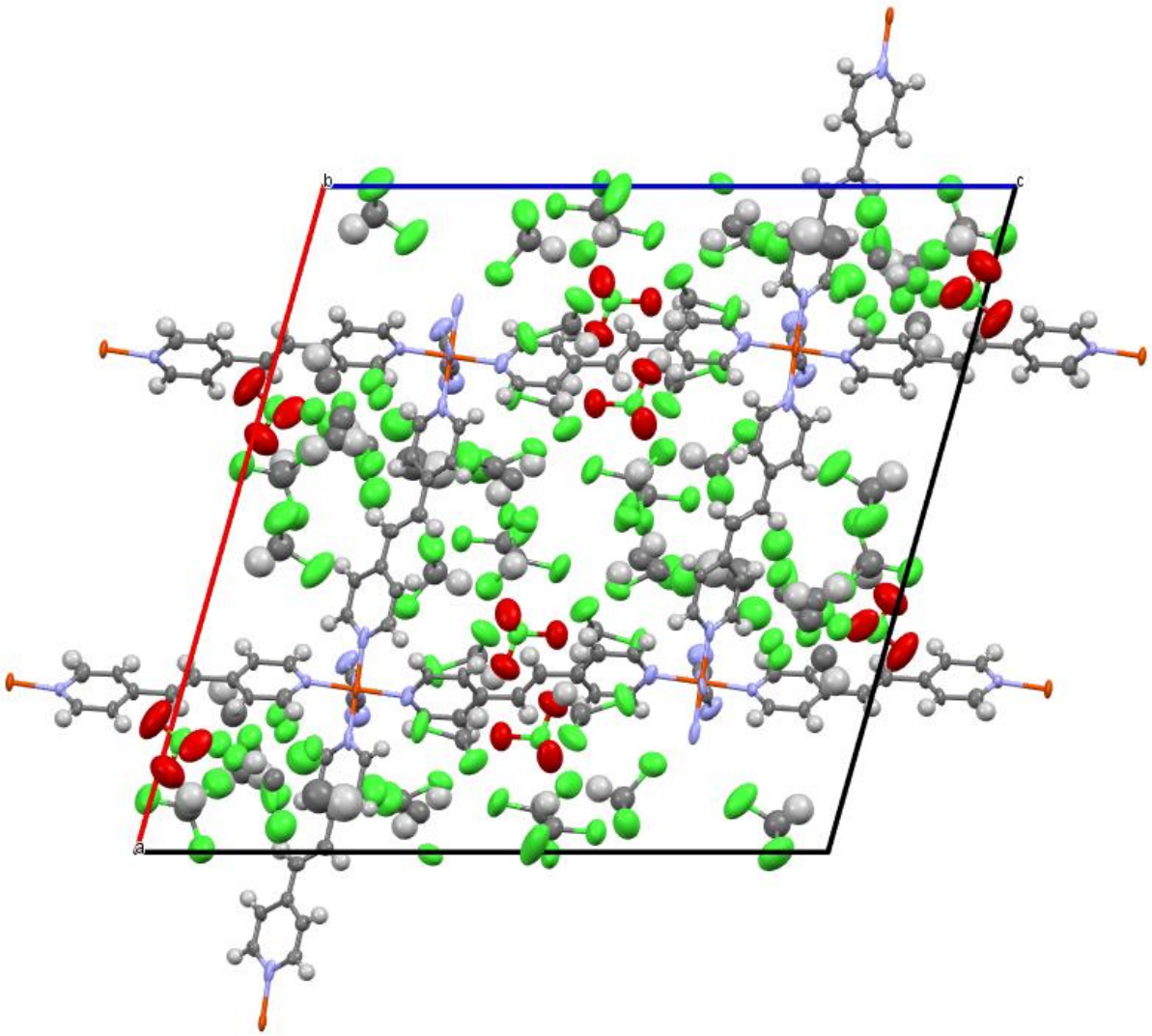

Figure 19a. Structure representation of LS6 (packing) following b axe's view. Atom labels: orange = Fe, light grey = H, dark grey = C, blue = N, red = O, green = Cl

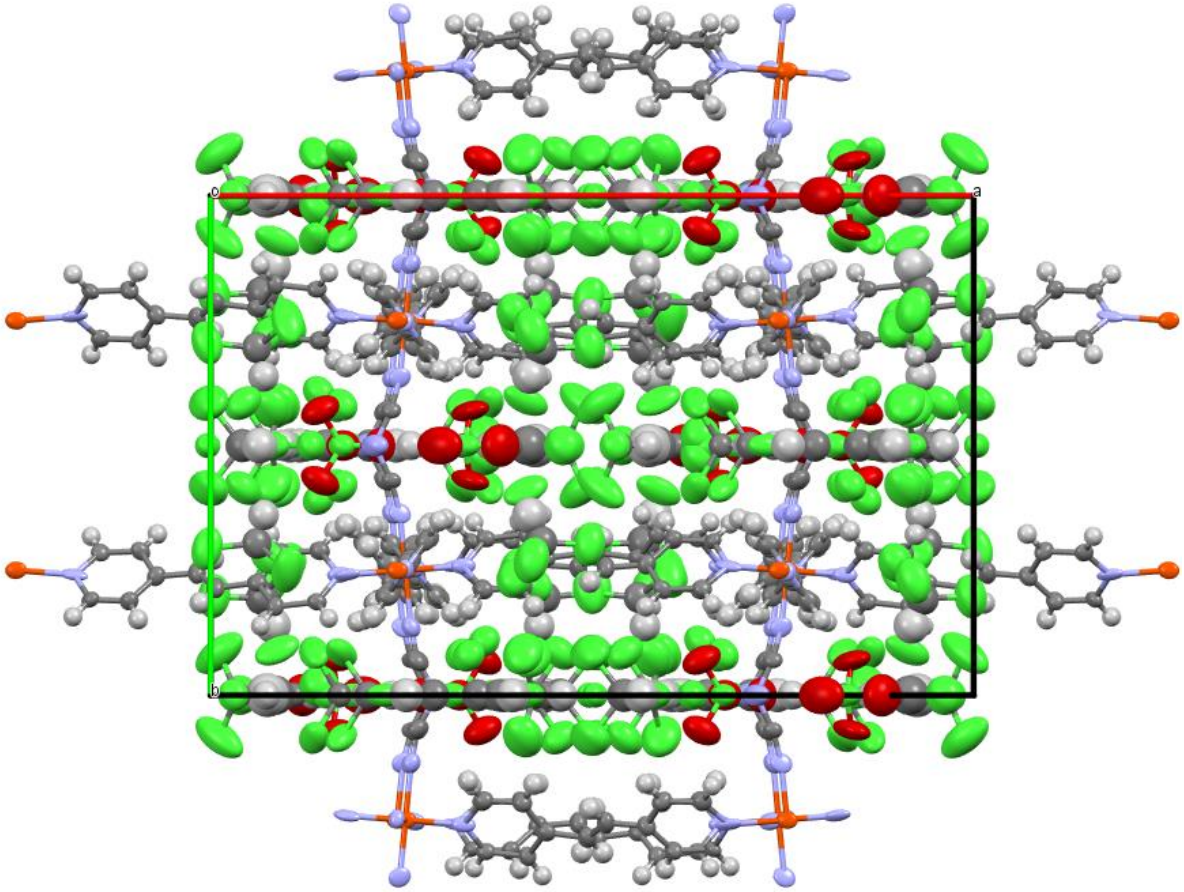

Figure 19b. Structure representation of LS6 (packing) following c axe's view. Atom labels: orange = Fe, light grey = H, dark grey = C, blue = N, red = O, green = Cl

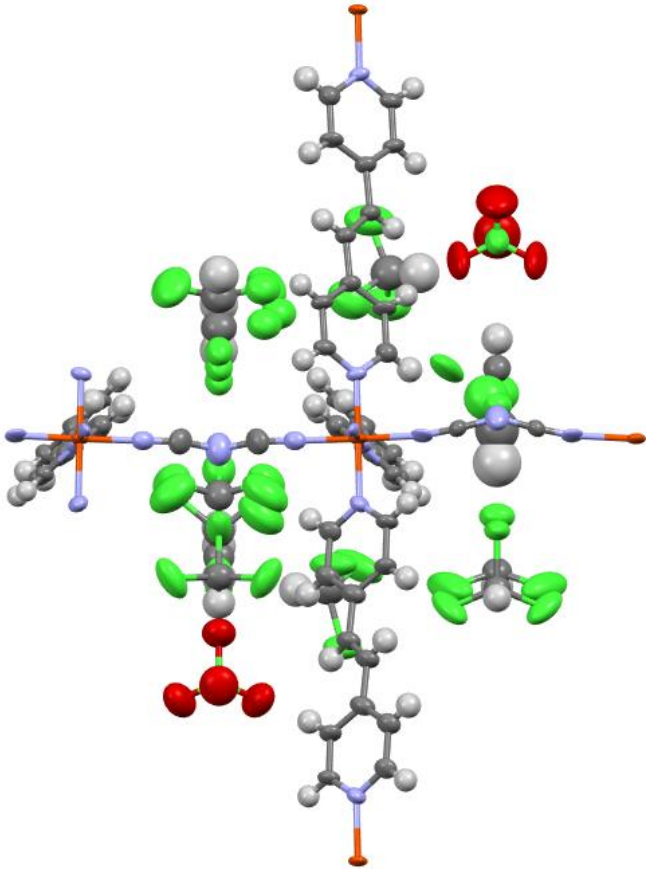

Figure 20. Structure representation of LS6 (unit cell) following a axe's view. Atom labels: orange = Fe, light grey = H, dark grey = C, blue = N, red = O, green = Cl

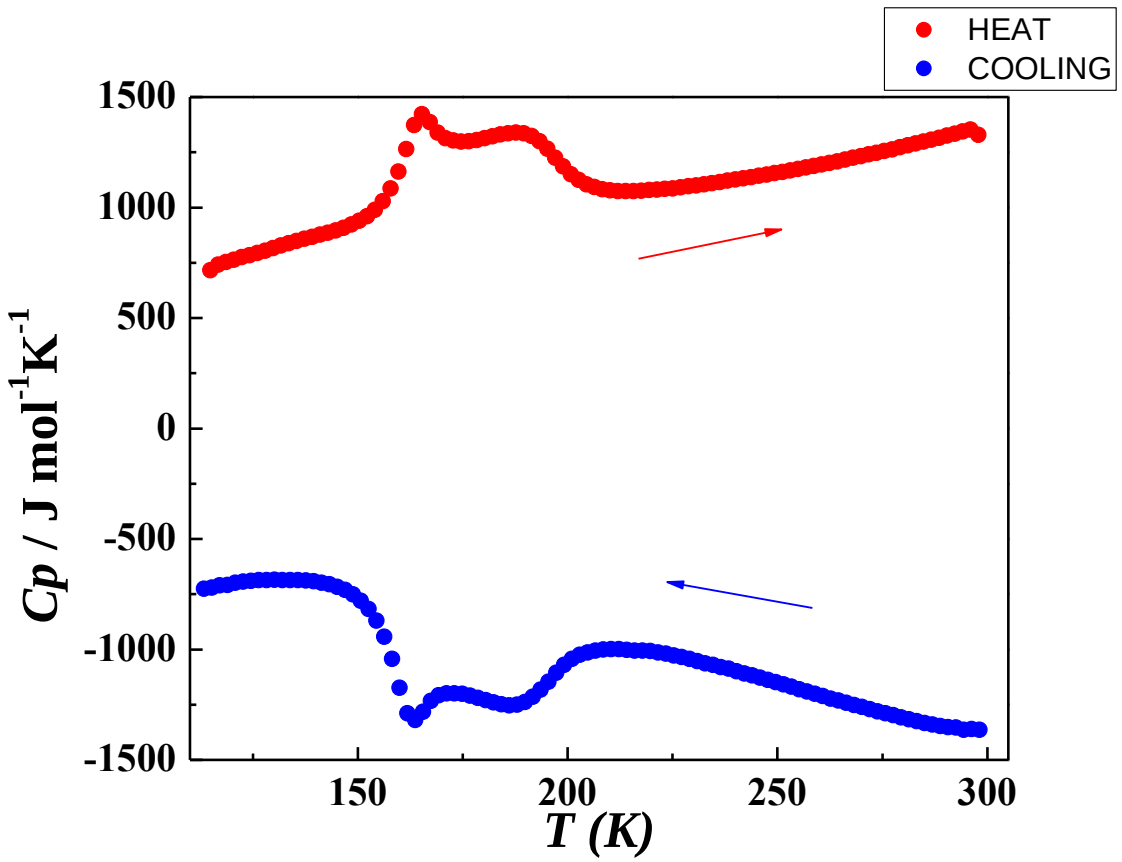

Figure 21. DSC graph for sample LS6 with the cooling branch in blue and the heating branch in red

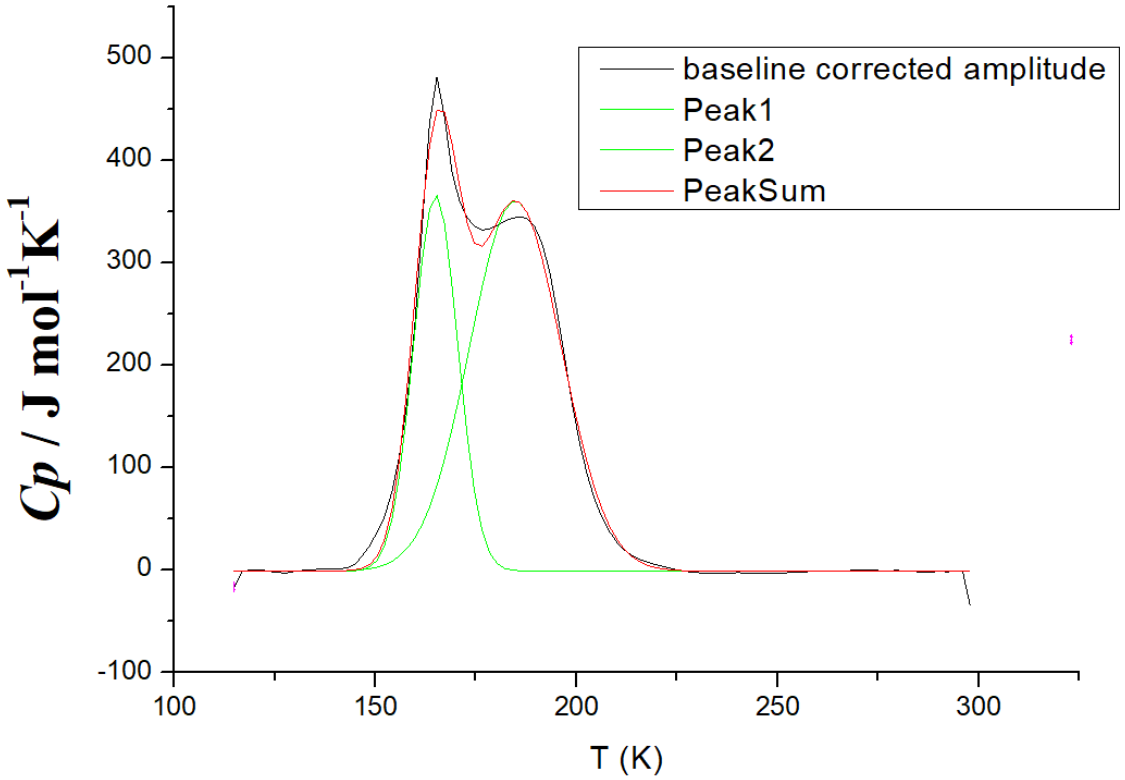

Figure 22a. DSC graph corrected and approximate by Gaussian for sample LS6 with the heating branch

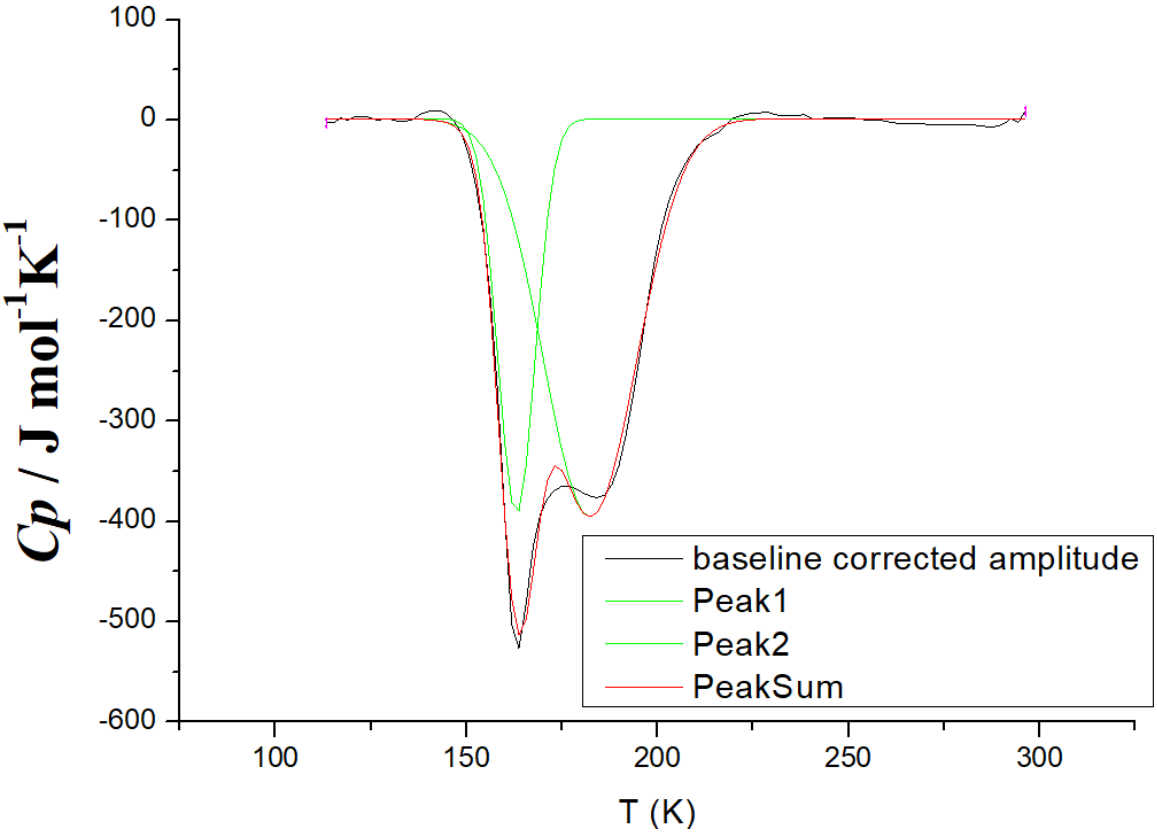

Figure 22b. DSC graph corrected and approximate by Gaussian for sample LS6 with the cooling branch

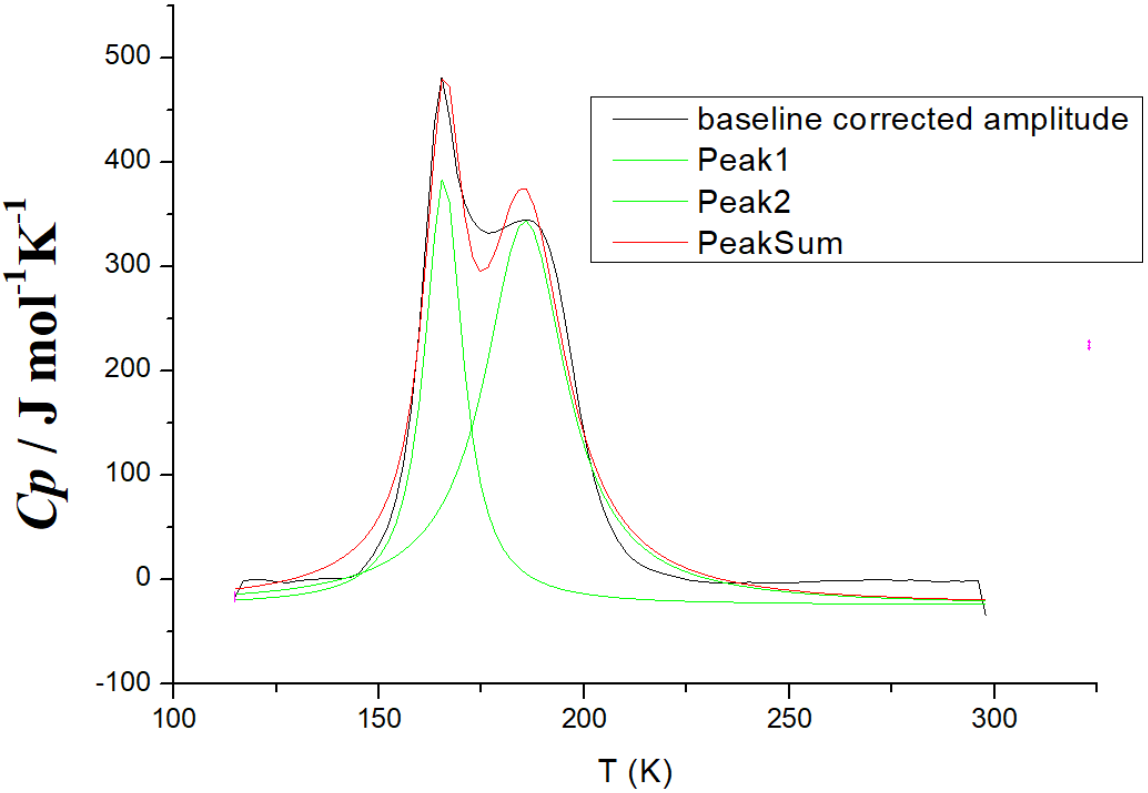

Figure 23a. DSC graph corrected and approximate by Lortenz for sample LS6 with the heating branch

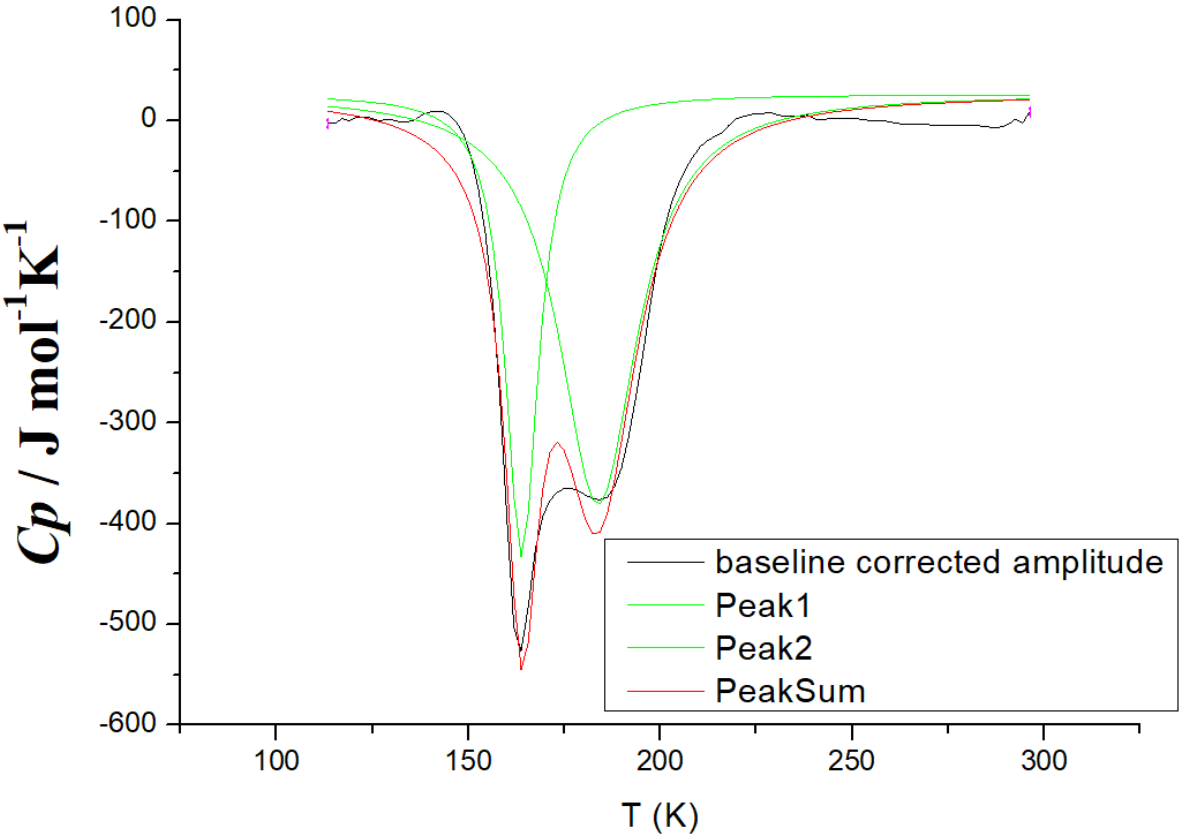

Figure 23b. DSC graph corrected and approximate by Lortenz for sample LS6 with the cooling branch

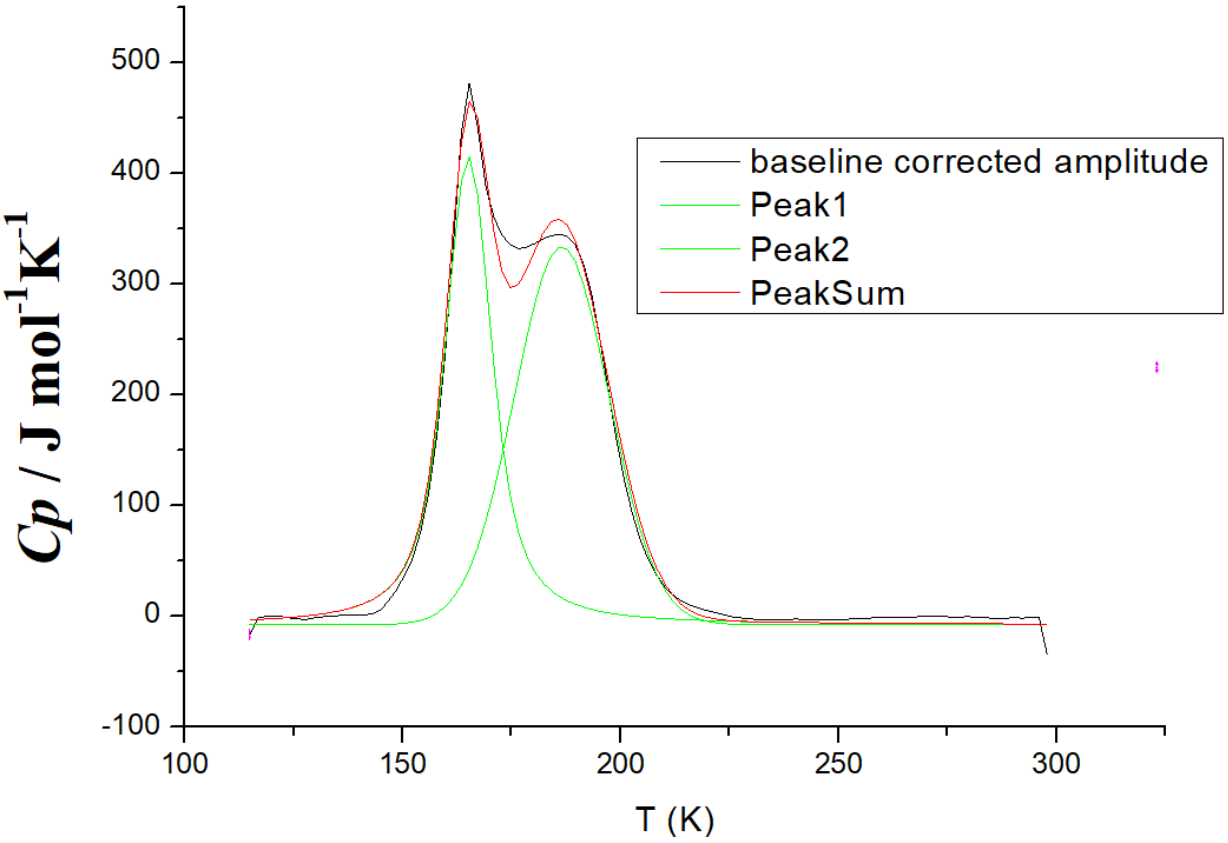

Figure 24a. DSC graph corrected and approximate by Voigt for sample LS6 with the heating

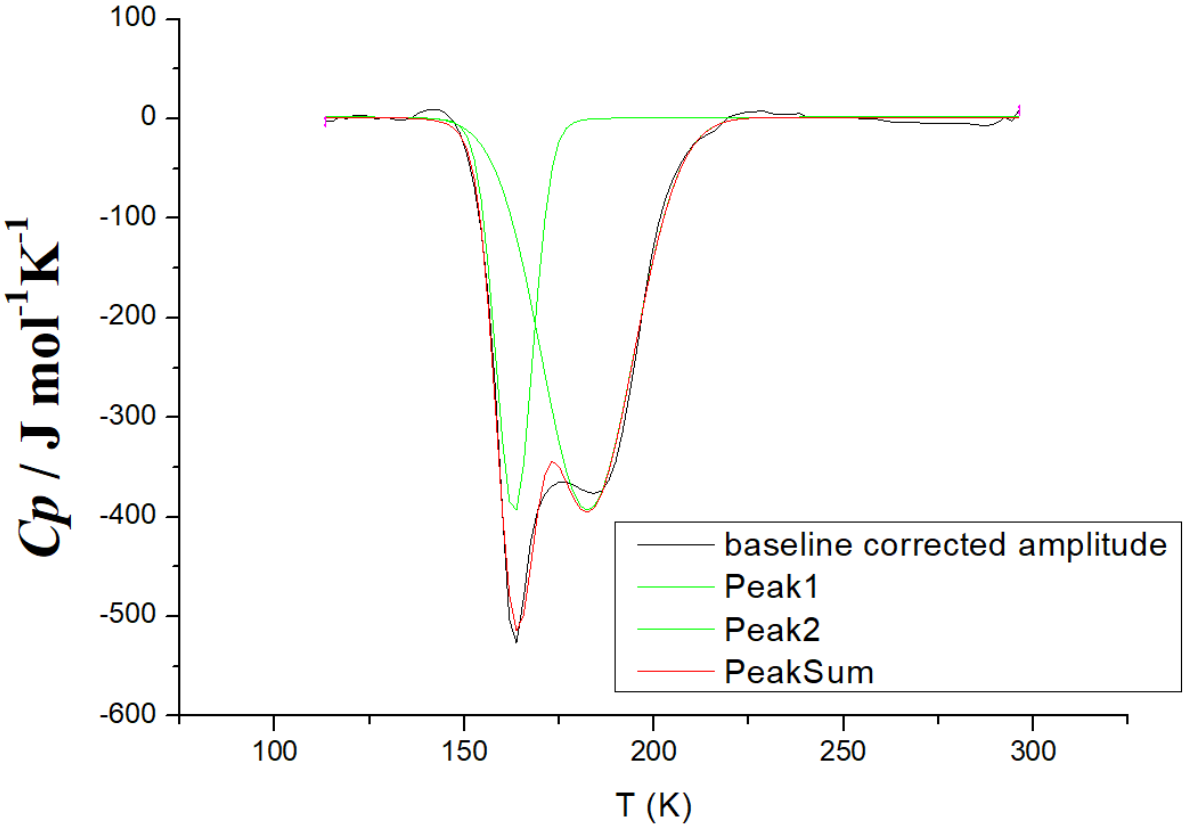

branch

Figure 24b. DSC graph corrected and approximate by Voigt for sample LS6 with the cooling branch

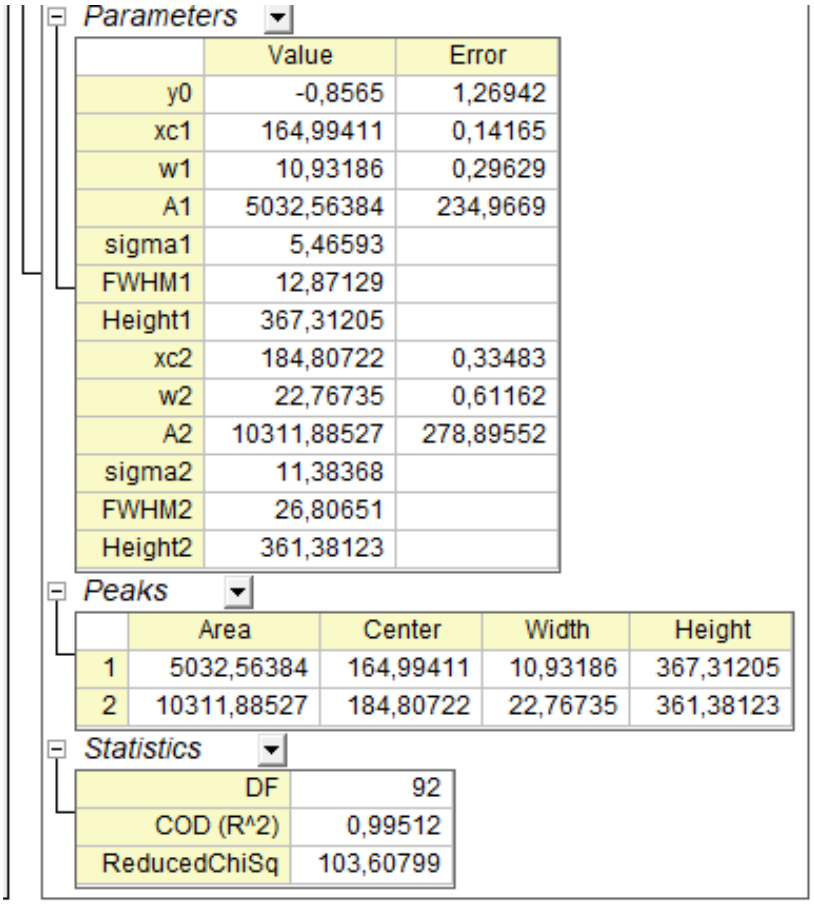

Parameters

	Value	Error
y0	-0,8565	1,26942
xc1	164,99411	0,14165
w1	10,93186	0,29629
A1	5032,56384	234,9669
sigma1	5,46593	
FWHM1	12,87129	
Height1	367,31205	
xc2	184,80722	0,33483
w2	22,76735	0,61162
A2	10311,88527	278,89552
sigma2	11,38368	
FWHM2	26,80651	
Height2	361,38123	

Peaks

	Area	Center	Width	Height
1	5032,56384	164,99411	10,93186	367,31205
2	10311,88527	184,80722	22,76735	361,38123

Statistics

DF	92
COD (R^2)	0,99512
ReducedChiSq	103,60799

Figure 25a. Data from the DSC approximation by Gauss for sample LS6 with the heating branch

Parameters

	Value	Error
y0	1,41512	1,17184
xc1	163,09277	0,09386
w1	9,77649	0,24173
A1	-4831,20497	203,40258
sigma1	4,88825	
FWHM1	11,51094	
Height1	-394,28706	
xc2	182,37593	0,27987
w2	24,39006	0,51971
A2	-12131,2899	260,79633
sigma2	12,19503	
FWHM2	28,7171	
Height2	-396,85718	

Peaks

	Area	Center	Width	Height
1	-4831,20497	163,09277	9,77649	-394,28706
2	-12131,2899	182,37593	24,39006	-396,85718

Statistics

DF	92
COD (R^2)	0,99667
ReducedChiSq	85,72678

Figure 25b. Data from the DSC approximation by Gauss for sample LS6 with the heating branch

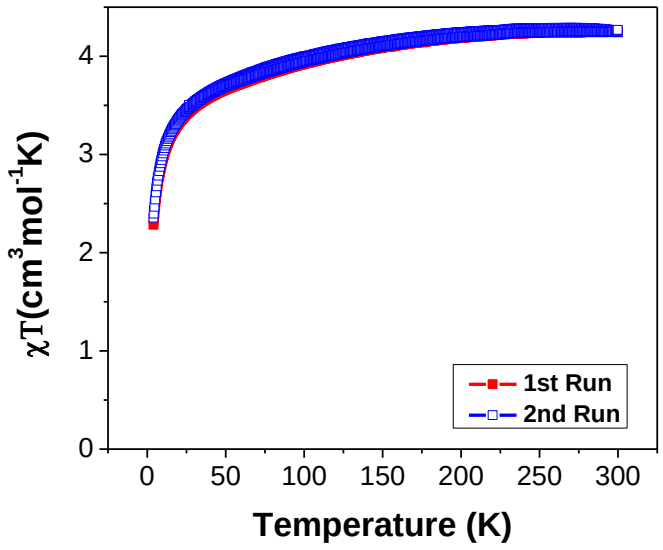

Figure 26a. SQUID graph with two different runs for fresh LS6 humidified by solvent, 2K/min, m = 6,29 mg

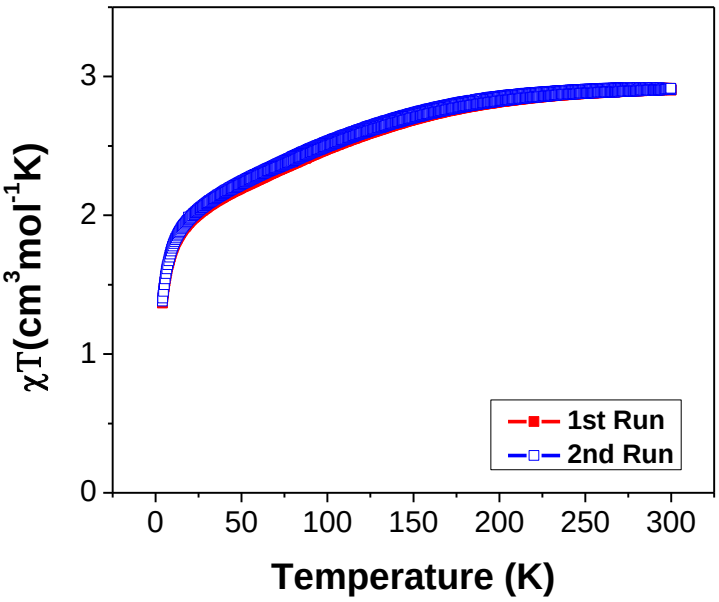

Figure 26b. SQUID graph with two different runs for fresh LS6 non humidified by solvent, 2K/min, m = 6,23 mg

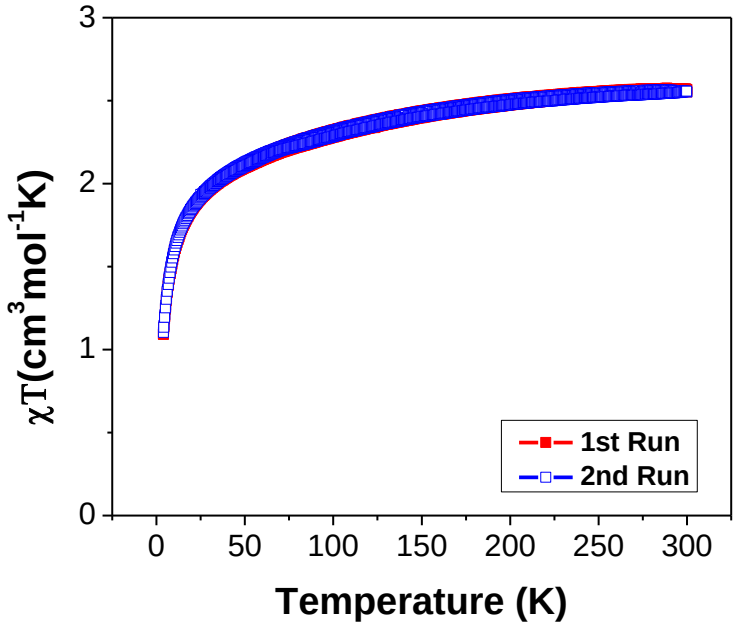

Figure 26c. SQUID graph with two different runs for fresh LS6 non humidified by solvent, 2K/min, m = 9,11 mg

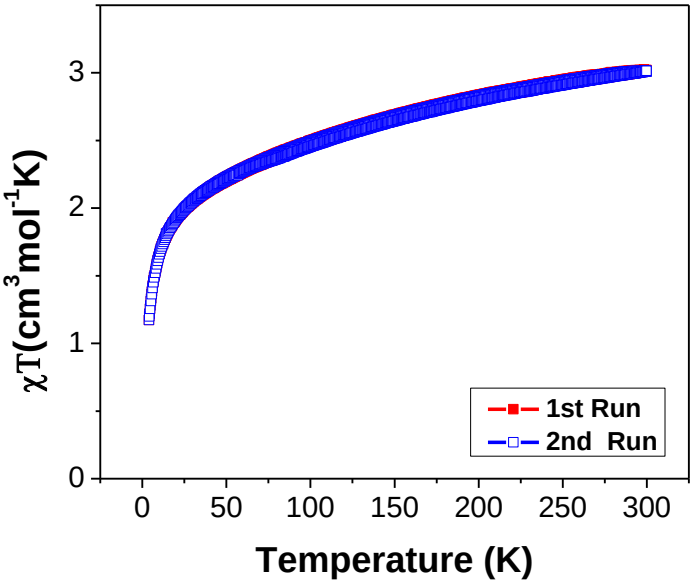

Figure 26d. SQUID graph with two different runs for fresh LS6 non humidified by solvent, 2K/min, m = 6,26 mg

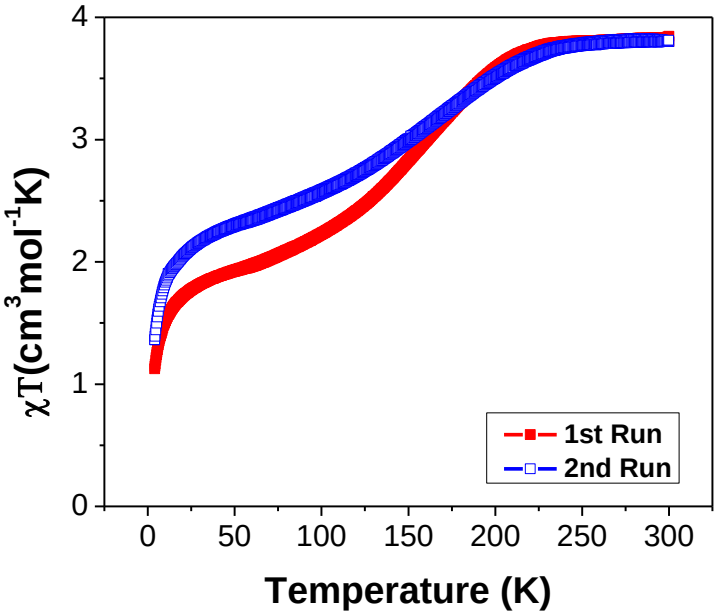

Figure 26e. SQUID graph with two different runs for fresh LS6 humidified by solvent, 2K/min, m = 7,05 mg

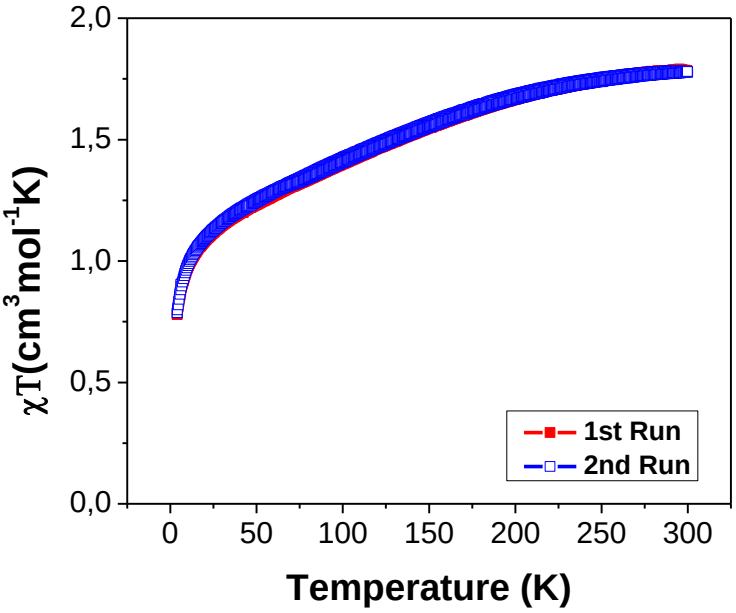

Figure 26f. SQUID graph with two different runs for fresh LS6 non humidified by solvent, 2K/min, m = 4,24 mg

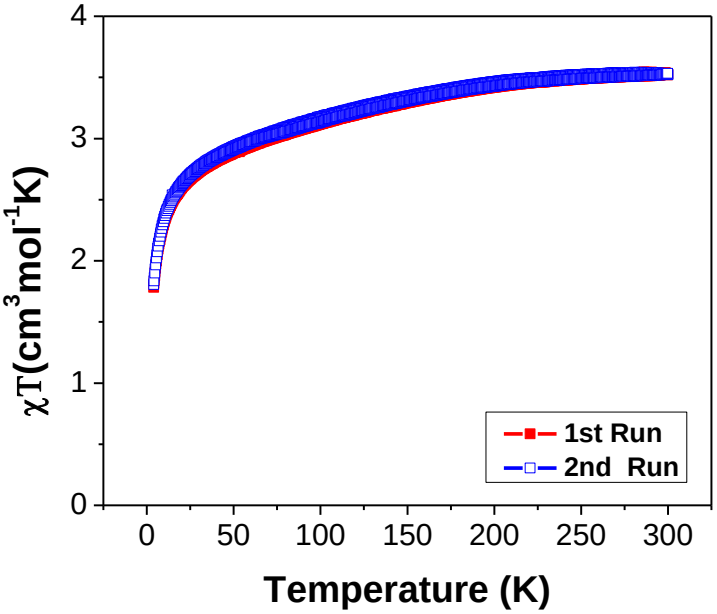

Figure 26g. SQUID graph with two different runs for fresh LS6 non humidified by solvent, 2K/min, m = 4,64 mg

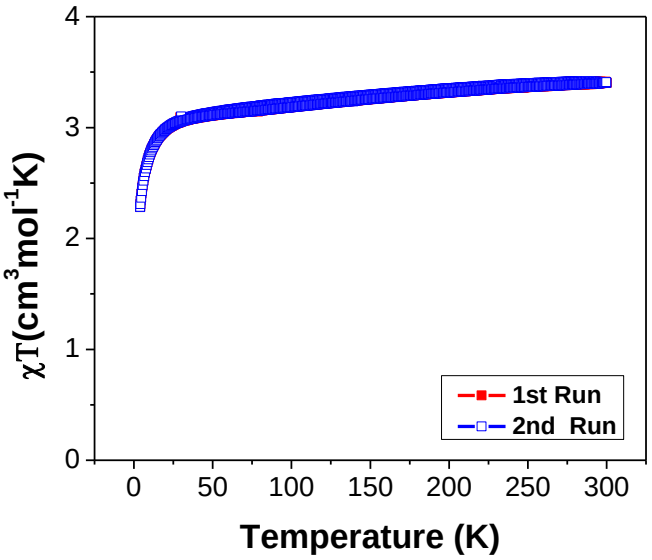

Figure 26h. SQUID graph with two different runs for fresh LS6 non humidified by solvent, 2K/min, m = 6,99 mg

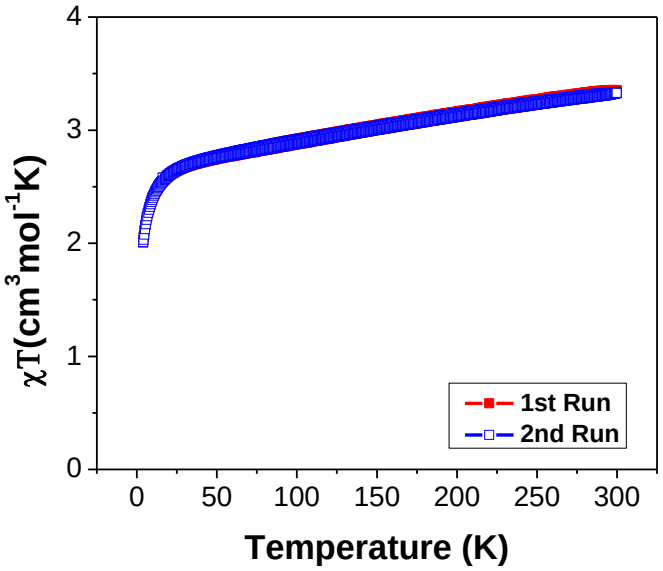

Figure 26i. SQUID graph with two different runs for fresh LS6 non humidified by solvent, 2K/min, m = 5,56 mg

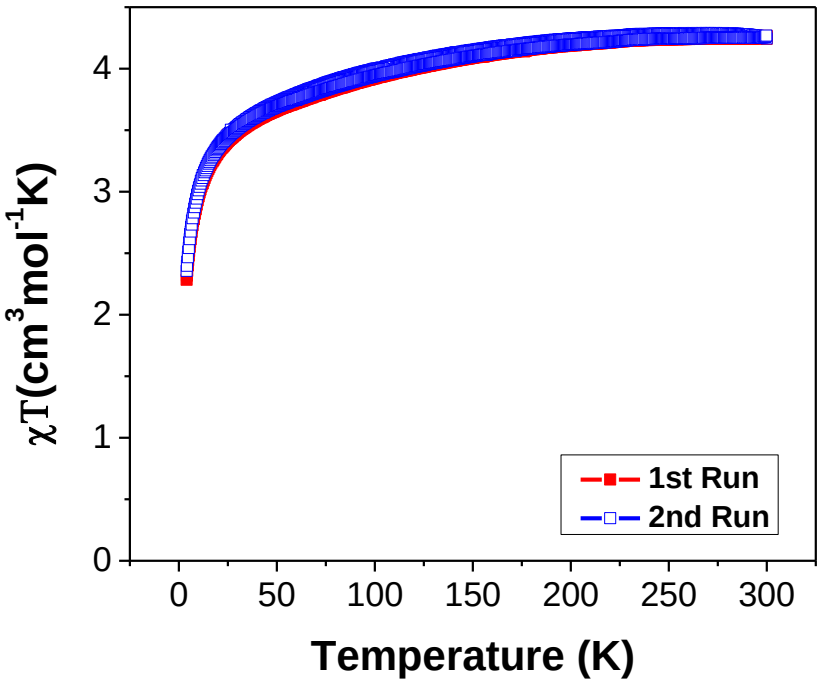

Figure 27a. SQUID graph with two different runs for LS6 at RT 1 day humidified by solvent, 2K/min, m = 6,29 mg

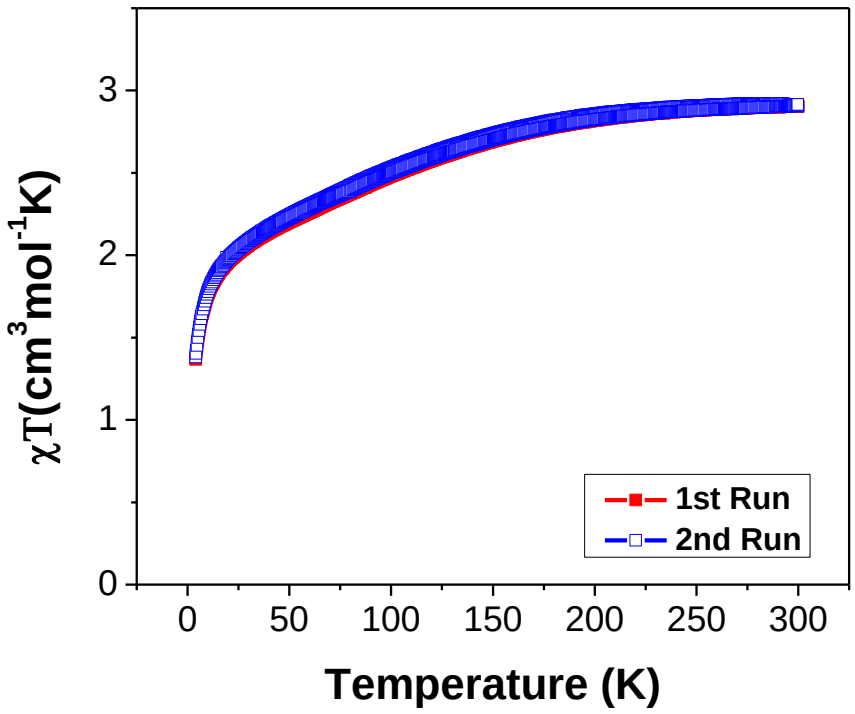

Figure 27b. SQUID graph with two different runs for LS6 at RT 1 day non humidified by solvent, 2K/min, m = 6,23 mg

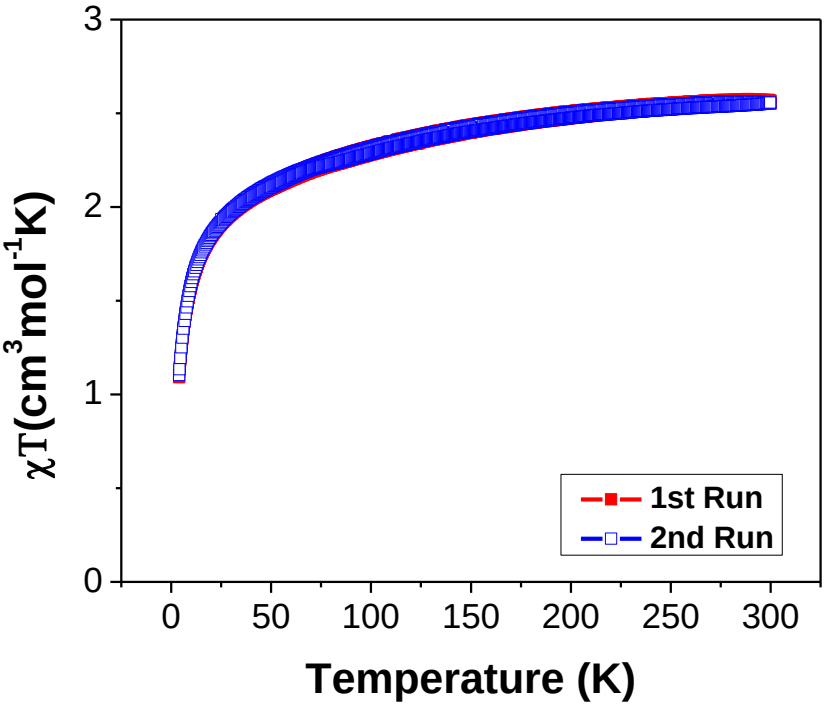

Figure 27c. SQUID graph with two different runs for LS6 at RT 1 day non humidified by solvent, 2K/min, m = 9,11 mg

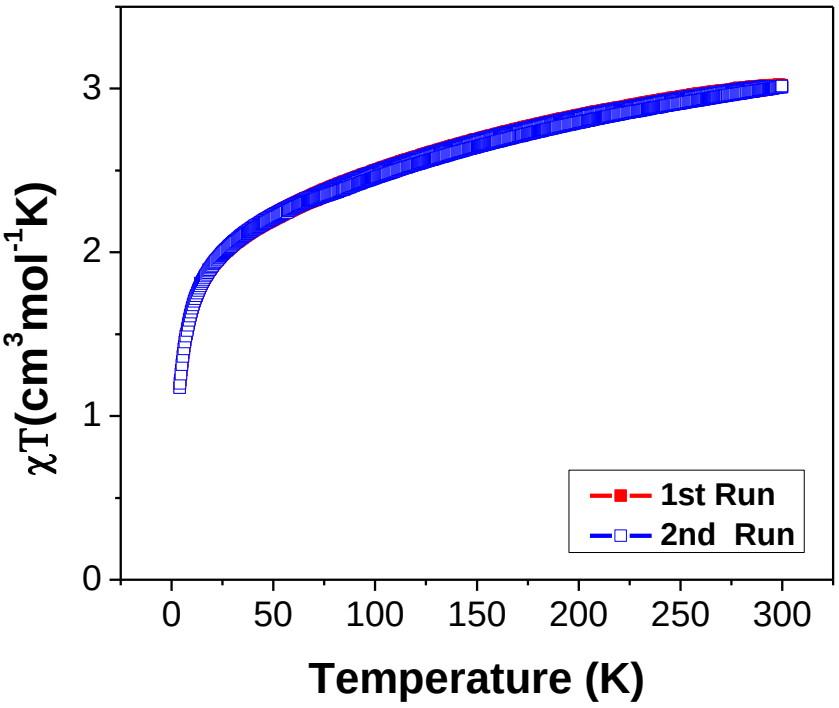

Figure 27d. SQUID graph with two different runs for LS6 at RT 1 day non humidified by solvent, 2K/min, m = 6,26 mg

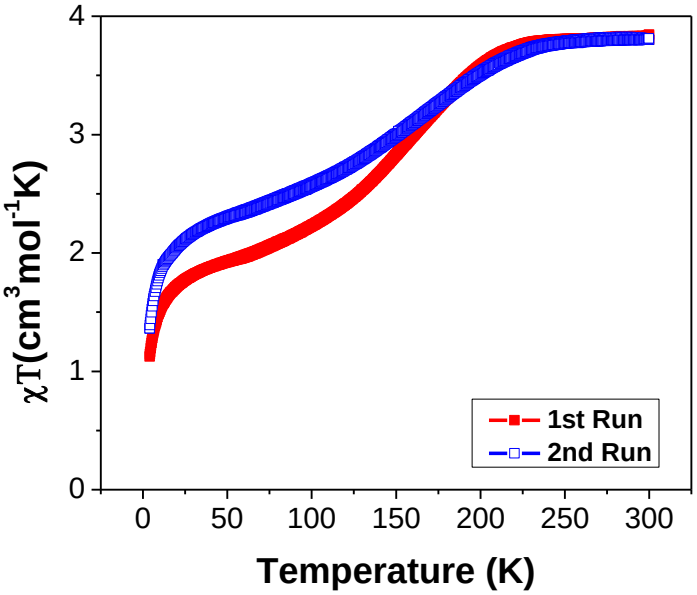

Figure 27e. SQUID graph with two different runs for LS6 at RT 1 day humidified by solvent, 2K/min, m = 7,05 mg

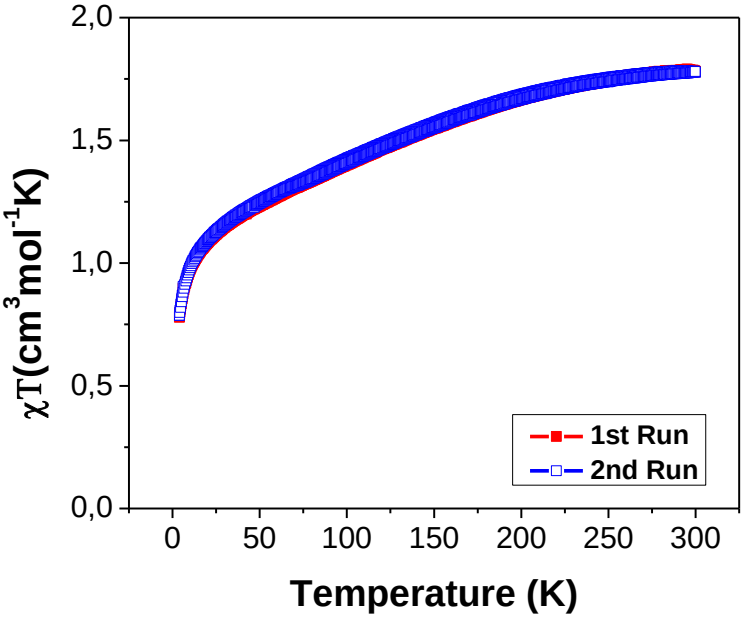

Figure 27f. SQUID graph with two different runs for LS6 at RT 1 day non humidified by solvent, 2K/min, m = 4,24mg

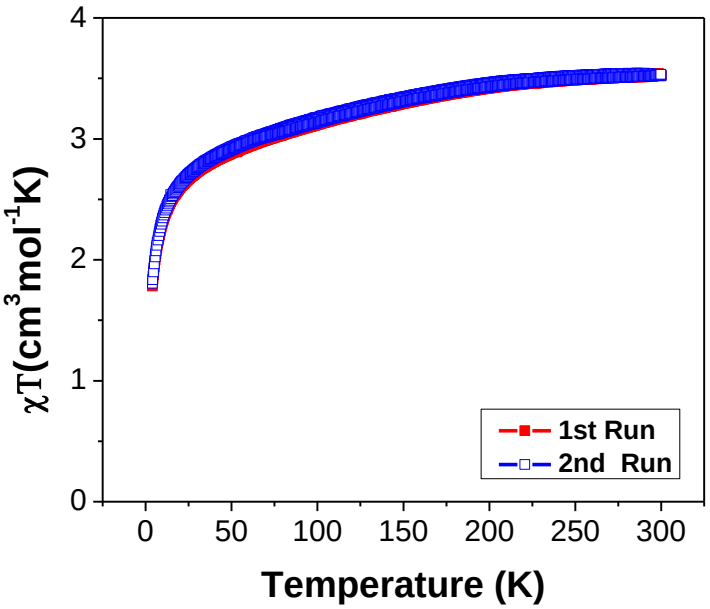

Figure 27g. SQUID graph with two different runs for LS6 at RT 1 day non humidified by solvent, 2K/min, m = 4,64 mg

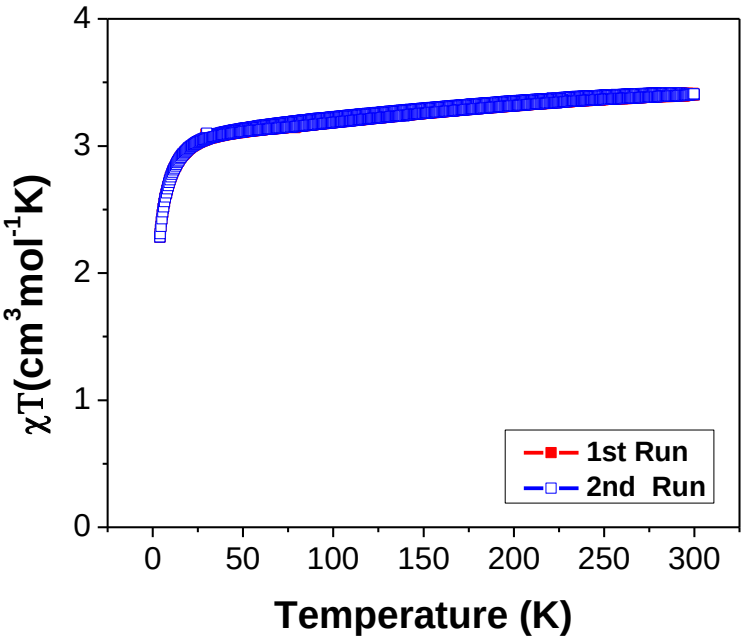

Figure 27h. SQUID graph with two different runs for LS6 at RT 1 day non humidified by solvent, 2K/min, m = 6,99 mg

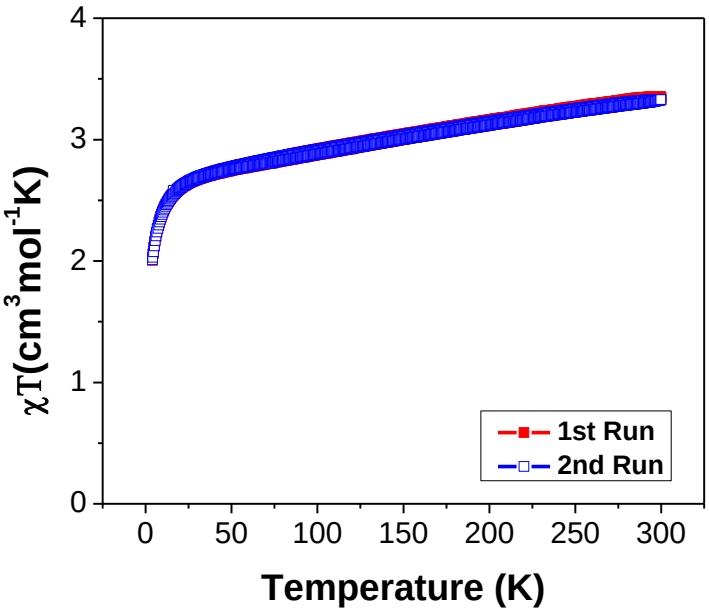

Figure 27i. SQUID graph with two different runs for LS6 at RT 1 day non humidified by solvent, 2K/min, m = 5,56 mg

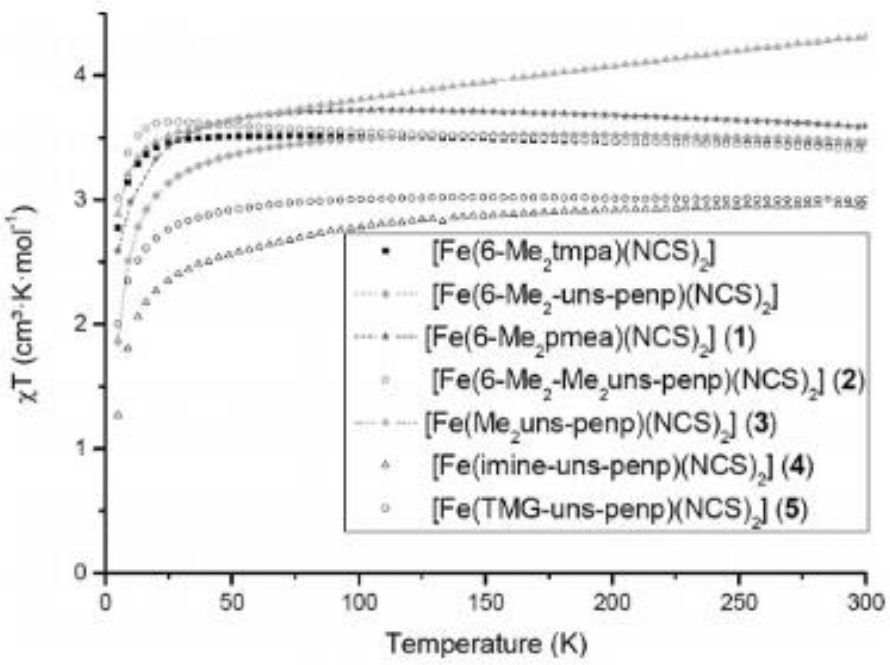

Figure 28. SQUID measurements of compounds 1–5, as well as of [Fe(6-Me_2tmpa)$(NCS)_2$] and [Fe(6-Me_2-uns-penp)$(NCS)_2$] (coolingmode) between 300 K and 5 K

Source : Sandra Kisslinger, Harald Kelm, Sipeng Zheng, Alexander Beitat, Christian Würtele, Ramona Wortmann, Sylvestre Bonnet, Sonja Herres-Pawlis, Hans-Jörg Krüger, and Siegfried Schindler, Z. Anorg. Allg. Chem. 2012, 638, (12-13), 2069–2077

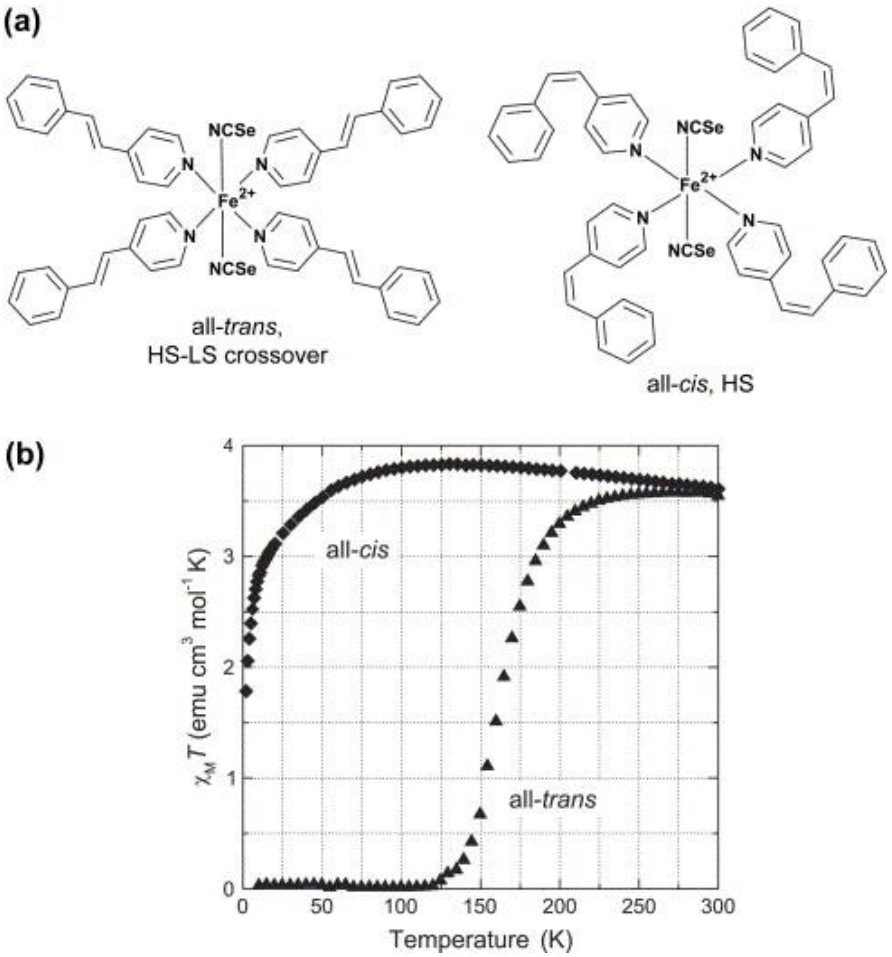

Figure 29. (a) Compounds under study, Fe(stpy)4(NCSe)2, with synthetically prepared all-trans or all-cis stpy isomer conformations. (b) Corresponding SQUID magnetization curves vs temperature.

Source: Johanna S. Kolb, Mark D. Thomson, Miljenko Novosel, Katell Sénéchal-David, Éric Rivière, Marie-Laure Boillot, Hartmut G. Roskos, Comptes Rendus Chimie, Volume 10, Issues 1–2, January–February 2007, Pages 125-136

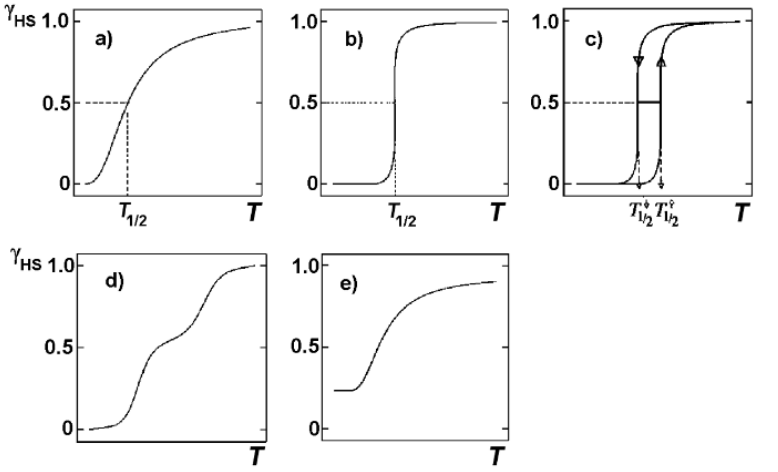

Figure 2: Types of spin transition curves in terms of the molar fraction of HS molecules, $\gamma_{HS}(T)$, as a function of temperature [23]. (Reproduced with permission from [27]. Copyright 2003 Wiley-VCH Verlag GmbH & Co. KGaA).

Figure 30. Types of spin transition curves in terms of the molar fraction of HS molecules, γHS(T), as a function of temperature

Source: Figure 2 of "Spin state switching in iron coordination compounds", Philipp Gütlich, Ana B. Gaspar, Yann Garcia, Beilstein Journal of Organic Chemistry, 2013, 9, 342-391

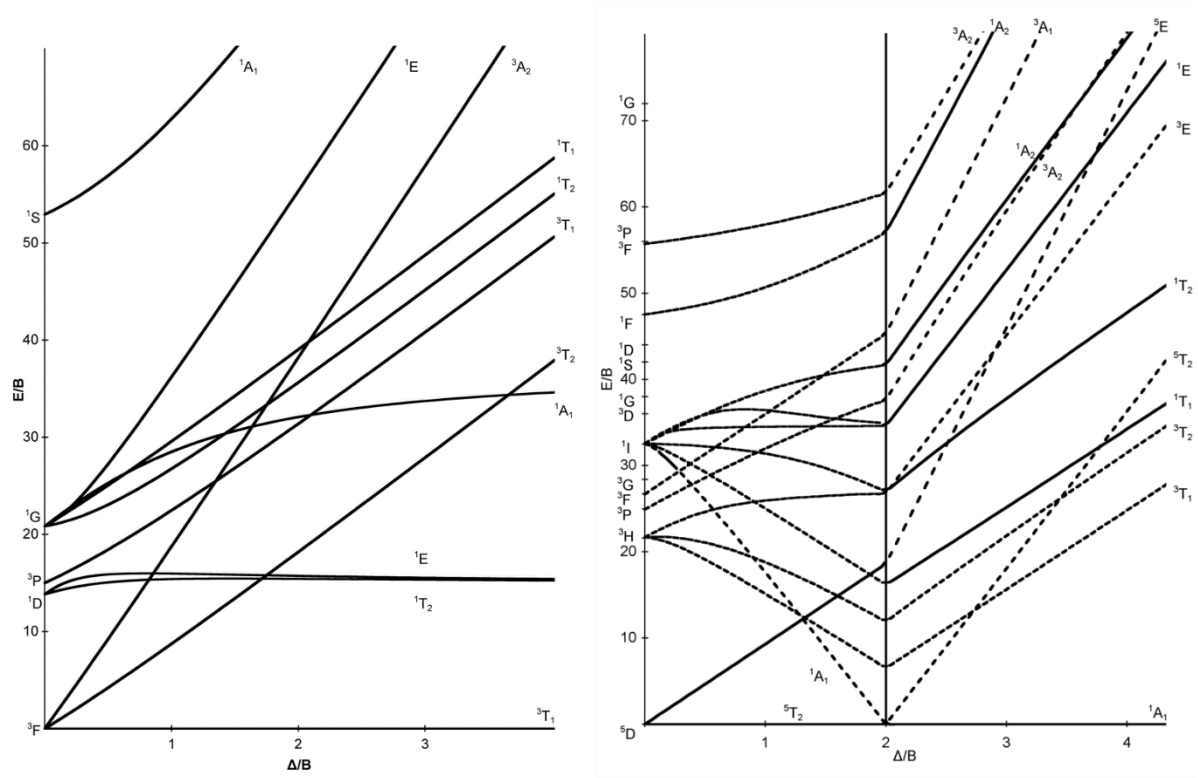

Figure 31. Tanabe-Sugano diagram for electronic configurations: respectively d^2 and d^6

Source : Wikipedia.org

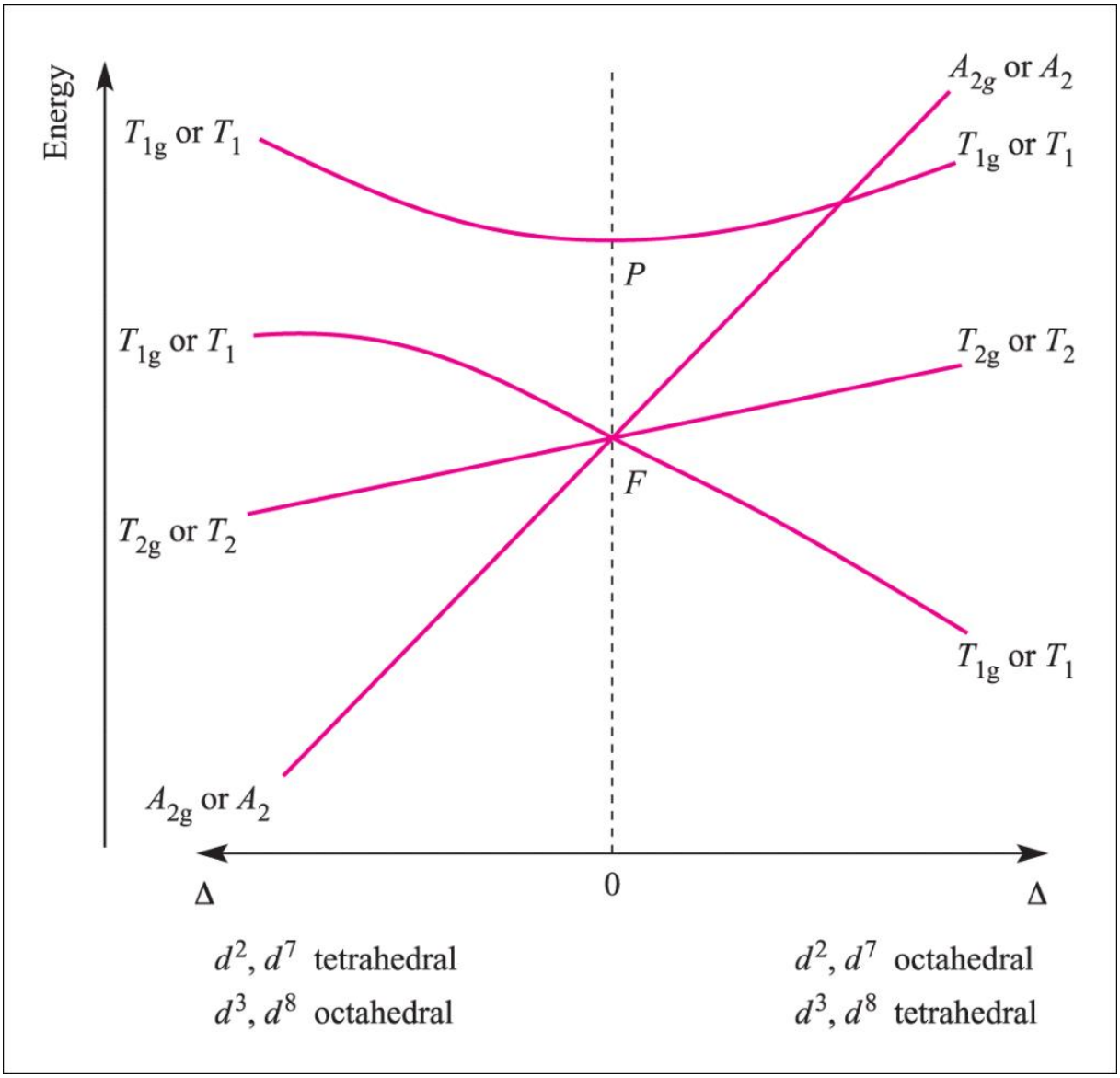

Figure 32. Orgel diagram for electronic configurations: respectively d^2/d^7 and d^3/d^8

Source : Chegg.com

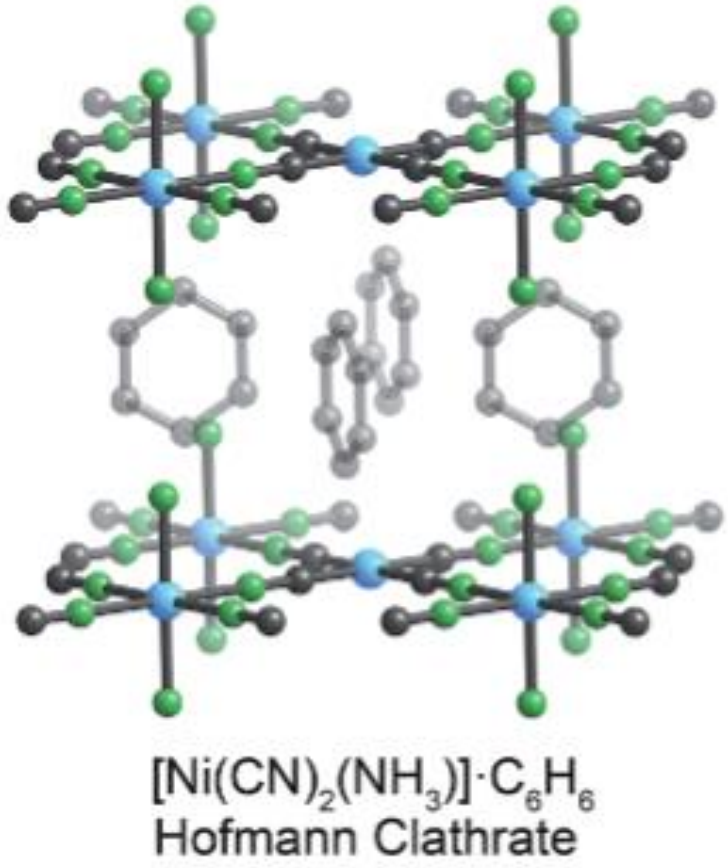

Figure 33. Hofmann clathrates withbenzene molecules occupying the space between the layers.9 Atom labeling scheme: C,black; N, green; metals, blue. H atoms are omitted for clarity

Source : Bunyarat Rungtaweevoranit, Christian S. Diercks,Markus J. Kalmutzki and Omar M. Yaghi, "Spiers Memorial Lecture:. Progress and prospects of reticular chemistry", The Royal Society of Chemistry 2017 Faraday Discuss., 2017, 201, 9–45

Atom 1	Atom 2	Length (Å)
Fe1	N2	1,99
Fe1	N22	2,00
Fe1	N32	1,98
Fe1	N41	1,94
Fe1	N44	1,93
Fe1	N13	2,00

Table 1. Distance Fe-N for a centre and the six nitrogen surrounding it, distance repeated for all the iron centres.

Atom 1	Atom 2	Atom 3	Angle (°)
N2	Fe1	N22	90,6
N2	Fe1	N32	90,0
N2	Fe1	N41	91,2

N2	Fe1	N44	88,8
N2	Fe1	N13	179,3
N22	Fe1	N32	179,3
N22	Fe1	N41	90,8
N22	Fe1	N44	90,3
N22	Fe1	N13	90,0
N32	Fe1	N41	89,1
N32	Fe1	N44	89,8
N32	Fe1	N13	89,3
N41	Fe1	N44	178,9
N41	Fe1	N13	88,9
N44	Fe1	N13	91,1

Table 2. N-Fe-N angles for a centre and the six nitrogen surrounding it

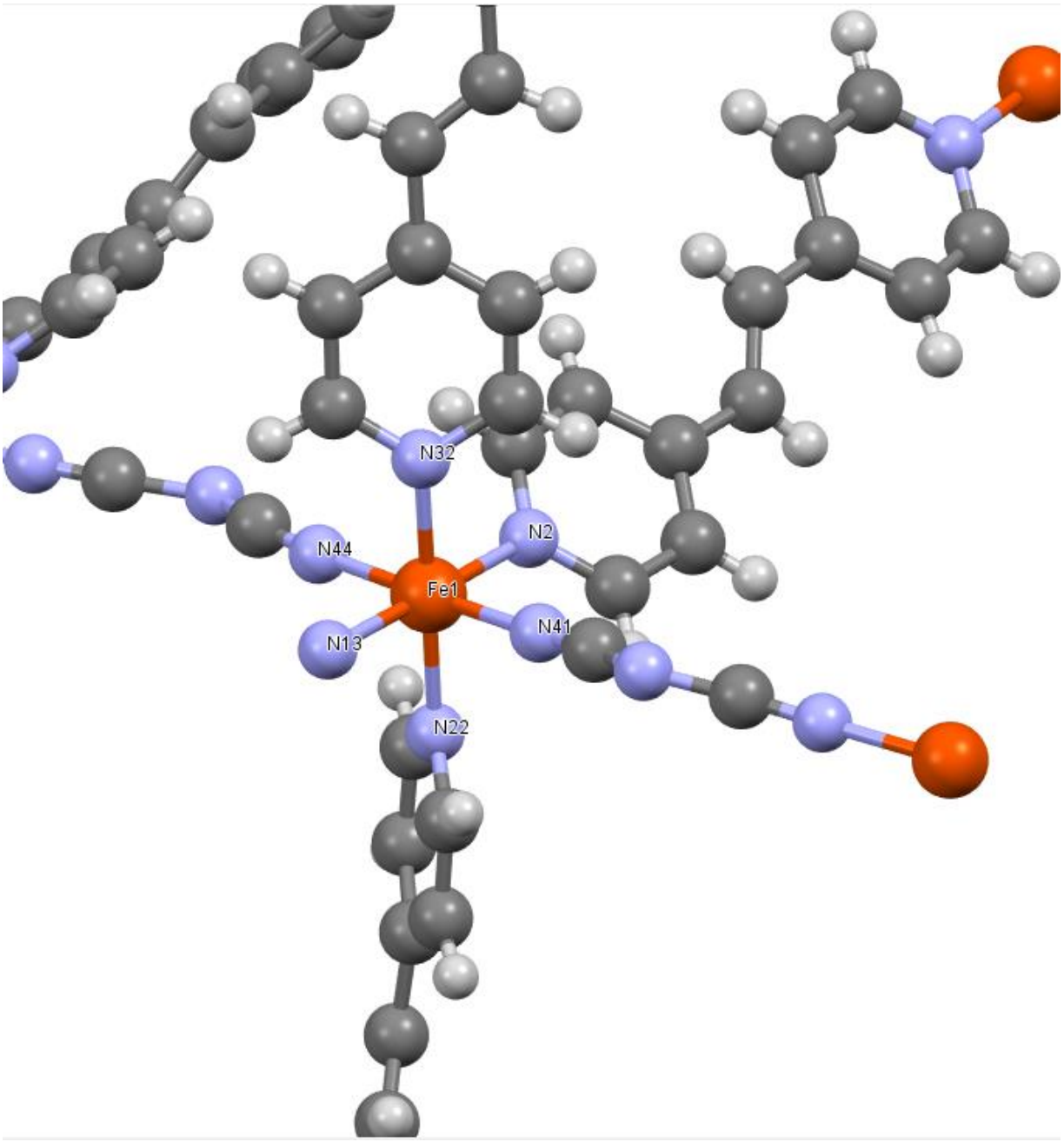

Supporting representation for table 2. Some atoms and molecules have been removed for clarity, a axis is in the depth, N44-N41 follow the b axis and N32-N22 follow the c axis

Atom 1	Atom 2	Atom 3	Angle (°)
O52	Cl51	O53	109
O52	Cl51	O54	112
O52	Cl51	O54	112
O53	Cl51	O54	106
O53	Cl51	O54	106
O54	Cl51	O54	111
O56	Cl55	O57	93
O56	Cl55	O58	106
O56	Cl55	O57	93
O57	Cl55	O58	114
O57	Cl55	O57	127
O58	Cl55	O57	114

Table 1. Distance O-Cl-O for a perchlorate nitrogen

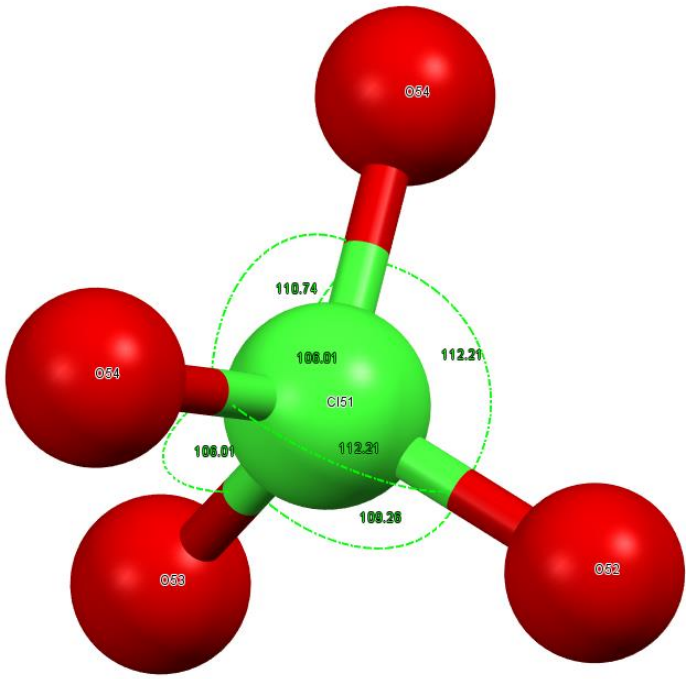

Supporting representation for table 3. Perchlorate anion representation and labelling for 1 molecule

Picture 1. Fresh LS6 crystals at room temperature

Picture 2. Fresh LS6 crystals just removed from liquid nitrogen

Picture 3. red crystals made of a composition of $Fe(BF_4)_2.6H_2O$, L_5 and SCN^-. The ones made of a composition of $FeCl_2$, L_5 and SCN^- look similar. When it is freshly made and before the collect, we can observe a sort of planar crystals but it disintegrates into smaller particles when collected.

Picture 4. Fresh composition of $FeCl_2$, L_5 and SCN^-, here are some orange crystals at top of the tube which look deliquescent

Picture 5. Fresh composition of $Fe(BF_4)_2.6H_2O$, L_5 and NH_4SCN, here are some crystals obtained on the right, the green powder collected on the left

Picture 6. Fresh orange crystals made of orthoxylene, L_4 and dca

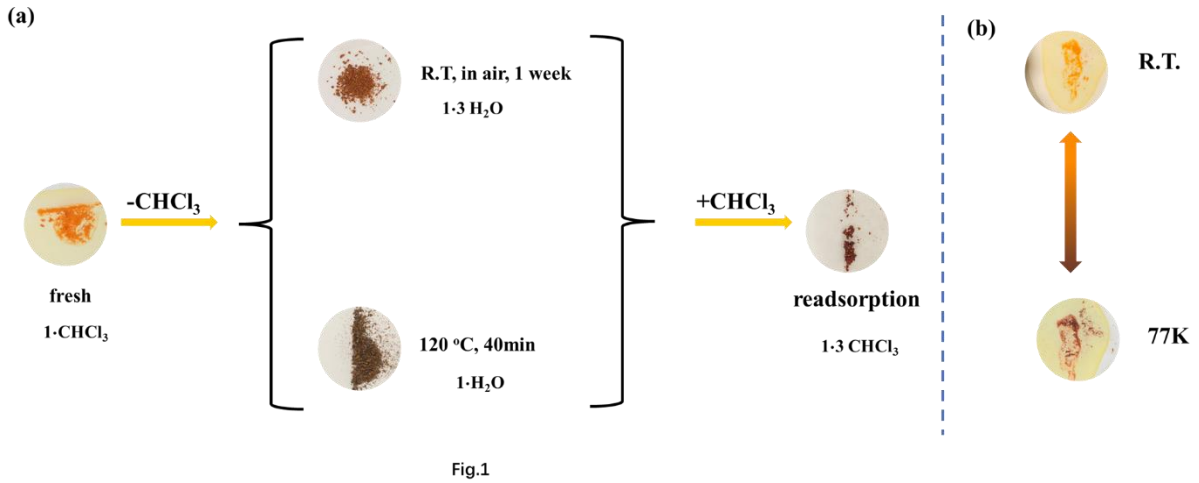

Fig.1

Supporting data 1. Representation of the colour and properties change with the variation of the conditions for $[Fe(L_1)_2dca]ClO_4 \cdot CHCl_3$ (**1·CHCl3**). This represents an adsorption-desorption process

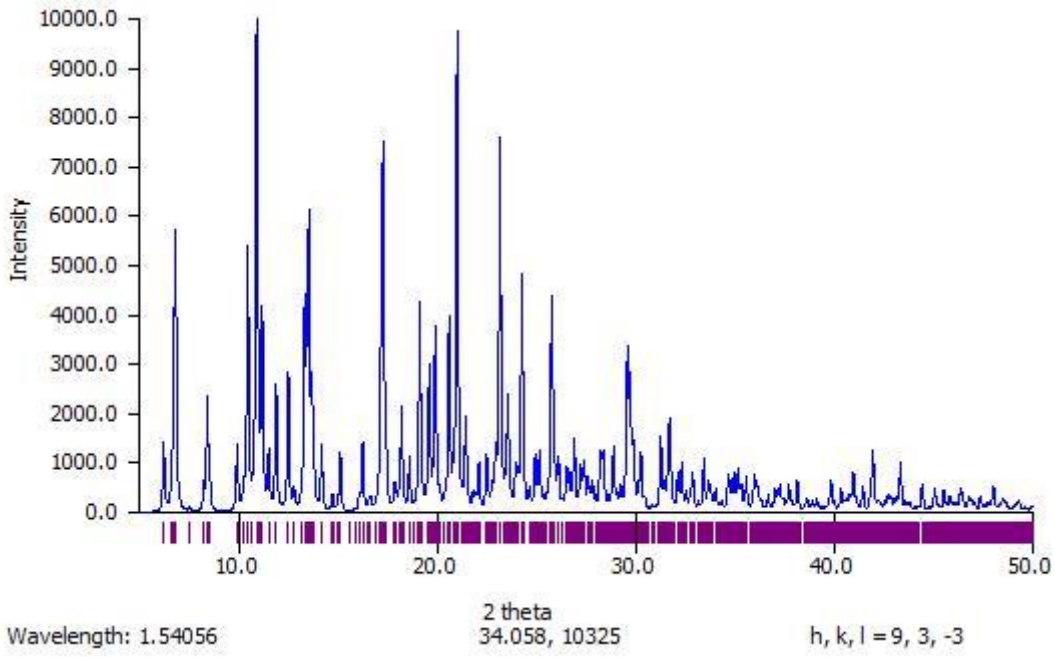

Supporting data 2. PXRD of LS6 at 100K that was designed on the basis of Single crystal XRD

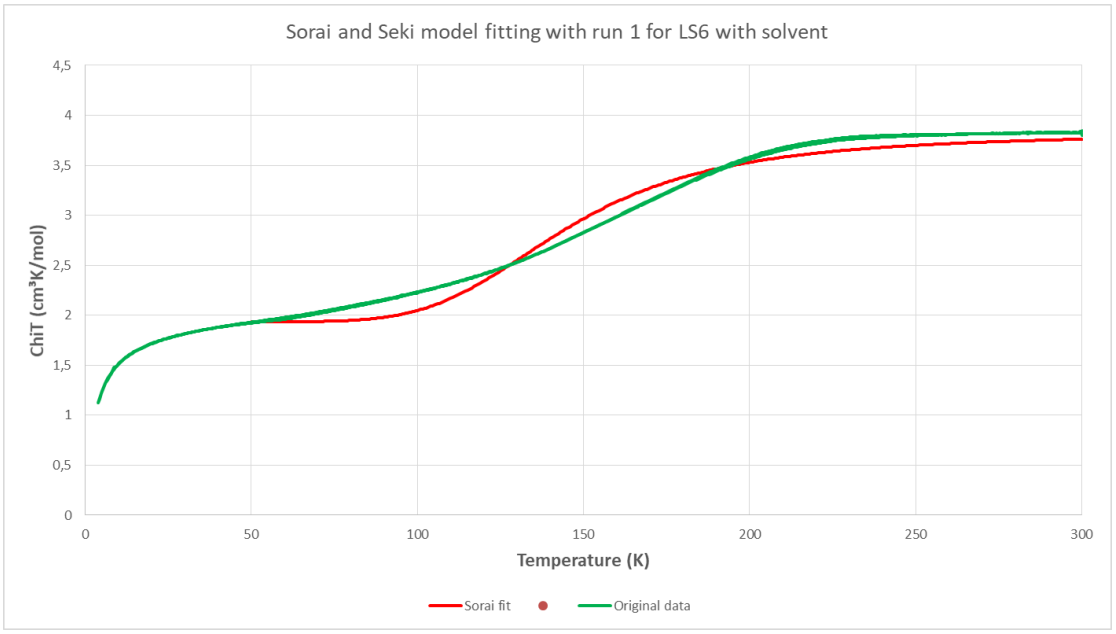

Supporting data 3. Sorai and Seki fit of the SQUID data of LS6 with solvent (run 1 only) showing SCO

Bibliography

[1] Oliver S. Siig and Kasper P. Kepp, Iron(II) and Iron(III) Spin Crossover: Toward an Optimal Density Functional, J. Phys. Chim. A 2018 , 122 , 16 , 4208–4217

[2] Gütlich, P.; Goodwin, H. A. Spin Crossover—an Overall Perspective. In Spin Crossover in Transition Metal Compounds I; Springer: 2004; pp 1– 47

[3] Kepp, K. P. Consistent Descriptions of Metal–ligand Bonds and Spin crossover in Inorganic Chemistry. Coord. Chem. Rev. 2013, 257 (1), 196– 209, DOI: 10.1016/j.ccr.2012.04.020

[4] Toftlund, H. Spin Equilibrium in Solutions. Monatsh. Chem. 2001, 132 (11), 1269– 1277, DOI: 10.1007/s007060170017

[5] Kershaw Cook, L. J.; Kulmaczewski, R.; Mohammed, R.; Dudley, S.; Barrett, S. A.; Little, M. A.; Deeth, R. J.; Halcrow, M. A. A Unified Treatment of the Relationship between Ligand Substituents and Spin State in a Family of Iron (II) Complexes. Angew. Chem., Int. Ed. 2016, 55 (13), 4327– 4331, DOI: 10.1002/anie.201600165

[6] P. Gütlich, A.B. Gaspar, Y. Garcia, Beilstein J. Org. Chem., 9 (2013), pp. 342-391

[7] S.A. Goudsmit, « Discovery of the spin of the electron / La découverte du spin de l'électron », Journal de Physique, vol. 28, 1967, p. 6 , DOI 10.1051/jphys:01967002801012301

[8] G. E. Uhlenbeck, S. Goudsmit, « Ersetzung der hypothese vom unmechanischen Zwang durch eine forderung bezglich des inneren Verhaltens jedes einzelnen elektrons », Naturwissenschaften, vol. 13, 1925, p. 953

[9] W. Kutzelnigg, J.D. Morgan III, Hund's rules, Z. Phys. D 36, 197-214 (1996)

[10] J.H. Van Vleck, « Theory of the Variations in Paramagnetic Anisotropy Among Different Salts of the Iron Group », Physical Review, vol. 41, no 2, 1932, p. 208-215 (DOI 10.1103/PhysRev.41.208)

[11] Petrucci, Ralph H. General Chemistry Principles and Modern Applications. 9th ed. Upper Saddle River: Pearson Prentice Hall, 2002, Chapter 24

[12] Rodgers, Glen E. Descriptive Inorganic, Coordination, and Solid-State Chemistry. 2nd ed. McGraw-Hill: New York, 1994, Chapter

[13] J. S. Griffith et L. E. Orgel, « Ligand-field theory », Quarterly Reviews, Chemical Society, vol. 11, no 4, 1957, p. 381-393 (DOI 10.1039/QR9571100381)

[14] F. Albert Cotton, “Ligand Field Theory”, resource papers-I , Journal of Chemical Education, vol.9, no 9, 1964, p 466-476

[15] Gary L. Miessler et Donald Arthur Tarr, Inorganic Chemistry, 1999, p. 338.

[16] Frank Albert Cotton, Geoffrey Wilkinson et Carlos A. Murillo, Advanced Inorganic Chemistry, 1999

[17] Yukito Tanabe et Satoru Sugano, « On the absorption spectra of complex ions I », Journal of the Physical Society of Japan, vol. 9, no 5, 1954, p. 753–766 (DOI 10.1143/JPSJ.9.753)

[18] Giulio Racah, « Theory of complex spectra II », Physical Review, vol. 62, nos 9–10, 1942, p. 438–462

[19] Chr Klixbüll Jørgensen, Carl-Henric De Verdier, John Glomset et Nils Andreas Sörensen, « Studies of absorption spectra IV: Some new transition group bands of low intensity », Acta Chem. Scand., vol. 8, no 9, 1954, p. 1495–1512

[20] Andrei L. Tchougréeff et Richard Dronskowski, « Nephelauxetic effect revisited », International Journal of Quantum Chemistry, vol. 109, no 11, 2009, p. 2606-2621

[21] Nenad. Juranic, « Nephelauxetic effect in paramagnetic shielding of transition metal nuclei in octahedral d6 complexes », Journal of the American Chemical Society, vol. 110, no 25, décembre 1988, p. 8341-8343

[22] Claus E.Schäffer et C. Klixbüll Jørgensen, « The nephelauxetic series of ligands corresponding to increasing tendency of partly covalent bonding », Journal of Inorganic and Nuclear Chemistry, no 8, 1958, p. 143-148

[23] C. E. Housecroft et A. G. Sharpe, (2004). Inorganic Chemistry, Prentice Hall, 2e édition, 2004, p. 578

[24] M. Getzlaff , Fundamentals of Magnetism, Springer, 2008, p25-39

[25] B.M. Moskowitz, Hitchhiker’s Guide to Magnetism, 1991, p1-14

[26] Cambi, L.; Szegö, L. Uber die magnetische Susceptibilitat der komplexen Verbindungen. Ber. Dtsch.Chem. Ges. 1931, 64, 2591–2598

[27] R. Carl Stoufer; Daryle H. Busch; Wayne B. Hadley (1961). "Unusual magnetic properties of some six-coordinate cobalt(II) complexes' electronic isomers". J. Am. Chem. Soc. 83 (17): 3732–3734

[28] Baker, W. A., Bobonich, H. M. (1964) Magnetic Properties of Some High-Spin Complexes of Iron(II). Inorganic Chemistry, 3 (8). 1184-1188

[29] Ewald, A.H.; Martin, R.L.; Sinn, E.; White, A.H. Electronic equilibrium between the 6A1 and 2T2 states iniron(III) dithio chelates. Inorg. Chem. 1969, 8, 1837–1846

[30] Decurtins, S.; Gütlich, P.; Köhler, C.P.; Spiering, H.; Hauser, A. Light-induced excited spin state trappingin a transition-metal complex: The hexa-1-propyltetrazole-iron(II) tetrafluoroborate spin crossover system.Chem. Phys. Lett. 1984, 105, 1–4.

[31] P. G. Sim and E. Sinn, J. Am. Chem. Soc. 103, 241 (1981)

[32] D.M. Halepoto, et al., J. Chem. Soc., Chem. Commun., 1989, 1322.

[33] Kahn, O.; Kröber, J.; Jay, C. Spin Transition Molecular Materials for Displays and Data Recording. Adv. Mater.1992, 4, 718–728

[34] Kröber J, Audière JP, Claude R, Codjovi E, Kahn O, Haasnoot JG, Grolière F, Jay C, Bousseksou A, Linarès J, Varret F, Gonthier-Vassal A (1994) Chem Mater 6:1404

[35] Vreugdenhil W, van Diemen JH, De Graaff RAG, Haasnoot JG, Reedijk J, van der Kraan AM, Kahn O, Zarembowitch J (1990) Polyhedron 9:2971

[36] Real JA, Andrés E, Muñoz MC, Julve M, Granier T, Bousseksou A, Varret F (1995) Science 268:265

[37] Garcia Y, Guionneau P, Bravic G, Chasseau D, Howard JAK, Kahn O, Ksenofontov V, Reiman S, Gütlich P (2000) Eur J Inorg Chem 1531

[38] Garcia Y, van Koningsbruggen PJ, Lapouyade R, Fournès L, Rabardel L, Kahn O, Ksenofontov V, Levchenko G, Gütlich P (1998) Chem Mater 10:2426

[39] Zhao-Ping Ni, Jun-Liang Liu, Md. Najbul Hoque, Wei Liu, Jin-Yan Li, Yan-Cong Chen, Ming-Liang Tong, Coordination Chemistry Reviews Volume 335, 15 March 2017, Pages 28-43

[40] K.A Hofmann, F. Küspert, Z. Anorg, Chem., 15 (1897), pp.204-207

[41] K.A Hofmann, F. Höchtlen, Ber. Dtsch. Chem. Ges., 36 (1903), pp.1149-1151

[42] K.A Hofmann, H. Arnoldi, Ber. Dtsch. Chem. Ges., 39 (1906), pp. 339-344

[43] H.M. Powell, J.H. Rayner, Nature, 163 (1949), pp.566-567

[44] J.H. Rayner, H.M. Powell, J.Chem. Soc. (1952), pp. 319-328

[45] R.Baur, G. Schwarzenbach, Helv. Chim. Acta, 43 (1960), pp. 842-847

[46] S.-I. Nishikiori, H. Yoshikawa, Y. Sano, T. Iwamoto, Acc. Chem. Res., 38 (2005), pp. 227-234

[47] T. Kitazawa, Y. Gomi, M. Takahashi, M. Takeda, M. Enomoto, A. Miyazaki, T. Enoki, J. Mater. Chem., 6 (1996), pp. 119-121

[48] V. Niel, J.M. Martinez-Agudo, M.C. Munoz, A.B. Gaspar, J.A. Real, Inorg. Chem., 40 (2001), pp. 3838-3839

[49] Yuqi Yang, Xiaoping Shen, Hongbo Zhou, Leiming Lang, Guoxing Zhu, Zhenyan Ji, Controlled synthesis of [Fe(pyridine)2Ni(CN)4] nanostructures and their shape-dependent spin crossover properties, Journal of Magnetism and Magnetic Materials, vol. 496, 15 february 2020, n° 165938

[50] V. Martinez, A.B. Gaspar, M.C. Munoz, G.V. Bukin, G. levchenko, J.A. Real, Chem. Eur. J., 15 (2009), pp. 10960-10971

[51] W. Liu, L. Wang, Y.-J. Su, Y-C. Chen, J. Tucek, R. Zboril, Z.-P. Ni, M.-L. Tong, Inorg. Chem., 54 (2015), pp. 8711-8716

[52] M.Seredyuk, A.Gaspar, V. Ksenofontov, M. Verdaguer, F. Villain, P. Gütlich, Inorg. Chem., 48 (2009), pp. 6130-6141

[53] C. Bartual-Murgui, N.A. Ortega-Villar, H.J. Shepherd, M.C. Munoz, L. Salmon, G. Molnar, A. Bousseksou, J.A. Real, J. Mater. Chem., 21 (2011), pp. 7217-7222

[54] F.J. Munoz-Lara, A.B. Gaspar, M.C. Munoz, V. Ksenofontov, J.A. Real, Inorg. Chem., 52 (2013), pp. 3-5

[55] M.C. Munoz, J.A. Real, Coord. Chem. Rev., 255 (2011), pp. 2068-2093

[56] V. Niel, M.C. Munoz, A.B. Gaspar, A. Galet, G. Levchenko, J.A. Real, Chem. Eur. J., 8 (2002), pp. 2446-2453

[56a] J.E. Clements, J.R. Price, S.M. Neville, C.J. Kepert, Angew. Chem. Int. Ed., 53 (2014), pp. 10164-10168

[56b] J.-Y. Li, Z.-P. Ni, Z. Yan, Z.-M. Zhang, W. Liu, M.-L. Tong, CrystEngComm, 16 (2014), pp. 6444-6449

[56c] J.-Y. Li, Y.-C. Chen, Z.-M.Zhang, W. Liu, Z.-P. Ni, M.-L. Tong, Chem. Eur. J., 21 (2015), pp. 1645-1651

[56d] J.-Y. Li, C.-T. He, Y.-C. Chen, Z.-M Zhang, W. Liu, Z.-P. Ni, M.-L. Tong, J. Mater. Chem. C, 3 (2015), pp. 7830-7835

[57] J. Cirera, Rev. Inorg. Chem., 34 (2014), pp. 199-216

[58] R. Ohtani, S. Hayami, Chem. Eur. J., 2016

[59] F.J. Munoz-Lara, A.B. Gaspar, D. Aravena, E. Ruiz, M.C. Munoz, M. Ohba, R. Ohtani, S. Kitagawa, J.A. Real, Chem. Commun., 48 (2012), pp. 4686-4688

[60] M. Ohba, K. Yoneda, G. Agusti, M.C. Munoz, A.B. Gaspar, J.A. Real, M. Yamasaki, H. Ando, Y. Nakao, S. Sakaki, S. Kitagawa, Angew. Chem. Int. Ed., 48 (2009), pp. 4767-4771

[61] P.D. Southon, L. Liu, E.A. Fellows, D.J. Price, G.J. Halder, K.W. Chapman, B. Moubaraki, K.S. Murray, J.-F. Létard, C.J. Kepert, J. Am. Chem. Soc., 131 (2009), pp. 10998-11009

[62] D. Aravena, Z.A Castillo, M.C. Munoz, A.B. Gaspar, K. Yoneda, R. Ohtani, A. Mishima, S. Kitagawa, M. Obha, J.A. Real, E. Ruiz, Chem. Eur. J., 20 (2014), pp. 12864-12873

[63] Y.H. Zhao, M.H. Abraham, A.M. Zissimos, J. Org. Chem., 68 (2003), pp.7368-7373

[64] A. Bondi, J. Phys. Chem., 68 (1964), pp. 441-451

[65] Z. Arcis-Castillo, F.J. Munoz-Lara, M.C. Munoz, D. Aravena, A.B. Gaspar, J.-F. Sanchez-Royo, E. Ruiz, M. Ohba, R. Matsuda, S. Kitagawa, Inorg. Chem., 52 (2013), pp. 12777-12783

[66] O. Shekhah, J. Liu, R.A. Fischer, C. Wöll, Chem. Soc. Rev., 40 (2011), pp. 1081-1106

[67] D. Zacher, R. Schmid, C. Wöll, R.A. Fischer, Angew. Chem. Int. Ed., 50 (2011), pp. 176-199

[68] A. Bétard, R.A. Fischer, Chem. Rev., 112 (2012), pp. 1055-1083

[69] K. Otsubo, H. Kitagawa, API. Mater., 2 (2014), p. 124105

[70] J.-L. Zhuang, A. Terfort, C. Wöll, Coord. Chem. Rev., 307 (2012), pp. 9605-9608

[71] S. Cobo, G. Molnar, J.A. Real, A. Bousseksou, Angew. Chem. Int. Ed., 45 (2006), pp. 5786-5789

[72] G. Molnar, S.Cobo, J.A. Real, F. Carcenac, E. Daran, C. Vieu, A. Bousseksou, Adv. Mater., 19 (2007), pp. 2163-2167

[73] C. Bartual-Murgui, A. Akou, L. Salmon, G. Molnar, C. Thibault, J.Antonio Real, A. Bousseksou, Small, 7 (2011), pp. 3385-3391

[74] C. Bartual-Murgui, A. Akou, C. Thibault, G. Molnar, C. Vieu, L. Salmon, A. Bousseksou, J. Mater. Chem. C, 3 (2015), pp. 1277-1285

[75] S. Sakaida, K. Otsubo, O. Sakata, C. Song, A. Fujiwara, M. Takata, H. Kitagawa, Nat. Chem., 8 (2016), pp. 377-383

[76] J. Larionova, L. Salmon, Y. Guari, A. Tokarev, K. Molvinger, G. Molnar, A. Bousseksou, Angew. Chem. Int. Ed., 47 (2008), pp. 8236-8240

[77] Y. Raza, F. Volatron, S. Moldovan, O. Ersen, V. Huc, C. Martini, F. Brisset, A. Gloter, O. Stéphan, A. Bousseksou, L. Catala, T. Mallah, Chem. Commun., 47 (2011), pp. 11501-11503

[78] A. Tokarev, J. Long, Y. Guari, J. Larionova, F. Quignard, P. Agulhon, M. Robitzer, G. Molnar, L. Salmon, A. Bousseksou, New J. Chem., 37 (2013), pp. 3420-3432

[79] Y. Inoue, H. Hoshi, M. Sakurai, R. Chujo, J. Am. Chem. Soc., 107 (1985), pp. 2319-2323

[80] T. Furuki, F. Hosokawa , M. Sakurai, Y. Inoue R. Chujo, J. Am. Chem. Soc., 115 (1993), pp. 2903-2911

[81] S.M. Neville, G.J. Halder, K.W. Chapman, M.B. Duriska, B. Moubaraki, K.S. Murray, C.J. Kepert, J. Am. Chem. Soc., 131 (2009), pp. 12106-12108

[82] T. Romero-Morcillo, N. De la Pinta, L.M. Callejo, Pineiro-Lopez, M.C Munoz, G. Madariaga, S. Ferrer, T. Breczewski, R. Cortés, J.A. Real, Chem. Eur. J., 21 (2015), pp. 12112-12120

[83] J.-Y. Li, Y.-C. Chen, Z.-M. Zhang, W. Liu, Z.-P. Ni, M.-L. Tong, Chem. Eur. J., 21 (2015), pp. 1645-1651

[84] L.J. Murray, M. Dinca, J.R. Long, Chem. Soc. Rev., 38 (2009), pp. 1294-1314

[85] B.-L. Chen, S.-C. Xiang, G.-D. Qian, Acc. Chem. Res., 43 (2010), pp. 1115-1124

[86] D.M. D'Alessandro, B. Smit, J.R. Long, Angew. Chem. Int. Ed., 49 (2010), pp. 6058-6082

[87] J.-R. Li, Y. Ma, M.C. McCarthy, J. Sculley, J. Yu, H.-K. Jeong, P.B. Balbuena, H.-C. Zhou, Coord. Chem. Rev., 255 (2011), pp. 1791-1823

[88] K. Sumida, D.L. Rogow, J.A. Mason, T.M. McDonald, E.D. Bloch, Z.R. Herm, T.-H. Bae, J.R. Long, Chem. Rev., 112 (2012), pp. 724-781

[89] Y.-B. He, W. Zhou, G.-D. Qian, B.-L. Chen, Chem. Soc. Rev., 43 (2014), pp. 5657-5678

[90] Y. Yan, S.-H. Yang, A.J. Blake, M. Schröder, Acc. Chem. Res., 47 (2014), pp. 296-307

[91] M.I. Nandasiri, S.R. Jambovane, B.P. McGrail, H.T. Schaef, S.K. Nune, Coord. Chem. Rev., 311 (2016), pp. 38-52

[92] J.-R. Li, R.J. Kuppler, H.-C. Zhou, Chem. Soc. Rev., 38 (2009), pp. 1477-1504

[93] Y.-S. Bae, R.Q. Snurr, Angew. Chem. Int. Ed., 50 (2011), pp. 11586-11596

[94] S.-L. Qiu, M. Xue, G.-S. Zhu, Chem. Soc. Rev., 43 (2014), pp. 6116-6140

[95] D. Banerjee, A.J. Cairns, J. Liu, R.K. Motkuri, S.K. Nune, C.A. Fernandez, R. Krishna, D.M. Strachan, P.K. Thallapally, Acc. Chem. Res., 48 (2015), pp. 211-219

[96] B. Seoane, J. Coronas, I. Gascon, M.E. Benavides, O. Karvan, J. Caro, F. Kapteijn, J. Gascon, Chem. Soc. Rev., 44 (2015), pp. 2421-2454

[97] J.-R. Li, J. Sculley, H.-C. Zhou, Chem. Rev., 112 (2012), pp. 869-932

[98] B. Van de Voorde, B. Bueken, J. Denayer, D. De Vos, Chem. Soc. Rev., 43 (2014), pp. 5766-5788

[99] M. Kurmoo, Chem. Soc. Rev., 38 (2009), pp. 1353-1379

[100] P. Dechambenoit, J.R. Long, Chem. Soc. Rev., 40 (2011), pp. 3249-3265

[101] S. Roy, A. Chakraborty, T.K. Maji, Coord. Chem. Rev., 273 (2014), pp. 139-164

[102] D.-F. Weng, Z.-M Wang, S. Gao, Chem. Soc. Rev., 40 (2011), pp. 3157-3181

[103] Z.-G. Gu, C.-H. Zhan, J.Zhang, X.-H. Bu, Chem. Soc. Rev., 45 (2016), pp. 3122-3144

[104] M. Yoon, R. Srirambalaji, K. Kim, Chem. Rev., 112 (2012), pp. 1196-1231

[105] S. Horike, D. Umeyama, S. Kitagawa, Acc. Chem. Res., 46 (2013), pp. 2376-2384

[106] L. Sun, M.G. Campbell, M. Dinca, Angew. Chem. Int. Ed., 55 (2016), pp. 3566-3579

[107] H. Furukawa, K.E. Cordova, M. O'Keeffe, O.M. Yaghi, Science, 341 (2013), p.974

[108] J.-W. Liu, L.-F. Chen, H. Cui, J.-Y. Zhang, L.Zhang, C.-Y. Su, Chem. Soc. Rev., 43 (2014), pp. 6011-6061

[109] T.Zhang, W.-B. Lin, Chem. Soc. Rev., 43 (2014), pp. 5982-5993

[110] M. Zhao, S. Ou, C.-D. Wu, Acc. Chem. Res., 47 (2014), pp. 1199-1207

[111] A.H. Chughtai, N.Ahmad, H.A. Younus, A. Laypkov, F. Verpoort, Chem. Soc. Rev., 44 (2015), pp. 6804-6849

[112] I. Nath, J. Chakraborty, F. Verpoort, Chem. Soc. Rev., 45 (2016), pp. 4127-4170

[113] J. Rocha, L.D. Carlos, F.A.A. Paz, D. Ananias, Chem. Soc. Rev., 40 (2011), pp. 926-940

[114] J. Heine, K. Müller-Buschbaum, Chem. Soc. Rev., 42 (2013), pp. 9232-9242

[115] Y.-J. Cui, B.-L. Chen, G.-D. Qian, Coord. Chem. Rev., 273-274 (2014), pp. 76-86

[116] Z.-C. Hu, B.J. Deibert, J.Li, Chem. Soc. Rev., 43 (2014), pp. 5815-5840

[117] R.-B. Lin, S.-Y. Liu, J.-W. Ye, X.-Y. Li, J.-P. Zhang, Adv. Sci., 3 (2016), pp. 150034-1500453

[118] M.D. Allendorf, C.A. Bauer, R.K. Bhakta, R.J.T. Houk, Chem. Soc. Rev., 38 (2009), pp. 1330-1352

[119] S.-L. Li, Q. Xu, Energy Environ. Sci., 6 (2013), pp. 1656-1683

[120] Y. Ren, G.H. Chia, Z. Gao, Nano Today, 8 (2013), pp. 577-597

[121] P. Falcaro, R. Ricco, C.M. Doherty, K. Liang, A.J. Hill, M.J. Styles, Chem. Soc. Rev., 43 (2014), pp. 5513-5560

[122] W. Xia, A. Mahmood, R.-Q. Zhou, Q. Xu, Energy Environ. Sci., 8 (2015), pp. 1837-1866

[123] M.-H. Sun, S.-Z. Huang, L.-H. Chen, Y. Li, X.-Y. Yang, Z.-Y. Yuan, B.-L. Su, Chem. Soc. Rev., 45 (2016), pp. 3479-3563

[124] L. Whang, Y.-Z. Han, X. Feng, J.-W. Zhou, P.-F. Qi, B. Wang, Coord. Chem. Rev., 307 (2016), pp. 361-381

[125] Kumar Biradha, Yoshito Hongo, Makoto Fujita, Angew. Chem. Int. Ed., 2000, 39, No 21, pp. 3843-3845

[126] Susanne Wöhlert, Mario Wriedt, Tomasz Fic, Zbigniew Tomkowicz, Wolfgang Haase and Christian Nather Inorg. Chem. 2013, 52, 2, 1061–1068, December 31, 2012

[127] Nakashima, S.; Yamamoto, A.; Asada, Y.; Koga, N.; Okuda, T. Inorg. Chim. Acta 2005, 358 (2), 257−264.

[128] Wöhlert, S.; Boeckmann, J.; Wriedt, M.; Nather, C. , Angew. Chem.,Int. Ed. 2011, 50 (30), 6920−6923

[129] Galina S Matouzenko, Monique Perrin, Boris Le Guennic, Serguei A Borshch, Caroline Genre, Gabor Molnar, Azzedine Bousseksou, Dalton Transactions, April 2007, 934-942

[130] Javier García-Ben, Lauren Nicole, McHugh Thomas, Douglas Bennett, Juan Manuel, Bermúdez-García, Coordination Chemistry Reviews, Volume 455, 15 March 2022, 214337

[131] Stuart R Batten, Keith S Murray, Coordination Chemistry Reviews, Volume 246, Issues 1–2, November 2003, Pages 103-130

[132] Ilya A. Shkrob, Timothy W. Marin, James F. Wishart, The Journal of Physical Chemistry B, May 2013, 117 (23), pp. 7084-7094

[133] Sandra Kisslinger, Harald Kelm, Sipeng Zheng, Alexander Beitat, Christian Würtele, Ramona Wortmann, Sylvestre Bonnet, Sonja Herres-Pawlis, Hans-Jörg Krüger, and Siegfried Schindler, Z. Anorg. Allg. Chem. 2012, 638, (12-13), 2069–2077

[134] Johanna S. Kolb, Mark D. Thomson, Miljenko Novosel, Katell Sénéchal-David, Éric Rivière, Marie-Laure Boillot, Hartmut G. Roskos, Comptes Rendus Chimie, Volume 10, Issues 1–2, January–February 2007, Pages 125-136

[135] Jarrod J. M. Amoore Dr.,Suzanne M. Neville Dr.,Boujemaa Moubaraki Dr.,Simon S. Iremonger Dr.,Keith S. Murray Prof.,Jean-François Létard Dr.,Cameron J. Kepert Prof, Chemistry Europe, Volume 16, Issue 6, February 8, 2010, Pages 1973-1982

[136] Rong-Jia Wei, Jun Tao, Rong-Bin Huang, and Lan-Sun Zheng, Inorg. Chem. 2011, 50, 17, 8553–8564

[137] P. Gütlich, Y. Garcia, H. A. Goodwin, Chem. Soc. Rev. 2000, 29, 419–427.

[138] N. O. Moussa, G. Molnár, X. Ducros, A. Zwick, T. Tayagaki, K. Tanaka, A. Bousseksou, Chem. Phys. Lett. 2005, 402, 503–509.

[139] P. Weinberger, M. Grunert, Vib. Spectrosc. 2004, 34, 175–186

[140] M. Kurzajewska, D.Kwiatek, M.Kubicki, B. Brzezinski, Z. Hnatejko, Polyhedron, Vol.148, 1 July 2018, pages 1-8

[141] P. Cardillo, E. Corradi, A. Lunghi, S. Valdo Mieille, M.T. Messina, P. Metrangolo, G. Resnati, Tetrahedron, Vol. 56, Issue 30, 21 July 2000, pages 5535-5550